

**Sandia
National
Laboratories**



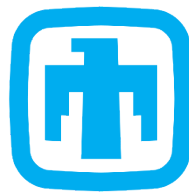
BGE TECHNOLOGY GmbH

RANGERS

State of the Art and Science on Engineered Barrier Systems in Salt Formations

BGE TEC 2021-13

Technical Report



Sandia
National
Laboratories



BGE TECHNOLOGY GmbH

RANGERS

State of the Art and Science on Engineered Barrier Systems in Salt Formations

BGE TEC 2021-13

Authors

Simo, Eric (BGE TEC)
Herold, Philipp (BGE TEC)
Keller, Andreas (BGE TEC)
Lommerzheim, Andree (BGE TEC)

Matteo, Edward N. (SNL)
Hagdu, Teklu (SNL)
Jayne, Richard S. (SNL)
Kuhlman, Kristopher L. (SNL)
Mills, Melissa M. (SNL)

Date 12.12.2021

Client BMWi

Funding contract number 02 E 11839

The report was compiled as part of the project:

"Methodology for design and performance assessment of geotechnical barriers in a HLW repository in salt formations (RANGERS)."

The research work that is the basis of this report was funded at BGE TEC by the German Federal Ministry for Economic Affairs and Energy (BMWi, Bundesministerium für Wirtschaft und Energie) represented by the Project Management Agency Karlsruhe (Karlsruhe Institute of Technology, KIT) under contract number FKZ 02 E 11839. The authors alone, however, are responsible for the contents of this study.

Gefördert durch:



Bundesministerium
für Wirtschaft
und Energie

aufgrund eines Beschlusses
des Deutschen Bundestages

BETREUT VOM



PTKA
Projektträger Karlsruhe

Karlsruher Institut für Technologie

This report describes objective technical results and analysis. Any subjective views or opinions that might be expressed in the paper do not necessarily represent the views of the U.S. Department of Energy or the United States Government.

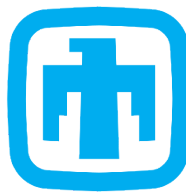
At Sandia, the work was funded by the US Department of Energy Office of Nuclear Energy, Spent Fuel and Waste Science and Technology program.



Sandia National Laboratories is a multimission laboratory managed and operated by National Technology and Engineering Solutions of Sandia LLC, a wholly owned subsidiary of Honeywell International Inc. for the U.S. Department of Energy's National Nuclear Security Administration under contract DE-NA0003525.



Sandia
National
Laboratories



Sandia National Laboratories



BGE TECHNOLOGY GmbH

RANGERS

State of the Art (SOTA) and Science on Engineered Barrier Systems in Salt Formations

BGE TEC 2021-13 / SAND2021-XXXXR

Authors Simo, Eric (BGE TEC)
Herold, Philipp (BGE TEC)
Keller, Andreas (BGE TEC)
Lommerzheim, Andree (BGE TEC)

Matteo, Edward N. (SNL)
Hagdu, Teklu (SNL)
Jayne, Richard S. (SNL)
Kuhlman, Kristopher L. (SNL)
Mills, Melissa M. (SNL)

Date 12.12.2021

Client BMWi

Funding contract number 02 E 11839

Number of pages: 106

BGE TECHNOLOGY

Edited by:

Reviewed by:

Quality assurance by:

Approved by:

Date/Signature

Date/Signature

Date/Signature

Date/Signature

SANDIA

Edited by:

Reviewed by:

Quality assurance by:

Approved by:

Date/Signature

Date/Signature

Date/Signature

Date/Signature

Contents

1	Introduction	1
2	Overview of research projects and state of research	3
2.1	ELSA	3
2.1.1	Overview	3
2.1.2	Shaft sealing concepts for salt formations	4
2.1.3	Filling columns made of compacted crushed salt	5
2.1.4	Cast in place concrete made of MgO-concrete	15
2.1.4.1	First large-scale test	17
2.1.4.2	Second large-scale test	18
2.1.5	Asphalt and bitumen sealings	20
2.1.5.1	Bitumen filled gravel columns	20
2.1.5.2	Dense stone asphalts	21
2.1.5.3	"Hard shell – soft core"	21
2.2	Preliminary safety analysis for the Gorleben site - VSG	26
2.2.1	Safety concept	26
2.2.2	Safety assessment concept	28
2.2.3	Shaft sealing concept	29
2.2.4	Drift sealing concept	31
2.2.5	Safety demonstration and verification concept	32
2.3	ISIBEL	37
2.4	Waste Isolation Pilot Plant	40
2.4.1	Cement Seal Experiments	40
2.4.1.1	Borehole Plugging Program	40
2.4.1.2	Small-Scale Seal Performance Test (SSSPT)	44
2.4.2	WIPP Salt Backfill Reconsolidation Research	46
2.4.2.1	Field Tests	48
2.4.2.2	Laboratory Tests	52
3	Case study: Asse II (Germany)	55
3.1	Introduction	55
3.2	Salt concrete to test long-term sealing of horizontal drifts in rock salt	56
3.3	Sorel concrete for the construction of flow barriers	58
3.4	Selected further learnings	63
3.4.1	Well installation for monitoring	63
3.4.2	Crushed salt as backfill	63
3.4.3	EDZ size and healing	64
3.4.4	Shaft sealing	65
4	Case study: Morsleben	67
4.1	Introduction and Project Description	67
4.2	Geology and mine openings	67
4.3	Geotechnical Barriers within the Safety Concept	69
4.4	Salt concrete for horizontal sealings in rock salt layers – category I	71
4.4.1	ERAM in situ Test Seal - main Hydraulic Test at 2 nd Level	72
4.4.2	Destruction free quality measuring of seals	73
4.5	Sorel concrete for horizontal seals in anhydrite – category I	74
4.5.1	Conceptual seal in anhydrite at ERAM	74
4.5.2	Sorel concrete seals – cast in situ – test site Bleicherode	75
4.5.3	Sorel concrete seals – shotcrete and bitumen	76
4.6	Salt concrete as backfill for large cavities to maintain the integrity of the impermeable barrier in the hanging wall of the repository (category II)	77

5	Case study: WIPP Site	79
5.1	Introduction	79
5.2	Project Description	79
5.3	Geology	79
5.4	Geotechnical Barrier	82
6	Closure of Industrial Rock Salt and Potash Mines in Germany	85
7	Summary and Next Steps	89
8	References	91
	List of Figures	104
	List of Tables	108

1 Introduction

The construction of deep geological repositories (DGR) in salt formations requires penetrating through naturally sealing geosphere layers. While the emplaced nuclear waste is primarily protected by the containment-providing rock zone (CRZ), technical barriers are required, for example during handling. For closure geotechnical barriers seal the repository along the accesses against water or solutions from outside and the possible emission paths for radionuclides contained inside. As these barriers must ensure maintenance-free function on a long-term basis, they typically comprise a set of specialized elements with diversified functions that may be used redundantly. The effects of the individual elements are coordinated so that they are collectively referred to as the Engineered Barrier System (EBS). The major radiation protection goals of the DGR and its EBS require a high hydraulic resistance that minimizes the movement of water and gas as transportation media. Article 26 of the German Repository Site Selection Act (In German: Standortauswahlgesetz, StandAG) stipulates but is not limited to the following objectives:

- To separate the radionuclides of spent fuel (SF) and high-level waste (HLW) from the biosphere and contain them within the main barriers until they are no longer harmful
- To limit the exposure due to radioactive emissions to a value that is small in comparison to the natural radiation
- To protect humans and the environment from harmful effects of ionizing radiation or other harmful effects of the SF/HLW

The high hydraulic resistance fosters the non-radiation safety goal of groundwater protection against harmful pollution as required by § 48 of the German Federal Water Act (In German: Wasserhaushaltsgesetz, WHG). In addition, it indirectly limits subsidence due to reduced cavities in the underground, which in turn protects buildings and infrastructure on the earth's surface.

Besides the hydraulic resistance, the EBS needs to be chemically and mechanically stable, stiff, strong and the elements need to be produced and processed in situ. A barrier only works in combination with the surrounding rock mass, as there are three important potential paths for migration (see Figure 1-1). All pathways must be addressed to ensure containment:

- Barrier
- Contact zone between barrier and rock mass
- Rock mass, predominantly the excavation damaged zone (EDZ)

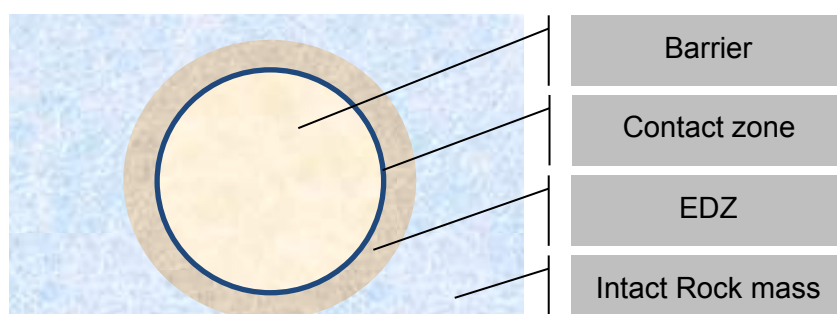


Figure 1-1: Schematic cross-section of potential pathways at a circular geotechnical barrier

Barriers protect operational parts of mines against gases or liquids from the surrounding area or from abandoned mining areas. Geotechnical barriers for nuclear waste repositories have the additional demand that requires maintenance-free performance over a long timescale, typically hundreds of thousands of years. Several approaches have been used to identify adequate materials and how they should be applied to fulfill the requirements. The report summarizes research projects related to closure of mines or repositories in Germany and in the USA. The construction of barriers here is divided into vertical barriers and horizontal barriers, as these categories each face different challenges. Additionally, backfilling procedures are included. A summary of the planning and construction of geotechnical barriers will show best practices for a future site. This report therefore covers existing concepts of EBS and the conducted testing on sealing structures.

The international status of the design and construction of new types of geotechnical barriers that deviate from the approaches currently being pursued in Germany and the USA are not included here. They will be part of another report within the project RANGERS that will continue with new and emerging concepts and materials.

2 Overview of research projects and state of research

Salt has been considered a viable host rock for DGR since early investigations of radioactive waste disposal in Germany and the USA. Not just the favorable geo-mechanical and geological properties, but also the presence of large and various salt formations justified these considerations. In addition, more than one hundred years of industrial mining and decades of disposal of chemo-toxic waste provide a technical base and wide knowledge in underground activities in salt formations. Additional R&D activities focused on the special issues of radioactive waste disposal. With respect to the disposal of HLW and SNF in German salt formations, a common thread in the R&D activities can be drawn from the 1990s until today. BGE TEC contributed to this in several R&D projects. The two-phase project ISIBEL (Buhmann et al., 2008) reviewed and appraised the tools available for a safety assessment of final disposal. Subsequently the preliminary safety assessment for the Gorleben site (German acronym: VSG) (Fischer-Appelt et al., 2013) applied the best theoretical understanding to the site based existing knowledge including the exploration results. This project therefore represents the state of the art at the time. Through the KOSINA project (Bollingerfehr et al., 2018), this knowledge was transferred to bedded salt formations in Germany. Finally, within the two-phase ELSA project (Kudla et al., 2021) shaft sealing concepts were developed and different sealing elements tested. The projects ISIBEL, VSG and ELSA will be summarized in the following sections. In the USA the Waste Isolation Pilot Plant (WIPP) had conducted research on borehole, drift, and shaft sealing components from the 1970s through the early 2000s. The Bell Canyon Test was a field experiment conducted in two boreholes before the construction of the WIPP facility. The test involved emplacing and measuring permeability for a plug emplaced in the anhydrite stratigraphically below the WIPP Salado horizon, to test the ability to seal against possibly pressurized formations. The WIPP Small-Scale Seal Performance Tests (SSSPT) studied plugging and sealing through multi-part tests conducted in the WIPP underground. The test plan included the emplacement of different seals made from different materials, including clay, salt, and clay/salt blocks, salt cement, and grouting fractures in the near-drift damaged zone. This summary presents some of the plugging and sealing tests that explored materials and focused on *in situ* measurements of permeability for seals and plugs. Additional underground tests, examining thermal-structural interactions (TSI) and crushed salt compaction are also summarized.

2.1 ELSA

The following sections summarize the results of the ELSA phase 2 project, relevant for RANGERS. Focus lies on sealing systems suitable for the application in rock salt. The summary is based on Kudla et al. (2021) and corresponding technical reports of the project, while additional relevant sources are referenced.

2.1.1 Overview

The present Phase 2 of the ELSA R&D Project follows Phase 1 of the ELSA project, which described the state of the art in science and technology up to 2013, the safety demonstration concept for sealing (shaft) elements, the boundary conditions for the salt and clay host rocks and the regulatory requirements for the shaft seals of future HAW repositories. The results of the ELSA - Phase 1 project allowed important conclusions to be drawn for the basic concept

of future shaft seals in saline and clay rock with increased requirements. The ELSA - Phase 2 project used these results and put them into practice by means of laboratory and semi-technical tests. Objectives of the ELSA - Phase 2 project were the development of site-independent and modular shaft sealing concepts for salt and claystone formations, testing of individual elements of a shaft sealing in the laboratory and in semi-technical experiments with development, testing and calibration of material models for the model-theoretical description of the material behavior for mathematical verification. By this, the following possible shaft seal components have been investigated as the focus of the project:

- Filling columns made of compacted rock salt - material selection and installation methods for the realization of a low porosity < 10% (for sites in salt formations),
- Abutment elements made of MgO concrete with the long-term stable 3-1-8 binder phase (recipe type C3) in in-situ concrete construction (for locations in salt formations),
- Further development of the construction and quality control of asphalt seals (for sites in salt formations and clay),
- Integration of equipotential segments into bentonite sealing systems (for sites in salt formations and clay).

An important contribution of the project is the further development of the methodology of verification (theoretical and experimental). The modular design of the shaft closure concept eases an adaptation to future site conditions.

2.1.2 Shaft sealing concepts for salt formations

For each of the two host rock options (rock salt and argillaceous rock), a generally applicable shaft sealing concept was developed, which is modular and can be adapted to local conditions. The existing concepts from the work on the "Salzdetfurth" project (Breidung, 2002) and the Preliminary Safety Analysis for the Gorleben site (VSG) (Müller-Hoeppel et al. 2012) represent starting point for this.

The geological model considered for salt rocks covers salt deposits that were formed under arid climatic conditions, such as those which prevailed geologically in Central Europe, especially during the Permian, Mesozoic and Tertiary periods. In Germany, the salt rocks of the Zechstein (Upper Permian) are most widespread. These are periodic sequences of clays, carbonates, sulfates, and chlorides, whereby seven main cycles (z1 to z7) can be distinguished. As an example of "salt cushion with flat support" rock salt type, a site was selected in the already considered in the project "Preservation of evidence on the geomechanical behavior of saline barriers after strong dynamic loading and development of a dimensioning guideline for permanent containment" (Minkley et al. 2010; Bollingerfehr et al. 2018).

In addition to the basic components, gravel-based filling columns and bentonite sealing elements following functional elements was proposed to consider in the sealing concept:

- filling columns made of compacted crushed salt
- MgO-based concrete cast in place
- concrete, including ordinary Portland cement (OPC) or salt concrete
- asphalt and bitumen
- equipotential segments as an addition/further development of bentonite sealings

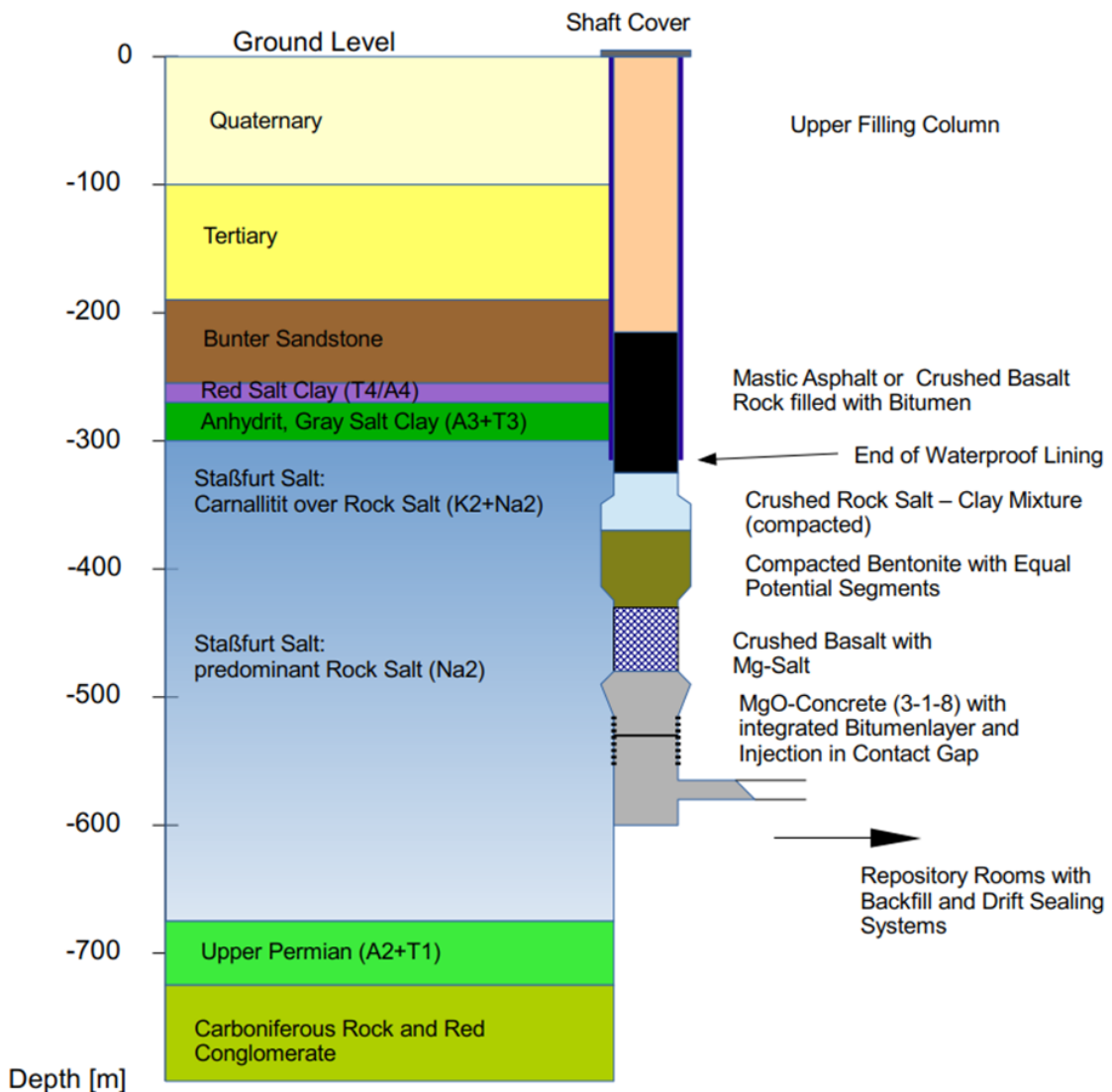


Figure 2-1: Conceptual design of the shaft sealing system (Kudla et al., 2021)

Bentonite sealing elements should always be positioned in rock salt (halite). If placed in contact with carnallitite there is an unfavorable influence on the swelling behavior (competitive reactions during water absorption). In carnallitite, sealing elements made of bitumen/asphalt or MgO concrete (with contact area injection) are preferable. For the element made of MgO concrete the formula C3 should be used. To ensure the stability of the element when exposed to solution, the Mg^{2+} content of the solution must be at least 0.5 mol / kg H_2O at 25 °C.

A more detailed concept is only possible once the measured values for the depth-dependent phase inventory, permeability and porosity of the individual geological layers are available through site investigations. For this purpose, the final position of the required watertight shaft lining, the position and extent of other lined areas of the shaft contour, the local thickness and sealing effect of the salt clay horizons and the distribution and location of carnallitite in the evaporite sequence must be known.

2.1.3 Filling columns made of compacted crushed salt

An alternative to gravel columns for sites in rock salt are filling columns made of a material that is specific to the host rock and is compacted as much as possible during installation. The material is further compacted by the convergence process which progresses over time and ideally the filling column material becomes a monolith with the surrounding rock. The materials used and the installation methods should allow a porosity of < 10% and if possible, about 5% after installation. This should be possible using material mixtures with optimized grain size distribution and optimum moisture content, such as salt-clay mixtures, the use of pressed shaped salt bricks or the use of multi-component systems consisting of pellets of different sizes and a fine fraction of salt breeze with clay powder. Within the ELSA 2 project the focus was on the first option, the optimization of the grain size distribution and moisture content. In a first step, based on laboratory tests, an optimized grain size distribution was determined. The tests were performed with crushed salt from Sondershausen salt mine. The grain size distribution depends on the filters in the production line. The goal for the optimization was the highest possible density based on a FULLER-line with exponent $n = 0.5$. An additional increase of the density was produced by the input of material with grain sizes lower than the finest salt fraction. The clay Friedländer Ton (associated with the 0.01 to 0.08 mm fraction) was chosen for the further optimization of the density and the moisture content. Finally, three different mixtures were developed, see Table 2-1.

Table 2-1: Grain-size distribution of the different mixtures (Kudla et al., 2021)

Fraction [mm]	STG-1 (Knorr- EBSM) (mass-%)	STG-2 (OBSM) (mass-%)	STG-3 (mOBSM) (mass-%)
3 to 10	24.8	48.1	--
0.4 to 4	23.1	19.8	58.5
0.1 to 1	37.6	10.9	17.5
0.03 to 0.3	--	13.4	13.5
0.01 to 0.08	14.6	7.8	10.5
Sum	100.0	100.0	100.0
Water input to the dry mass	5.1	3.4	4.2

For compaction tests an adapted ramming compaction with a Marshall device was used. The compaction work per hit was 20.5 N-m. Depending on the number of hits and amount of material, different specific compaction energies can be achieved. In this way, the evaluation of the laboratory tests showed the porosity of the compacted body achieved by the compaction as a function of the specific compaction energy related to the solid volume (grain volume).

Typical compaction curves are shown in Figure 2-2. For the mixtures at hand, minimum values of the specific compaction energy of 3 MJ/m³ are required. With moderate specific compaction energies of 3 to 5 MJ/m³, a porosity of approximately 11% could be achieved with the clay rich STG-1 formulation. In this case higher compaction energies are not required. Porosities < 9% could only be achieved with mixtures poor in clay and water (formulations STG-2 and STG-3) at very high specific compaction energies of approximately 15 MJ/m³. In addition, long term test for liquid permeability were performed, see Figure 2-3.

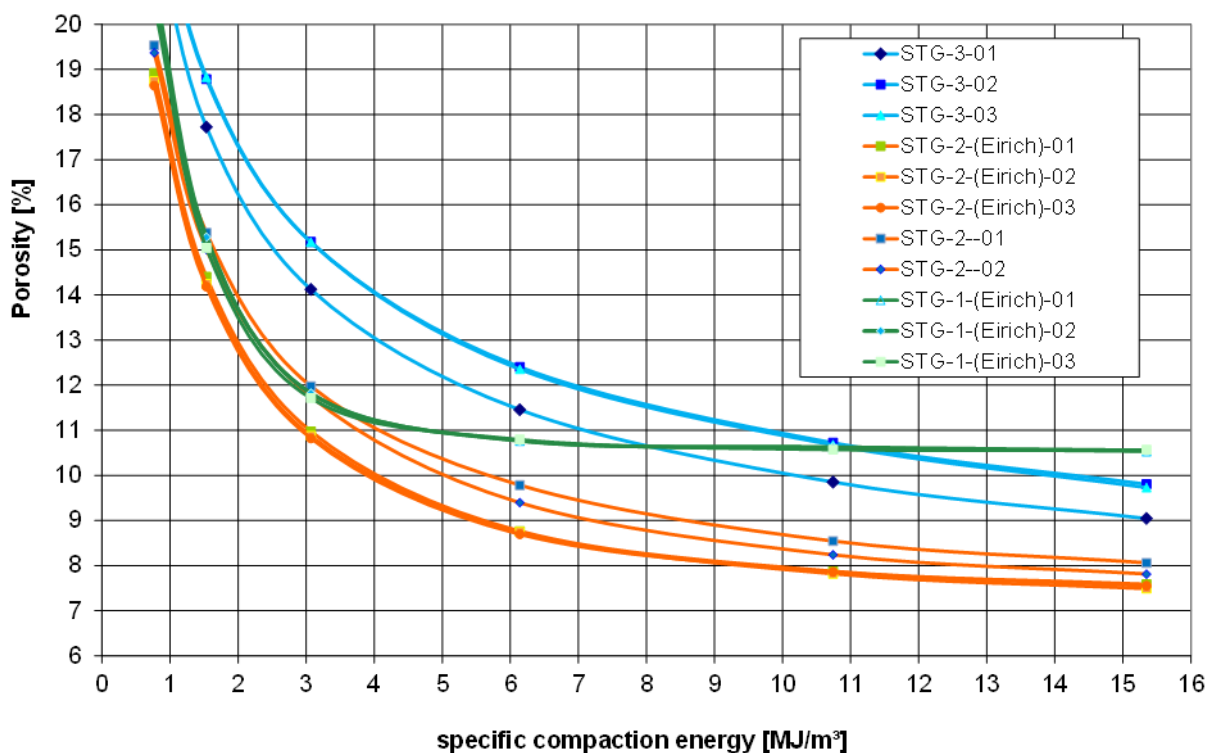


Figure 2-2: Achieved total porosity based the introduced engery for the three diffrent mixtures (Kudla et al., 2021)

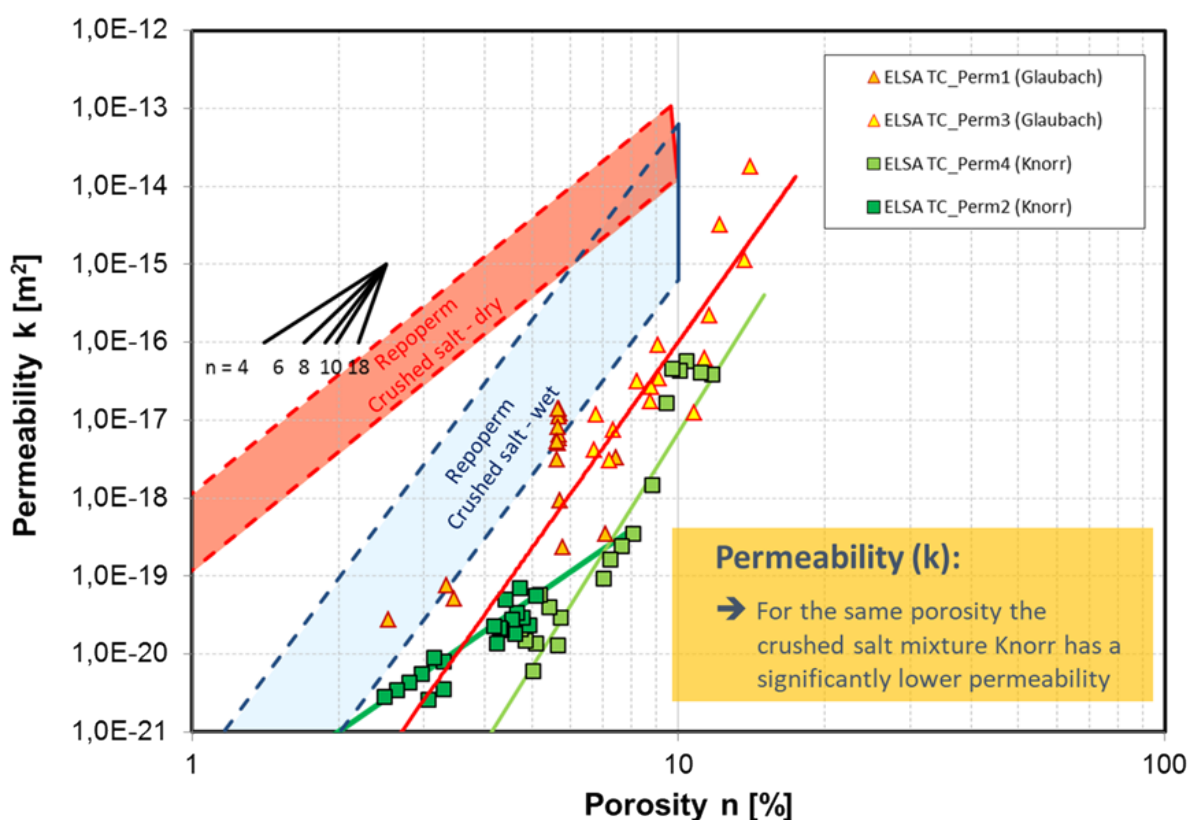


Figure 2-3: Achieved brine permeability as a function of porosity in comparisn to other mixtures and projects (Kudla et al., 2021)

The three different mixtures in combination with potential installation methods were tested in different half-scale in situ tests. The first test focuses on conventional compaction by vibrator

plates and vibratory trench rollers. The tests were performed underground in the Sondershausen salt mine.

During the tests it turned out that the mixer used was not suitable to produce a homogeneous mixture. Adhesions and partial segregations occurred during emptying. In addition, the average water content of 2.93 mass-% in the mix was too low, so that optimum compaction was not possible for this reason either.

With the STG-2 (OBSM) mixture, a porosity between 17% and 18% was achieved when paving in layers with layer thicknesses of approximately 10 cm. Due to the depth effect of the compaction equipment, the individual layers were compacted several times.

The n STG-1 (EBSM) mixture was only tested in the upper 2 layers of second test field, whereby a porosity of approximately 14% was achieved. As the two uppermost layers did not experience the same amount of accumulated compaction as the lower layers, this porosity should be viewed conservatively.

In both test fields, it was deduced that a light vibratory plate with an operating weight of less than 200 kg is optimal for pre-compaction of the loosely placed salt-crushed clay mixture. By driving over the compaction area in a spiral, an optimum compaction result for light pre-compaction is achieved after only 2 passes. Subsequent compaction should be carried out in a further pass using a heavy vibratory plate with a minimum of 600 kg and an adjustable amplitude. Here, too, 2 spiral passes are sufficient to achieve an optimum compaction result. At the first pass, the amplitude should first be lowered to a minimum level and only at the second pass can the amplitude be increased to the maximum level. However, a porosity < 10% in the newly developed salt-clay mixtures cannot be achieved with conventional compaction technology used in road construction. Therefore, an impulse compaction was tested additionally. A corresponding device is shown in Figure 2-4.

"The principle of impulse compaction consists of dropping a weight of up to 9 metric tonnes with a high frequency from a defined height repeatedly on to a steel plate, the so called "Compactor foot". The plate remains in constant contact with the to be compacted ground, thus ensuring an efficient energy transfer. In this way the sub-soil is locally compacted by every impact. The thus formed crater is filled in with suitable material and in turn compacted by the impulse compactor. In this manner an additional homogenisation of the sub-soil takes place." (Terramix, 2020)

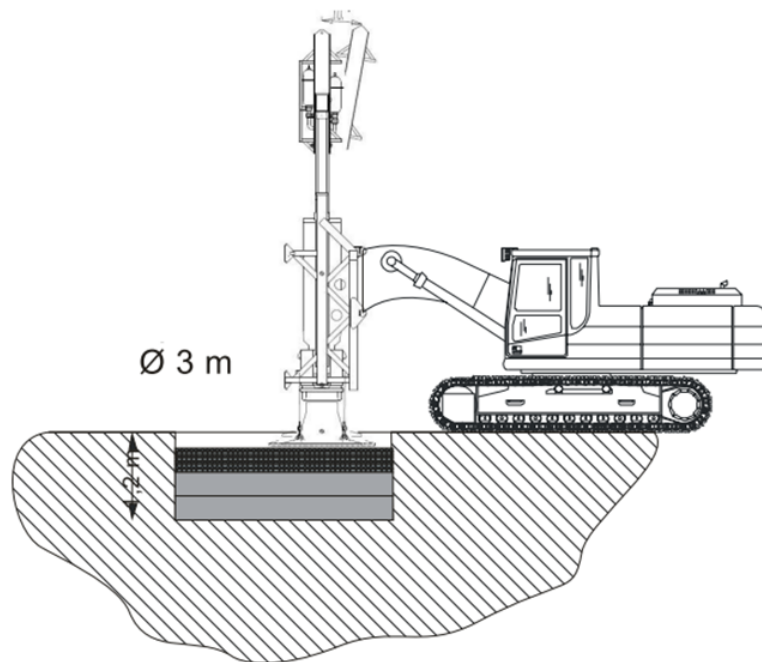


Figure 2-4: General design of the impulse compaction device and the in situ test (Kulda et al., 2020)

After a first preliminary test and core sampling, two in situ experiments were performed at an open pit mine. Due to the large dimensions of the impulse compaction device, it was not possible to perform the experiments in the underground. The test field was designed as a circular pit 3 m in diameter and 1.2 m in depth. The pit edge was lined by a steel wall that was backfilled with concrete and anchored in the surrounding rock as well. Within the first test all three mixtures were used.

The lower layer consisted of recipe STG-2 (OBSM), the middle layer of recipe STG-3 (mOBSM) and the upper layer of recipe STG-1 (EBSM). Each layer consisted of 8 individual installation layers. The average dumping height of each layer was 0.07 m. After spreading or before compacting, a horizontal surface was created by levelling with a straight edge and a spirit level.

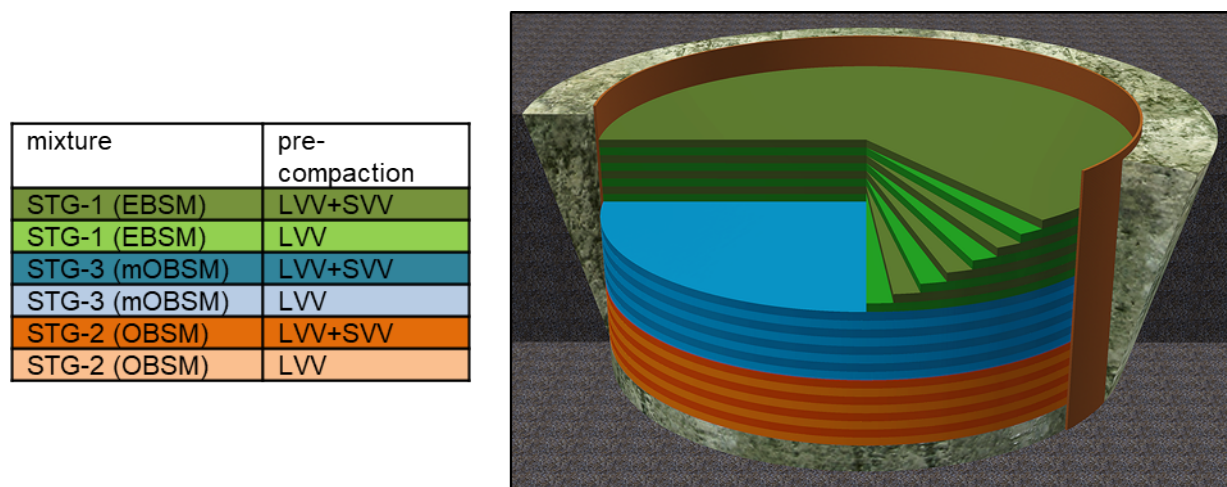


Figure 2-5. Illustration of the different mixtures in layers with the colour code the pre-compaction process in layers (right) and colour code of the pre-compaction (left) (Kudla et al., 2021)

Each layer was compacted conventionally by light pre-compaction and every second layer by heavy pre-compaction. After light and heavy pre-compaction, the 8th installation layer, and thus each layer, was finally compacted using impulse compaction. Compaction was carried out in a spiral in 2 passes from the outside to the inside. The use of the light vibratory plate has proved to be successful. The handling of the heavy vibratory plate was comparatively complex due to the limited space in the die. However, the circular geometry made it possible to compact the material flush with the edges without any problems.

The target for impulse compaction was to introduce a specific compaction energy of 15 MJ/m^3 into each individual layer. The specific compaction energy is only related to the volume of the solid content in the building material. This volume of solid matter was 2.17 m^3 in each of the 3 layers. As a result, an absolute compaction energy of 32.5 MJ had to be introduced into each layer.

To introduce the required compaction energy into the layer surface as evenly as possible, the impulse compaction was divided into 4 passes (IPV1 to IPV4). Furthermore, the compaction energy was increased in a defined manner during the 4 passes to avoid the formation of deep depression funnels, especially in the first pass IPV1. In the first pass 9.1%, in the second pass 16.5%, in the third pass 24.8% and in the fourth pass 49.6% of the total compression energy of 32.5 MJ was introduced. The variation of the compaction energy was achieved by increasing the height of fall of the drop weight, starting at 30 cm in the first pass IPV1, 40 cm in the second pass IPV2, 60 cm in the third pass IPV3 and finally 120 cm in the fourth pass IPV4.



Figure 2-6: Pictures from the test field surface after impulse compaction at the first layer and in all four compaction points (Kudla et al., 2021)

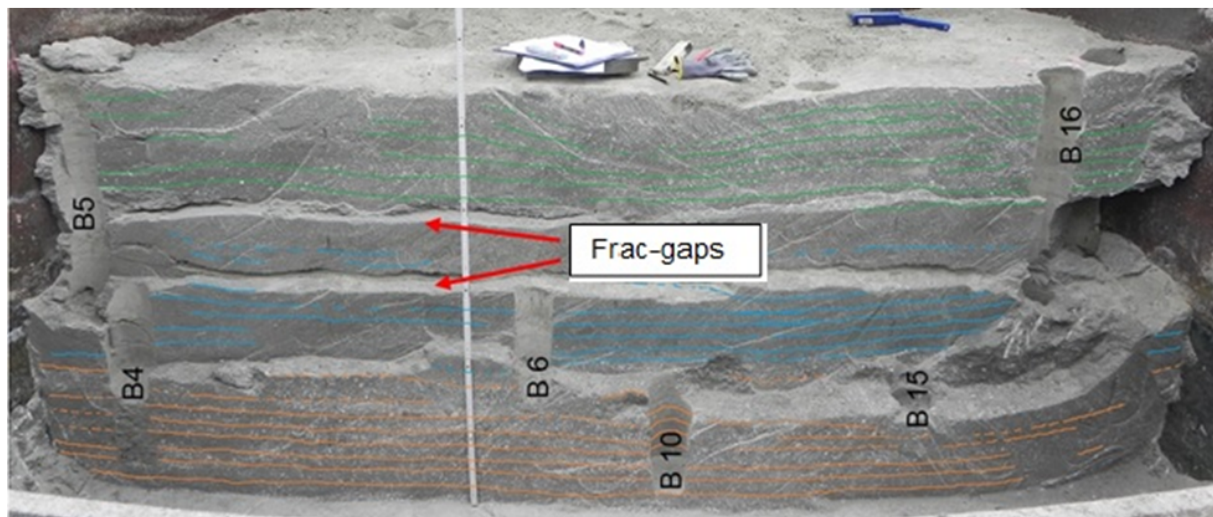


Figure 2-7: Post-test investigation of the compacted material (Kudla et al., 2021)

Afterwards the compacted soil was sampled with 22 drillings. Based on the data obtained, vertical and horizontal sections of the distribution of the total porosity with its distribution were made. Figure 2-8 shows the distribution of total porosity in the vertical sections at angles of 0°, 45°, 90° and 135°. In addition, the layer boundaries determined at the core marshes are shown as red lines.

The formulation STG-2 (OBSM), which was installed in the lowest (1st) layer, showed a uniform distribution of porosity in the range between 7.2% and 10.5%. The formulation STG-3 (mOBSM), which was incorporated in the middle (2nd) layer, also showed a relatively homogeneous distribution of porosity in the range between 9.2% and 12.4%. In both layers it is clearly visible that the lowest porosity tended to occur in the lower area and the highest porosity in the upper area of the layers. The same applies to the top (3rd) layer with the formulation STG-1 (EBSM). However, this showed a significantly more inhomogeneous distribution of porosity between 10.9% and 15.9%. This may be because the last (upper) layer was not post-compacted by a layer above it.

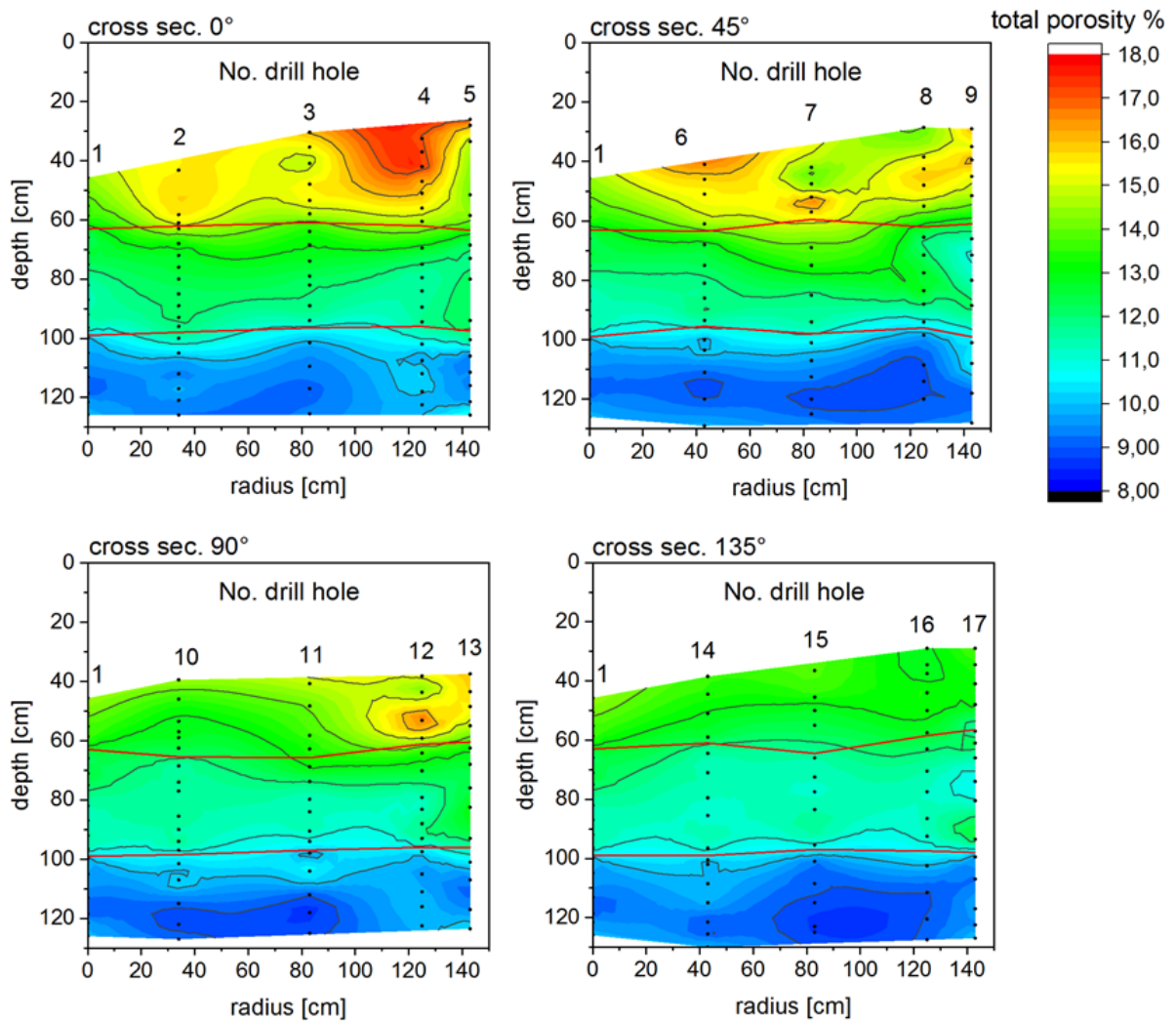


Figure 2-8: Achieved total porosity in four different cross sections of the first in situ test (Kudla et al., 2021)

The second die test was performed at the same site and in the same general operation mode. STG-2 mixture was used exclusively as this formulation has so far achieved the lowest porosities. Furthermore, a new compaction foot with optimized geometry and with counterweights (weight plates) was tested on the impulse compressor. The counterweights are intended to reduce the loosening and bulging of the near areas around the compressor foot, which was detected in the first test. The compaction scheme was adjusted as well so that the compaction energy is distributed more evenly over the surface.

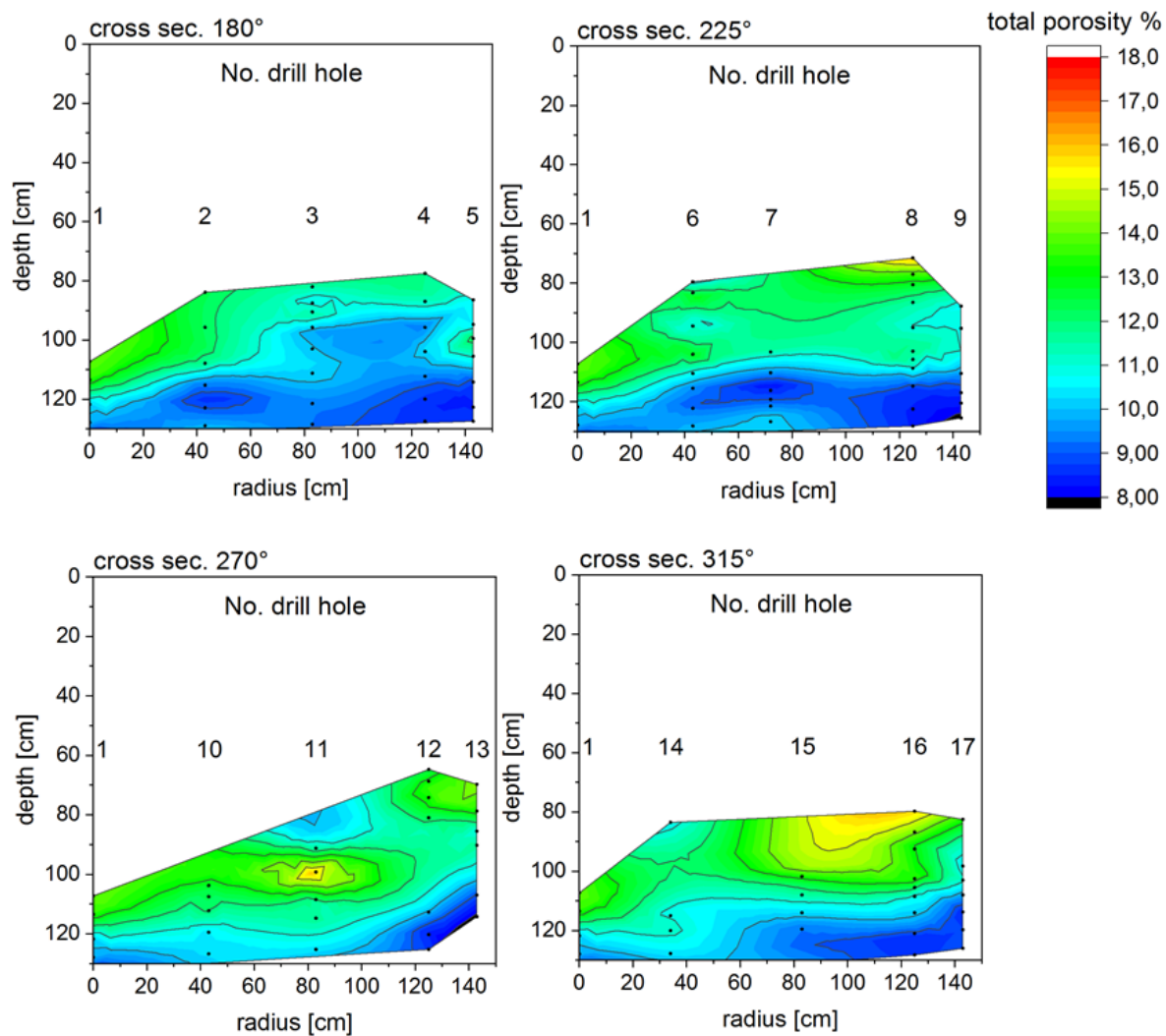


Figure 2-9: Achieved total porosity in four different cross sections of the second in situ test (Kudla et al., 2021)

The integral porosity is shown in Table 2-2-2. In comparison with the first test, the compaction result was improved.

Table 2-2: Comparison of total porosity in two test setups (Kudla et al., 2021)

Treatment	1 st in situ test "STV-3"	2 nd in situ test "STV-4"
Total porosity in the first layer after precompaction	0.1915	0.1965
Total porosity in the first layer after impulse compaction	0.1221	0.1088
Total porosity in the second layer after impulse compaction (Integral for first and second layer)	0.1318*	0.1090

The following conclusions are derived from the performed laboratory and in situ tests:

- Very high specific compaction energies were introduced by impulse compaction. Under the conditions of the swage tests, a porosity of < 10% was reliably achieved. However, it was not possible under the given technical conditions to introduce a specific compaction energy $> 8 \text{ MJ/m}^3$ without secondary negative effects (re-loosening in the edge area) in a meaningful way. With high intensity (many blows at the same position), it is possible that the edge area may be loosened up again. In a future application this point must be recognized. Alternatively, the machine must be moved more often, but this increases the compaction time and the amount of work enormously.
- The results of the laboratory tests in the Marshall device can be a benchmark for the porosity that can be achieved in situ. A transferability of the laboratory results to the in situ conditions is well possible. However, in situ the same density as in laboratory tests is only achieved under favorable conditions. For a conservative evaluation, it should be assumed that the density achievable in situ is approximately 97% of the density determined in the Marshall device, with the same specific compaction energy introduced.
- Under the given conditions, with the tested formulation STG-2 (OBSM) the input of a specific compaction energy of up to 7.54 MJ/m^3 is sufficient. Under these conditions a porosity of approximately 9% can be safely achieved. At a higher specific energy of compaction, no further improvement takes place.
- Although the use of the present compaction unit (without excavator) with technical adjustments for guiding the compaction unit in a shaft is quite conceivable, it is recommended for future use in the shaft to reduce the drop weight to approximately 2 t and to increase the drop height to approximately 1.5 to 2 m in compensation. According to verbal information from the company TerraMix, this would allow the compaction unit to be attached to a more compact mobile unit with hydraulic power unit. Such a unit could be built from existing assemblies according to the modular principle. As this would require further financial expenditure, which was not part of the present R&D project, no new compaction unit was developed.
- In case of practical implementation, the composition of the salt-clay mixture (clay content, water addition) may have to be adapted to the quality of the available salt-clay (grain band, grain shape) and the achievable compaction energy with the existing compaction equipment. Accompanying laboratory tests are to be carried out in the Marshall device.

2.1.4 Cast in place concrete made of MgO-concrete

Within the frame of the R&D project 02E10880 (Freyer et al. 2015) a long-term stable MgO construction material with the 3-1-8 binder phase was developed. In addition to the long-term chemical resistance to MgCl₂-containing solutions, the expansion behavior, and the time-dependent deformation behavior (relaxation behavior) was the focus of the investigations.

Table 2-3: Composition of the MgO-cast-in-place-concrete C3 (Freyer et al. 2015)

Component	Mass Fractions
MgO (medium reactivity)	0.0675
Quartz powder (M300)	0.2151
Aggregates (0-8 mm)	0.5591
MgCl ₂ -solution (5 molar)	0.1583

Within the ELSA phase 2 project laboratory tests were carried out with the MgO concrete of formula C3 (3-1-8 binder phase) with the aim of replacing the quartz powder used in this formula with another material. In the MgO-concrete mixture C3, quartz flour is used as an inert flour grain to achieve the sedimentation stability of the binder suspension. Without the addition of quartz flour, this concrete recipe is too liquid due to the high solution content and tends to bleed. In the original recipe, the addition of quartz flour is 2 kg per kg MgO. However, since quartz flour will be problematic in the future for large-scale underground use (dust pollution), an alternative flour grain additive is to be found. Further investigations have shown that a sedimentation-stable binder suspension can be achieved by adding finely ground salt in the quantity of 2 kg per kg MgO. Thus, in the C3N formulation, the quartz flour can be replaced by ground fine salt. The ratio of aggregate to binder suspension is adjusted to the desired consistency (spread). The optimized concrete mix C3N was used for concreting the second large borehole test. It is estimated, however, that the production of ground fine salt is very costly and will not be a practical and economical option.

The second large scale borehole test was accompanied by a mechanical, hydraulic, and mineralogical test program. Mean values of the cylinder compressive strength of the sampled batches are 37.7 MPa, 23.6 MPa, 39.9 MPa, and 40.9 MPa. The average values of the splitting tensile strength of the sampled batches of the main concrete are 3.47 MPa, 2.46 MPa, 1.99 MPa, 2.54 MPa, 2.25 MPa, and 2.39 MPa. The average ratio between the compressive strength and the splitting tensile strength is also different depending on the batch and varies between 10.9 and 17.7. As a result of additional strength tests with the restitution samples from the concreting, considerable differences in strength have also been found, but these are all in the range of the values known to date for the MgO building material C3 (Figure 13).

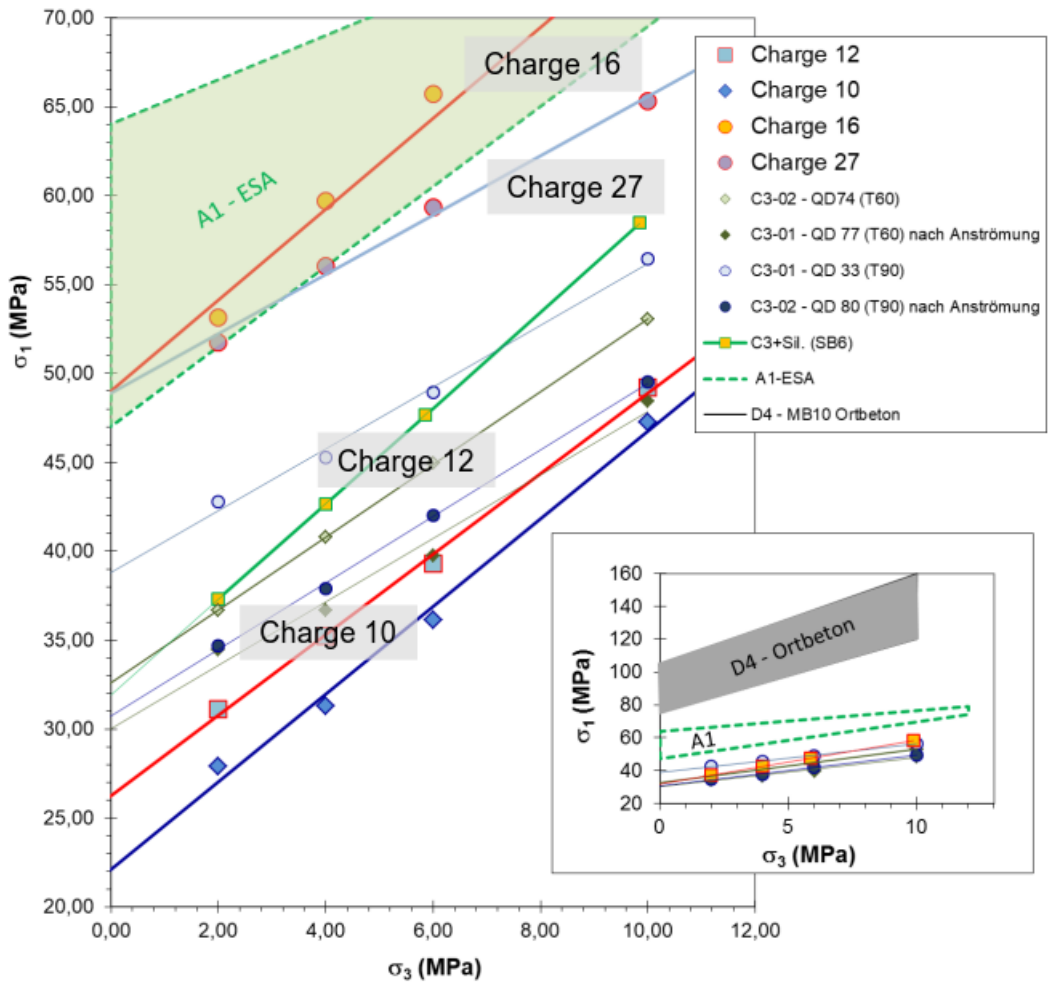


Figure 2-10: Strength of retained samples from the cast-in-place-concrete C3 (Kudla et al., 2021)

The phase development was reproduced in the laboratory on samples in the climatic chamber, whereby the same temperature curve was simulated in the climatic chamber as was measured in the large borehole test. Two typical temperature-time windows (TZF) were simulated: TZF-1 with a maximum temperature of 70 °C (TZF70) and TZF-2 with a maximum temperature of 40 °C (TZF40). The phase inventory of the temperature-time window 70 °C (typical for core) and 40 °C (typical for edge area to the rock salt contour) develops as follows: At the setting temperature 70 °C and subsequent cooling, the 3-1-8 binder phase is already detectable after 14 days. The primarily formed 5-1-8 binder phase is still present after 173 days. At the setting temperature of 40 °C and subsequent cooling, the 3-1-8 binder phase is clearly detectable after 9 days. The primarily formed 5-1-8 binder phase is still present after 183 days. In the following time, the proportion of the 5-1-8 binder phase formed primarily decreases further in both cases and the proportion of the 3-1-8 binder phase increases further. In the accompanying laboratory tests, lower expansion pressures are measured than after the same service life in the in-situ large borehole test (here approximately 5 MPa at the same time). The formation of the 3-1-8 binder phase is overlapped by the processes of thermal expansion/contraction in the initial phase, pore space formation through solution consumption from suspension and solidifying structure due to the formation of the 3-1-8 phase, crystallization of the 3-1-8 phase with degradation of the 5-1-8 phase and MgO as well as structural relaxation.

2.1.4.1 First large-scale test

The MgO-concrete mixture as developed in Freyer et al. (2015) was tested the very first time in situ at the Sondershausen salt mine. A borehole of 1.0 m in diameter and 2.0 m in depth was constructed. Focus of the related measuring program was the development of the temperature during hydration and the development of the expansion pressure inside MgO concrete. The main interest was the contact pressure developing at the rock contour to the rock salt. Based on the results of Freyer et al. (2015) the question arises how the contact pressure or expansion pressure developing from the crystallization of the 3-1-8 binder phase in a larger structure develops over time. Based on laboratory experiments (Freyer et al., 2015) it was assumed that the expansion pressure decreases again after some time after a maximum. A resulting question was also how high a residual expansion pressure is or whether the expansion pressure approaches zero pressure, used in conservative assumptions. To verify the pressure data, concrete stress sensors were installed near the pressure transducers. Under this condition of exact measurement of a falling or rather low pressure, plate pressure sensors with a measuring range up to 20 bar were selected. However, as can be seen below, this decision led to a loss of information in the pressure measurement of the present large borehole test.

Figure 2-11 shows the measured pressure curve. Experience shows that an immediate primary pressure development is caused by temperature development (thermal expansion with limited volume). As the concrete cools, a re-expansion takes place, which leads to a decrease in the restraint state (pressure). After approximately 4.5 to 5 days, a secondary pressure development was observed in the present experiment. Since the concrete has already cooled down to a large extent, this is a pressure development caused by reactions in the concrete that result in changes in volume.

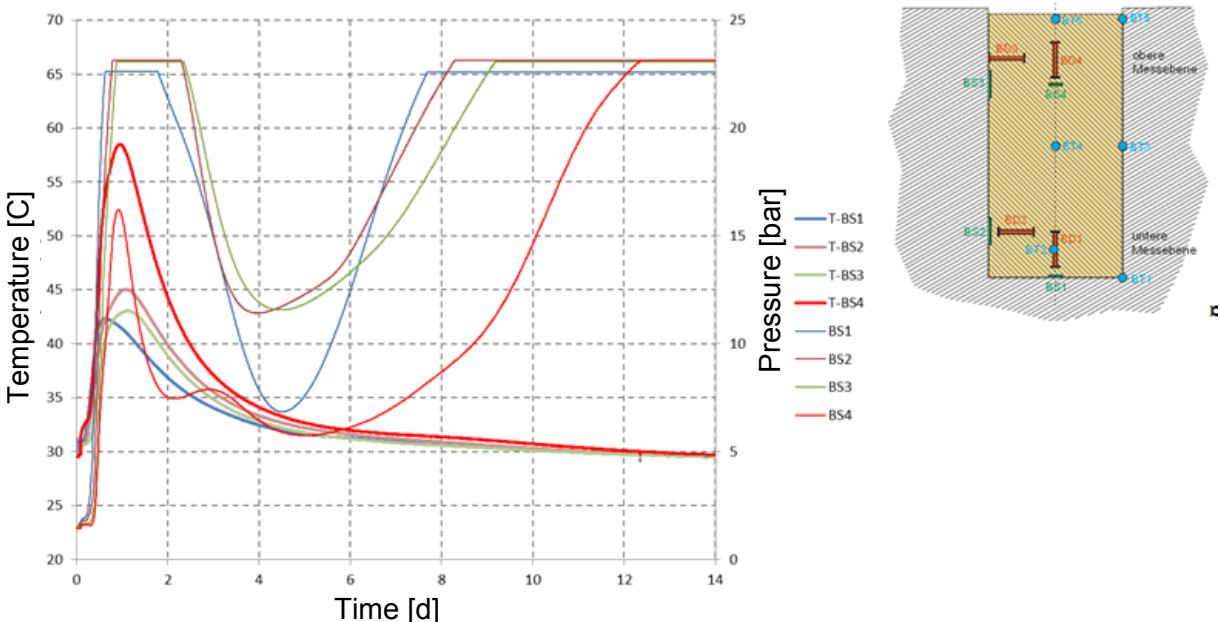


Figure 2-11: Measured pressures and temperatures in MgO concrete in the first 14 days - BS2 and BS3 as contact pressures, BS1 and BS4 as axial pressures (Kudla et al., 2021)

The developing pressures were outside the measuring range at > 22 bar for the reasons already mentioned above (selection of the measuring sensors). Therefore, no information is available about the maximum level of the expansion pressures and the further course over time. The pressure development measured at the beginning is in accordance with the previously known curves from laboratory investigations (Freyer et al., 2015) and is caused by the phase transformation (transformation of the primarily formed 5-1-8 phase with remaining pore solution into the stable 3-1-8 phase) in MgO concrete C3. This process takes place with an increase in volume, which leads to the formation of an expansion pressure under the existing boundary conditions (restraint in the rock).

2.1.4.2 Second large-scale test

The second in situ large scale borehole test with the MgO concrete C3 was initiated to close the knowledge gap regarding the temporal course of the expansion pressure and the radial contact pressure to the rock salt contour. The test setup was increased and accompanying laboratory tests on the expansion pressure development of the MgO concrete C3 in the same temperature-time window as in the large borehole test were performed, as described previously. A measurement of the permeability of the entire system with gas and brine was performed.

These requirements were implemented by selecting plate pressure transducers with a measuring range of up to 100 bar for the pressure measurements, increasing the length and diameter of the structure compared to the first large borehole test and installing a pressure chamber with an access borehole at the bottom of the structure. A pumping station was installed for the subsequent pressurization of the liquid over a longer test period.

After the cavity contour had been excavated and the pressure chamber had been accurately drilled, the pressure chamber construction was installed. Then the lower section was concreted, and the transducers were installed. The large bore hole was then concreted in two sections with MgO concrete C3. The concreting in two sections was necessary to enable the installation of the transducers. Figure 2-12 shows the test setup and the location of the installed sensors. Resulting pressures during the subsequent large borehole test no. 2 are shown in Figure 2-13.

Because of the expected very low permeability of the system uncertainties in the calculation of the permeability have a significant impact on the result. A defined-volume pressure chamber was installed to reduce uncertainties. Instead of using a porous soil (e.g., gravel), a steel construction was installed which allows a very accurate determination of the volume.

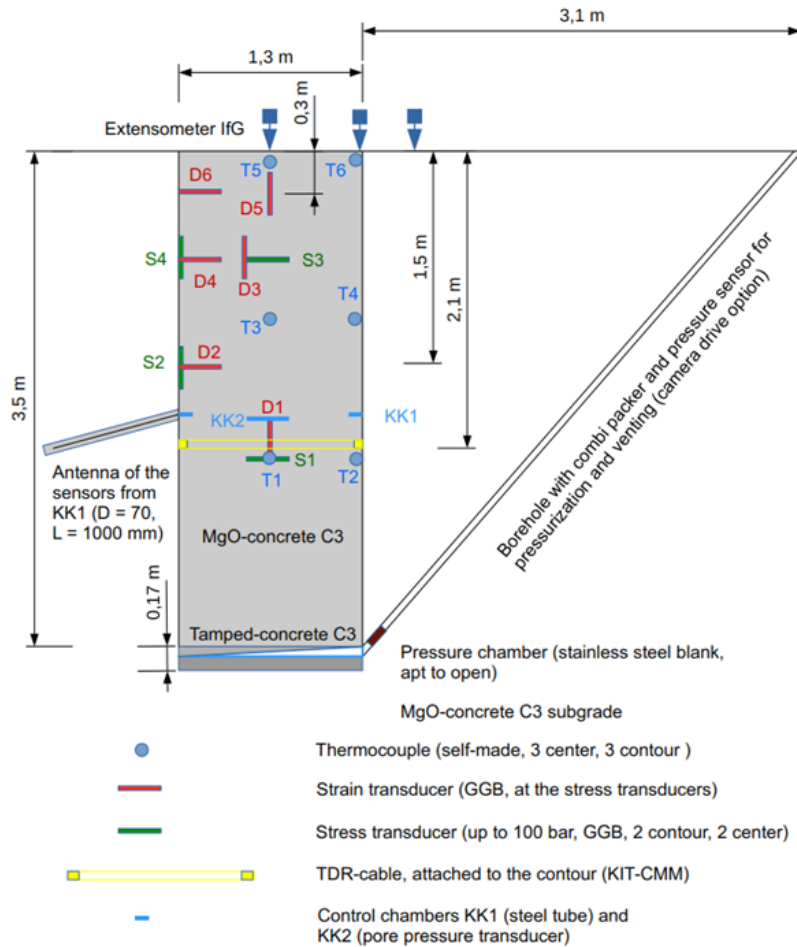


Figure 2-12: Test setup for the second in situ test (Kudla et al., 2021)

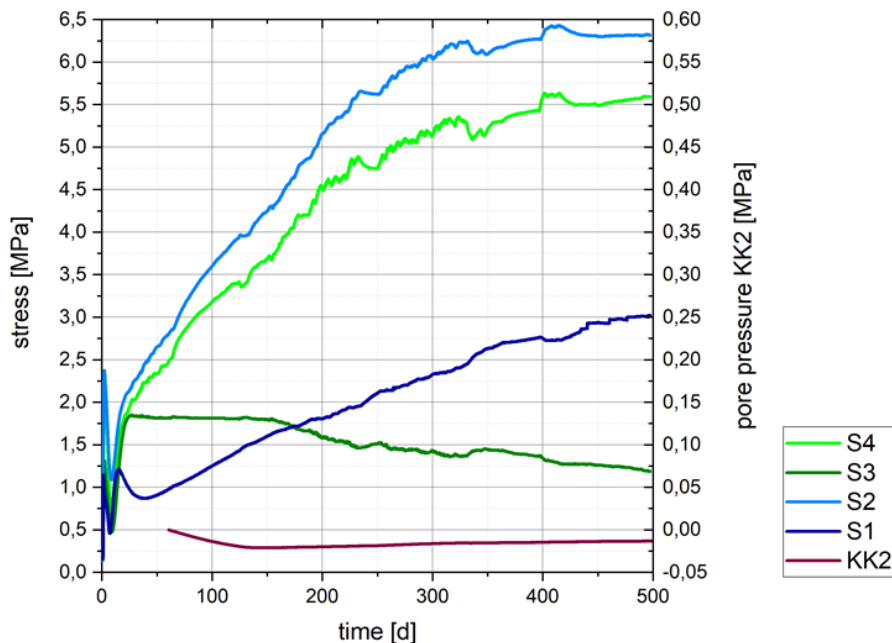


Figure 2-13: Radial (S2, S4) and axial (S1, S3) pressure and pore pressure in the control chamber 2 during the large borehole test 2 (Kudla et al., 2021)

2.1.5 Asphalt and bitumen sealings

Within phase 2 of the ELSA project three different types of bitumen based sealing elements were investigated:

- bitumen based sealing elements based on the principle "Hard shell – soft core" (Kudla et al., 2009)
- bitumen with inorganic filler (e.g., silica flour)
- bitumen filled gravel columns
- dense stone asphalt, in the style of Schönian (1999) and Van de Velde et al. (1985)

Basic questions regarding the material parameters of the used bitumen have already been investigated in earlier projects (Kudla et al., 2009). During ELSA phase 2 further laboratory tests were carried out to verify the input data for modelling (AP5) and in situ borehole tests with the three named sealing types were performed.

2.1.5.1 Bitumen filled gravel columns

A bitumen filled gravel column represents a combined abutment and sealing element was developed within the framework of the performance assessment of the Morsleben repository ERAM (Rauche et al., 2003; Rauche et al., 2004).

The pore space of a low-settling backfill column, made of gravel, is hot grouted in sections with bitumen or filled bitumen (asphalt). Pure or filled bitumen abutment sealing elements can be used against liquid ingress in either direction (i.e., with or against gravity).

The installation of a gravel column filled with bitumen is divided into two installation steps. At first the gravel is installed in layers and compacted. In a second step the bitumen is grouted into the pore space of the gravel. The installation technology for a gravel column filled with bitumen has been investigated and optimized by the TU Bergakademie Freiberg (Glaubach et al. 2013).

The basic requirements for the functionality of a bitumen-filled ballast column are a low-settling gravel framework and a sufficiently void-free grouting of the gravel pore space with bitumen. The last aspect in particular demanding in terms of implementation. As the gravel is always at ambient temperature, the hot bitumen cools down quickly during grouting. The resulting disproportionately increasing viscosity of the bitumen leads to a rapid stagnation of the grouting process. Following criteria were formulated to be in line with the basic requirements:

1. limitation of the moisture content of the gravel to 0.5 mass-%
2. limiting the dust content of the gravel to 0.5 mass-%
3. limiting the thickness of the gravel layer to be grouted to 0.6 m
4. if possible, continuous grouting of the bitumen with a density of the grouting points (EGP) on the gravel surface of at least 0.7 points per square meter
5. grouting of the bitumen as hot as possible with minimum 170 °C
6. volume flow of the bitumen at the grouting points of maximum 2 liters per second
7. a void content of the gravel column filled with bitumen of less than 3%

2.1.5.2 Dense stone asphalts

The installation process of bitumen filled gravel columns is connected to a high effort and several criteria as named before. As an alternative, simpler in installation, ready-to-install mixtures of filled bitumen (asphalt mastic) and a coarse grain size have been known in hydraulic engineering for a long time by the name "dense stone asphalt" (Schönian, 1999; Van de Velde et al., 1985) and were mainly used in Dutch coastal protection.

Dense stone asphalts are emplaced directly by free-fall, do not need to be compacted and are waterproof (void contents < 3%) due to the high bitumen content (saturation of the stone interstitial spaces) (Schönian, 1999). Based on these properties a dense stone asphalt is therefore very interesting for an abutment and sealing element made of bitumen and crushed stone. Within the scope of the ELSA phase 2 project, it is to be developed and investigated for underground use in shaft sealing.

A rounded-edge round-grain gravel has proven to be comparatively well compactable, low-settling, and stable against grain breakage under loads. Therefore, the suitability of the round-grain gravel for a low-settling grain structure for a dense stone asphalt is very promising compared to a ballast column filled with bitumen. Furthermore, the proportion of bitumen or filled bitumen in the mixture must be such that the pore space between the gravel grains stored in bulk density is nearly filled. The optimum proportion of bitumen or filled bitumen is therefore largely dependent on the storage density respectively porosity of the gravel. The proportion of bitumen in the mix is optimal when the bitumen level after installation is slightly below the upper edge (about half the maximum grain diameter) of the gravel. The exposed gravel grains allow low-settling grain to grain interlocking between the adjacent paving sections. For the practical application it seems to make sense to use bitumen with a somewhat too low content and, if necessary, to add bitumen or filled bitumen locally.

2.1.5.3 "Hard shell – soft core"

Bitumen based sealing elements designed against fluid attack from below must have a lower density than the attacking fluid. Therefore, only pure bitumen can be used here. A combination of a soft and a hard bitumen is recommended. Soft bitumens have a very good wetting capacity and, due to their more pronounced liquid character, are also better able to react to relatively rapid and short-term pressure changes. Hard bitumen reacts significantly more "sluggishly" to pressure changes, which also makes them more stable in place, in the long term. According to the "hard shell - soft core" idea, a bitumen seal should be constructed as presented in Figure 2-14. The design combines the useful properties of both types of bitumen. The combined use of distillation and oxidation bitumen does not represent a problem, as the two kinds of bitumen differ only in their colloidal composition. (Kudla et al., 2009)

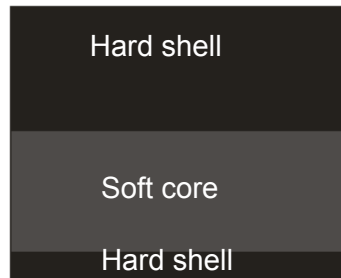


Figure 2-14: Schematic illustration of the construction "Hard shell – soft core", destillation bitumen (gray) covered by two layers of oxidation bitumen (black) (Kudla et al., 2009)

Within the frame of the ELSA phase 2 project different borehole tests in rock salt and clay were performed. The rock salt tests were performed in the underground at the Sondershausen mine, in parallel to the compaction tests of salt-clay mixtures. For salt four borehole were drilled. In two boreholes with a diameter of 0.3 meters the "Hard shell – soft core" system was tested. In two additional drillings with a diameter of 0.5 m the system of bitumen filled gravel column and dense stone asphalt were tested. Figure 2-15 and Figure 2-16 show the principal design of the test sealings installed in the boreholes.

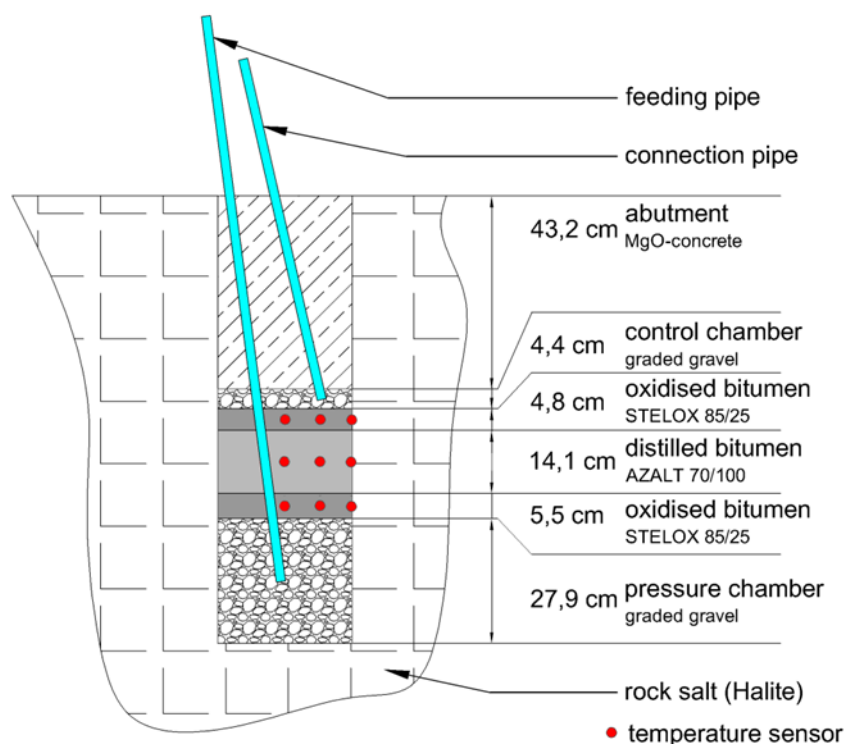


Figure 2-15: Design of the sealing system "Hard shell – soft core" as installed for the borehole test (Kudla et al., 2021)

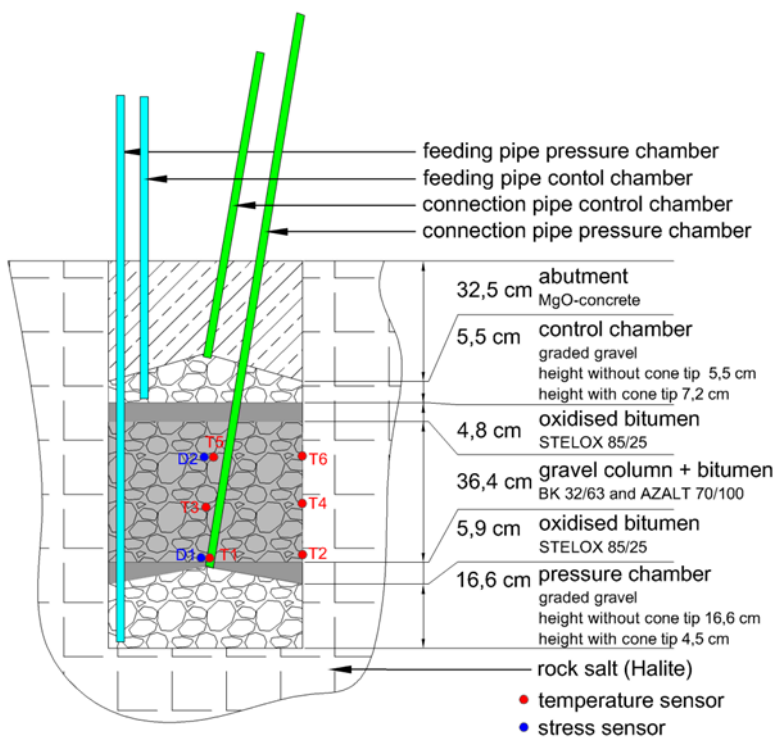


Figure 2-16: Internal design as installed for the borehole tests bitumen filled gravel column and dense stone asphalt (Kudla et al., 2021)

Small scale exploration drillings at the test side showed a gas permeability of the surrounded rock between $1 \cdot 10^{-22}$ and $5 \cdot 10^{-22}$ m². After the successful installation of all borehole sealings gas tests were performed. One of the boreholes with bitumen-filled gravel column and the borehole sealed with the dense stone asphalt were also tested with brine. The experiments showed integral (gas) permeability between $1 \cdot 10^{-20}$ and $3 \cdot 10^{-21}$ m². The liquid permeability for both tests was between $2 \cdot 10^{-20}$ and $6 \cdot 10^{-21}$ m². In none of the tests was a measurable flow around the sealing elements detected. The integral permeability of the systems seems to be driven by the EDZ around the drillings.

Finally, one of the smaller boreholes was overcored, de-constructed, and analyzed. To investigate how far the "soft core", the distillation bitumen, has penetrated the rock salt, thin sections were prepared from the removed salt, see Figure 2-17. Figure 2-18 shows two images of the thin sections taken with the transmitted light scanner. The edge of the bore hole, i.e., the contact with the bitumen, is on the left side of the images. The fine dark brown threads represent the penetrated bitumen. The black areas that can be observed deeper in the salt are faults, i.e., small air-filled cavities in the salt, which appear black in the image. The bitumen has penetrated fine cracks in the rock salt up to a maximum of 0.5 cm.

Figure 2-19 shows enlarged microscope images from the area near the borehole edge. The orientation of the fine cracks and thus also the penetration of the bitumen is usually radial, which is also to be expected due to the relaxation in the axial direction. Axial cracks only occur very locally. The bitumen fills the fine cracks very well.

Under higher resolution the flow of bitumen can be observed up to very fine cracks. It is even sufficient to fill subsequent larger cavities, see Figure 2-20. However, it appears the bitumen was not able to penetrate all the way into the last cavities. Small air-filled areas at the end of the cracks were not reached (see Figure 2-20). This may be because the pressure was no longer sufficient to push the bitumen further in. An estimate of the crack width showed that the bitumen was able to penetrate cracks up to a width of about 20 μm .



Figure 2-17: Image of sample from the borehole edge after removal of the test (Kudla et al., 2021)

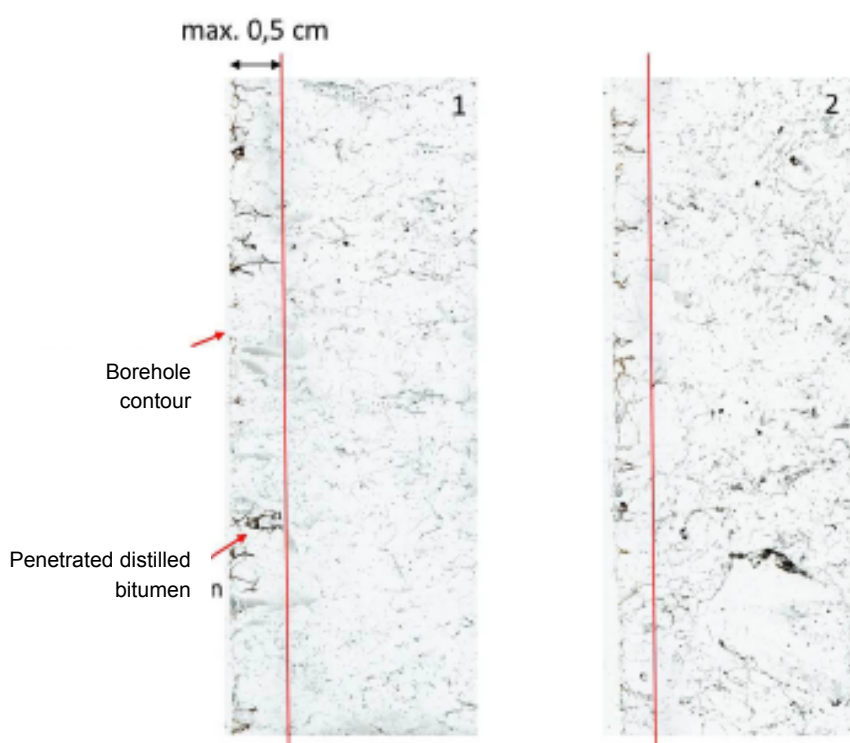


Figure 2-18: Thin sections showing penetration of the bitumen into the EDZ (Kudla et al., 2021)

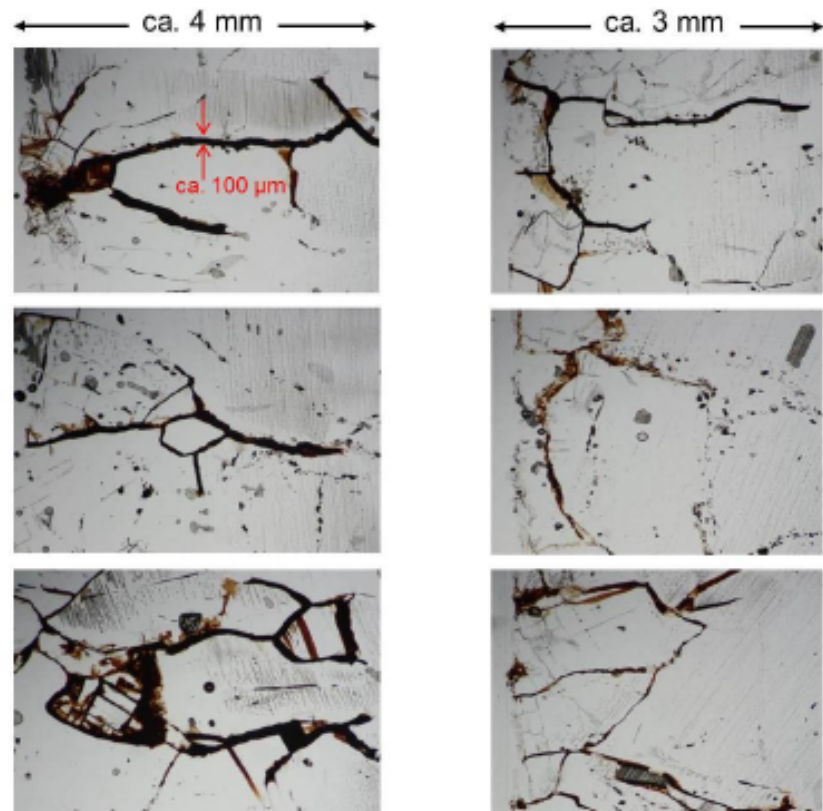


Figure 2-19: Images from the bitumen-filled cracks inside the EDZ (Kudla et al., 2021)

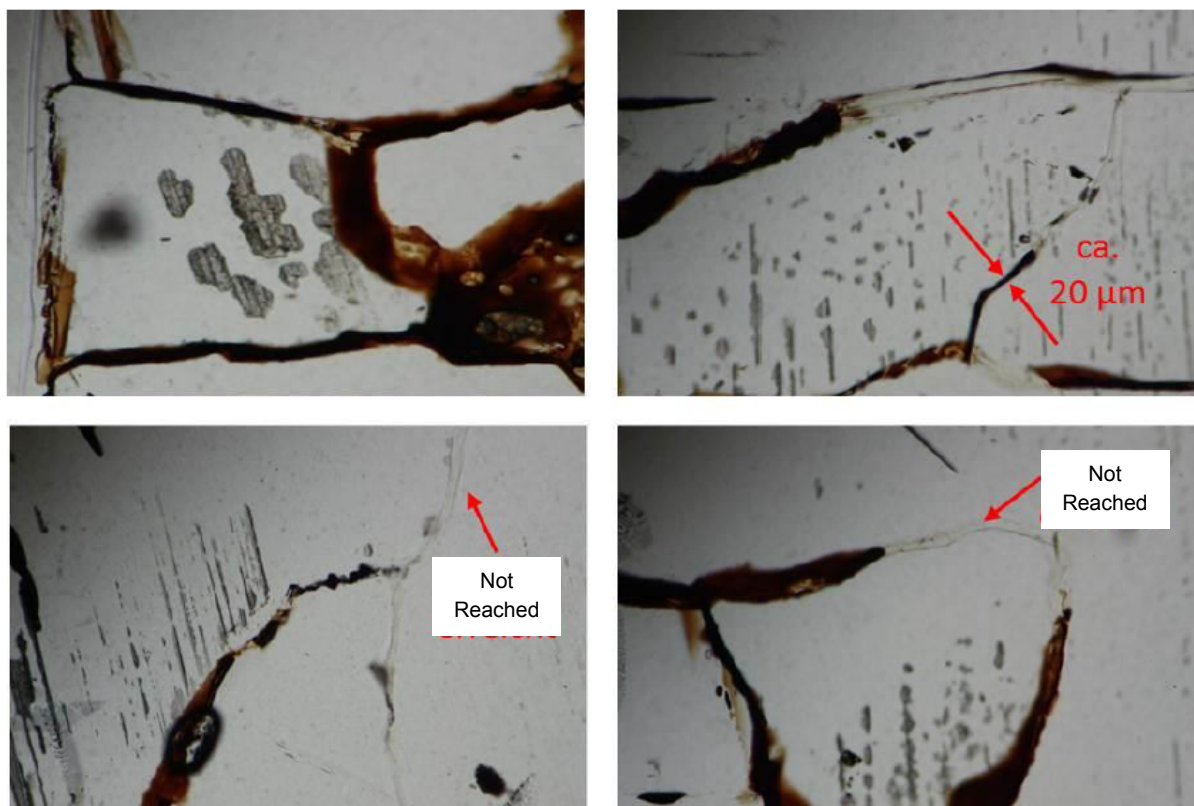


Figure 2-20: Images from the bitumen-filled cracks inside the EDZ, local and enhanced (Kudla et al., 2021)

2.2 Preliminary safety analysis for the Gorleben site - VSG

From 2011 to 2013, a working group of 11 institutions under the lead of GRS dealt with a wide range of questions concerning the Gorleben site and fundamental methodological issues of final disposal in the research project "Preliminary Safety Analysis Gorleben" (VSG). The project was funded by the German Federal Ministry for the Environment (BMU) (GRS, 2013).

The main goals of the project were to examine whether the repository concepts developed in the VSG project in combination with the geological barrier at the Gorleben site or a site with a comparable geological situation appear suitable to meet the safety requirements of the Federal Ministry for the Environment. The project was supplemented by the question of which methodological approaches of the VSG can be used for a future site selection procedure and for the comparison of repository sites. Regardless of the detailed design of the site selection procedure, it will always be necessary in the process to systematically summarize and evaluate the state of knowledge on the individual sites achieved. In addition, it was to be investigated which of the technical concepts developed in the VSG for emplacement of the radioactive waste and for closure of the repository mine are transferable to repository systems at sites with other geological conditions (GRS, 2013).

The results were published across a total of 24 reports. Within the following sections, the aspects relevant to the RANGERS project will be summarized. More detailed or further information can be found in the corresponding reports, given as reference.

2.2.1 Safety concept

The safety concept developed within the VSG and as described in (Mönig et al., 2012) bases on the Safety Requirements governing the final disposal of heat-generating radioactive waste (BMU, 2010). The following paragraphs summarizes (Mönig et al., 2012). Other references are marked.

The safety concept followed three basic ideas:

- achieve confinement of the radioactive waste in a defined rock area around the waste
- confinement should become effective immediately after closure of the repository mine and be ensured by the repository system on a permanent basis and free of human care
- immediate and permanent confinement of radioactive waste in a defined rock area around the waste should be achieved primarily by preventing or at least severely limiting the access of solutions to the waste

The containment providing rock zone (CRZ), as part of the geological barrier, must guarantee the long-term and maintenance free containment and isolation of the radioactive waste. The most important criterion for this is the practical impermeability of this CRZ. To achieve this, the integrity of the geological barrier must be given by the properties of the rock salt especially inside the CRZ and the design of the repository and the other (geo-)technical barriers. In this regard the self-sealing capacity of the rock salt, given by the creep behavior is a significant mechanism.

Mining activities inside the geological barrier are unavoidable but always creates direct pathways between the biosphere and the emplaced waste. In addition, the geological barrier damaged or at least disturbed in areas close to the contour and its effect is thus local weaknesses. The visco-elastic or visco-plastic behavior of the salt rock leads with time, to the closure of the mining openings such as shafts and drifts as well as the damages and disturbances, whereby the salt rock regains its original barrier-effective properties. Afterwards, the reconsolidated barriers and rock can fulfill their long-term safety function. The time-dependent processes can be influenced by the implementation of additional technical barriers. Backfilling the drifts represents such a measure. The backfill material should have long-term and permanent hydraulic, thermo-mechanical and geo-mechanical properties as similar as possible to those of the natural, undisturbed rock salt.

To ensure long-term stability filling of the mine openings, the backfill material to be used should therefore be the crushed rock salt produced during excavation, and thus the same salt rock as the surrounding geological barrier. Due to the compaction of the crushed salt, the backfill will develop a sealing effect over time that is comparable to that of the surrounding undisturbed geological barrier. Depending on the rate of convergence, moisture content, and ambient temperature, the time required to reach this final state ranges from several tens to several thousands of years.

In principle, it is possible to backfill the mine openings with backfill materials that lead to an effective seal immediately after closure of the repository. According to the state of the art, however, backfill materials would have to be used that differ significantly in composition from the granular salt rock derived from the geological barrier. This potentially leads to interactions between the backfill and the host rock and allows doubts to the effectiveness of such alternative backfill materials in the long term.

To guarantee containment and isolation during the process of backfilling compaction and self-sealing of the rock salt additional barriers are needed, such as drift and shaft seals. Both allow an intermediate sealing capacity after installation. The used materials are affected by corrosion processes. Their long-term stability as well as the effective sealing capacity could be limited. Thus, the drift and shaft sealings must be sufficiently tight at least until the hydraulic resistance of the backfill material is large enough to prevent the penetration of solutions to the waste or to limit it to such an extent that the protection level according to the safety requirements is achieved. Material selection and technical design of the barriers allows this.

Within Monig et al. (2012), three basic requirements were formulated to deduce the needed strategic measures:

- a. The disposed waste packages should be enclosed as quickly and tight as possible by the rock salt in conjunction with the geotechnical barriers
- b. The designated CRZ remains intact during the assessment period and its barrier function (geological barrier and geotechnical barriers) is not impaired by either internal or external procedures and processes
- c. Criticality must be excluded for every stage of repository lifetime

2.2.2 Safety assessment concept

The following paragraphs summarizes Mönig et al. (2012). Other references are marked.

The safe confinement of radionuclides and other constituents of the radioactive waste during the post-closure phase inside the CRZ represents the starting point for all considerations regarding the safety assessment concept. Safe confinement is defined as the condition of the repository system in which there is a minor release of radionuclides from the CRZ during the assessment period. This approach is based on the requirements according to BMU (2010). The releases of radioactive substances from the repository must only marginally exceed the risks resulting from natural radiation exposure in the long term. At the same time, it must be shown that its integrity of the CRZ can be demonstrated for all probable development possibilities.

All work within the framework of the system analysis in the VSG project is derived from the assessment concept, which is finally combined in the synthesis to form an overall statement. The assessment concept covers:

- Procedure for designating the location and boundary of the CRZ
- Integrity of the CRT during the verification period as thickness of the salt barrier inside the CRZ, integrity of the geological barrier and integrity of the geotechnical barriers
- Exclusion of criticality
- Containment of the radionuclides inside the CRZ
- Radiological consequences for the biosphere based on the criteria defined in BMU (2010) for the release of radionuclides from the CRZ

To demonstrate the preservation of the CRZ during the assessment period, a long-term geological prognosis for the site is required to verify whether the salt rock areas that can be removed by geological processes always lie outside the boundaries of the CRZ. This process must consider the uncertainties regarding the processes and their characteristics. Essential geological processes are subrosion and erosion, glaciers, and glacial channeling as well as salt uplift.

The integrity of the geological barrier demonstrated based on the dilatancy criteria (the stress state must remain below the dilatancy limit) and the fluid pressure criteria (the minimum principal stress must be greater than the calculated hydrostatic pressure at the corresponding depth).

The design of the geotechnical barriers is carried out with numerical calculations in which coupled thermo-mechanical, hydraulic, and geochemical processes are considered and investigating crack resistance, geo-mechanical stability, durability (resistance to aging), integral permeability and probability of failure. Technical feasibility is demonstrated verbal and by existing technical analogy.

The multiplication factor k_{eff} , which indicates how many neutrons are produced in a nuclear fission process relative to the number of neutrons previously present, is used as an indicator of criticality exclusion. Criticality can be excluded, if $k_{\text{eff}} < 0.95$ can be guaranteed.

BMU (2010) offers a simplified procedure for the evaluation of the containment. The potential release of radionuclides at the edge of the CRZ is considered. To evaluate the containment in an area, different receptor points are defined along the transport paths of the radionuclides. All pathways that can contribute to the transport of radionuclides out of the rock mass have to be considered. To evaluate the containment, the potential releases of radionuclides are analyzed at the receptor points and a radiological indicator is calculated separately for the solution path and the gas path.

2.2.3 Shaft sealing concept

The shaft sealing concept designed within the VSG project considers the actual geological situation at shaft 1 of the Gorleben site. The concept can be directly transferred to shaft 2. Both are located close to each other (approximately 300 m apart) and provide the same geological profile.

For shaft sealings in salt, different construction materials are available, such as crushed salt, salt bricks or salt pellets, basalt or other hard rocks, bitumen and asphalt bentonite, saltclay, concrete based materials or magnesia based concrete. Müller-Hoeppel et al. (2012) considered only materials which already provides an application in a comparable surrounding and scale. Large-scale testing provides information on the successful testing of the installation technology and enables the evaluation of performance. The practical examples demonstrate the feasibility of different necessary states of construction. The examples offers a minimal needed data base for the assessment and basic experiences in the design and implementation of quality management are available. Overall the consideration of comparable constructions demonstrated the technical feasibility of the corresponding element of the shaft seal. Large-scale testing with published results and material specifications were available from the following projects:

- Binary mixtures of bentonite based on the Salzdethfurth project (Breidung, 2002)
- Hard rock gravel based on Salzdethfurth project (Breidung, 2002)
- Salt concrete and salt based mortar based on BfS (2010) and Mauke et al. (2012)
- Magnesia based concrete (Sorel concrete) based on BfS (2009a)
- Compacted crushed salt (Hurtado et al., 1997)

Bitumen and Asphalt were not considered because of missing large scale experiments or applications at this time. Meanwhile such technical analogs are available, see section 4.

The listed materials were considered in the shaft sealing concept, see Figure 2-21.

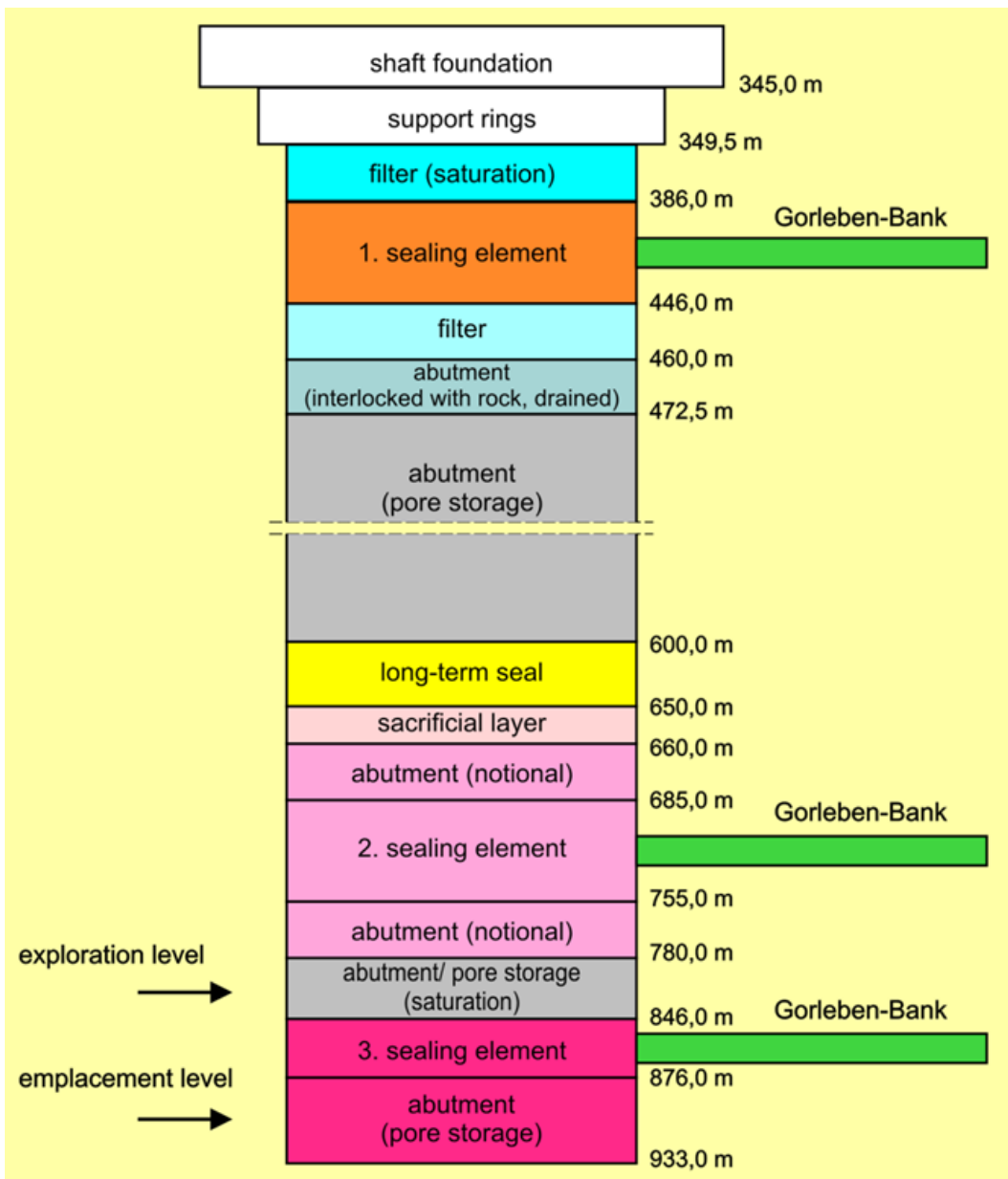


Figure 2-21: Shaft sealing concept based on preliminary design (Müller-Hoeppe et al., 2012)

The waterproof shaft liner between surface and the salt top will remain, following the design principles of shaft sealing for conventional salt and potash mines. In the area of the waterproof liner, a complete filling with gravel or comparable materials is foreseen. A separation between independent aquifers would be necessary and is not considered in this concept. The actual shaft sealing starts at the salt top or the location of the lining foundations. An element made of bentonite represents the upper sealing element, named “1. sealing element” in Figure 2-21. Bentonite is a material like salt clays, which are found several times in the natural sequence of different evaporite depositional cycles (e.g., gray or red salt clay). Gray salt clay is found above the cover anhydrite of Gorleben 2 shaft. This suggests the long-term stability of bentonite in the saline environment. Bentonite provides some swelling under salt solution influx, which also has a favorable effect on the residual EDZ even in this area of limited depth and low geo-mechanical pressures. Additionally, bentonite has a high ion exchange capacity, and promises that organic matter will be filtered if fluids pass the element.

The bentonite sealing is covered by filter elements made of gravel and sand. The stability of location is guaranteed by an abutment element made of salt concrete. Below that, an approximately 130 m long gravel-based filling column is considered. The large pore space within the gravel column represents an additional brine storage capacity. Brine passing the bentonite element will accumulate and create a steady and smooth pressure increase sealing elements below it. In the center of the shaft sealing a long-term relevant sealing element made of crushed rock salt is installed. The “2. sealing element” made of salt concrete is covered by two notional abutments and one sacrificial layer at the top. The sacrificial layer is made of salt concrete as well but is not considered as sealing element or abutment. If water or brine that is aggressive against the salt concrete enters the layer it is then used for saturation of the brine. Thus, the actual sealing and abutment is protected. Sealing and abutment consist of the same material. At the sealing location an additional re-excavation of the shaft contour is considered to remove parts of the EDZ. Within the safety assessment only the length of the sealing is considered for determination of the hydraulic resistance. In opposite for the evidence of local stability only the abutments are considered but not the sealing, which in fact provides compound with the rock as well. Overall, the separation of functions represents a conservative approach that underestimates the hydraulic and mechanical resistance of the salt concrete.

Shaft landing station of the exploration level is located below the salt concrete elements. In this area an approximately 60 m high gravel column is installed. The separation between exploration and emplacement level is guaranteed by the “3. sealing element”, made of magnesia concrete. Similar to the second sealing element a separation in sealing element and abutment is foreseen. At the sealing location the EDZ will be partly removed. The remaining shaft down to the shaft sump is filled with magnesia concrete as well. This lower part of the magnesia concrete represents the abutment but in parallel fills the additional connections between shaft and drifts such as skip filling bunker at the shaft landing station or maintenance drift down to the shaft sump.

2.2.4 Drift sealing concept

The drift seals represent the third part of the sealing system. Their sealing function is supplemented with increasing time by the compacting crushed salt backfill, which is finally able to take over the sealing function on its own.

According to the plans for the closure of the repository, each access drift is closed with two sealing elements, each 50 m long, made of Sorelbeton A1, which will be placed between abutments, see Figure 2-22. The abutments with a length of approximately 15 m are made of Sorelbeton A1 as well. They are arranged between 0.75 m thick formwork walls. The abutments are designed as simple cylindrical elements and fill the previous cross-section of the access drifts. The installation of cone-shaped or geared abutments should not be needed. The access drifts offer enough space to install long cylindrical abutments and the drift sealing concept follows the principle of being as simple as possible.

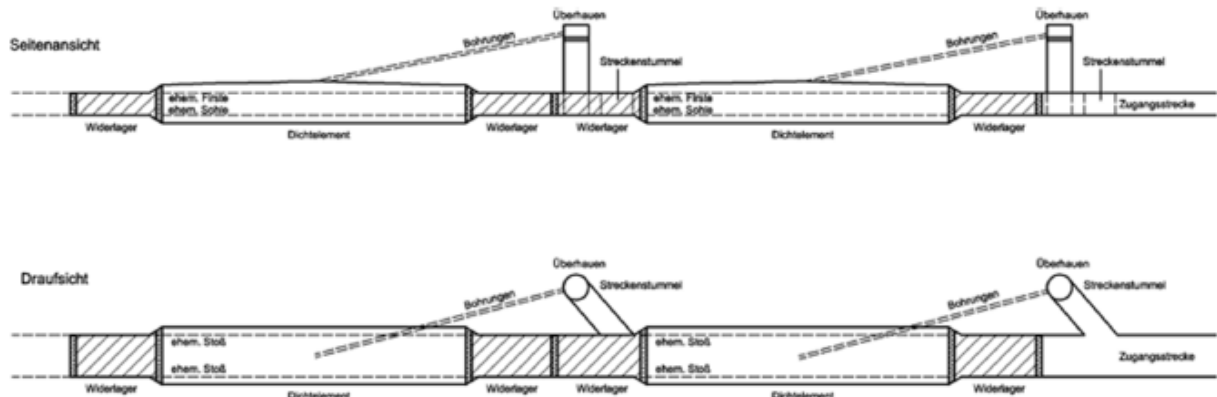


Figure 2-22: Drift sealing concept based on preliminary design, (Müller-Hoeppke et al., 2012b)

At the location of the sealing elements the contour of the drift will be re-cut to remove heavily damaged parts of the EDZ (the majority of the EDZ is associated with the first round of mining, when the change in stress is largest – subsequent mining creates a much smaller disturbance). To allow a complete filling of the sealing element and to avoid air filled gaps at the roof, it will be dome shaped. At the highest position at the center of the sealing element the Sorel concrete will be filled in. The filling is done via two boreholes: one for filling and one for air removal. Both boreholes start inside a short blind shaft or raise. The raise is located next to the drift. After installation the raise will be filled with Sorel concrete as well.

2.2.5 Safety demonstration and verification concept

The semi-probabilistic, reliability-oriented safety assessment concept using partial factors is based on the internationally recognized Eurocodes (DIN EN 1990). In engineering, it can thus be considered as state of the art for demonstrating the load bearing capacity (resistance) of a structure.

The actual safety case for the system as a whole and for the individual barriers consists of several individual safety assessments for various limit states that also include, e.g., the mechanical properties of the construction material. As a first step, the requirements for the multi-barrier system as a whole and for the individual subsystems need to be derived from the safety goals. Whether specific requirements are met is demonstrated by means of "assessment cases" (load cases). The term "assessment cases" was chosen analogous to the term used in long-term safety assessments as in addition to the load, other parameters need to be considered as well. The assessment cases are derived from the combinations of actions (impacts) and from the specific system characteristics. The respective states of the structure, e.g., the stress states, are to be determined by means of equilibrium considerations.

The proper demonstration is carried out by means of a limit value evaluation of the opposing actions and resistances, e.g., the (existing) stresses determined in the equilibrium considerations are compared with the nominal design stresses which can be calculated, e.g., from the material strengths. The actions on the structure are compared with the resistances of the structure by means of limiting criteria which are allocated to the combinations of actions.

The analyses by means of assessment cases must be carried out for all relevant combinations of actions as well as for their limit states. The reference to a limit state makes sense because both actions and resistances are determined from typical distribution functions. Because of the dispersion (variability) of the two parameters, several states are possible. The limit state describes the state of the structure when it just meets the requirements. If this state is exceeded, the structure no longer complies with the design requirements. Accordingly, to meet the design requirements, the resistances need to be higher than the actions.

According to Kreienmeyer et al. (2008) and Müller-Hoepppe et al. (2007), the following individual assessments are essential for a safety assessment according to the state of the art in technology. They must demonstrate:

- Sufficient hydraulic resistance (demonstration of tightness)
- Sufficient load bearing capacity (demonstration of structural integrity)
 - Structural stability
 - Crack limitation
 - Deformation limitation
 - Filter stability
 - Durability

These assessments are essential for demonstrating the effectiveness of the shaft seal. Furthermore, the feasibility needs to be assessed and demonstrated. Figure 2-23 shows the individual assessments and their connections to the overall demonstration of functionality. In addition to applying the method of partial factors, a reliability assessment based on empirical data needs to be carried out to quantify the reliability of using probabilistic methods. Methods to assess reliability are also used in risk analyses (Müller-Hoepppe & Krone, 1999).

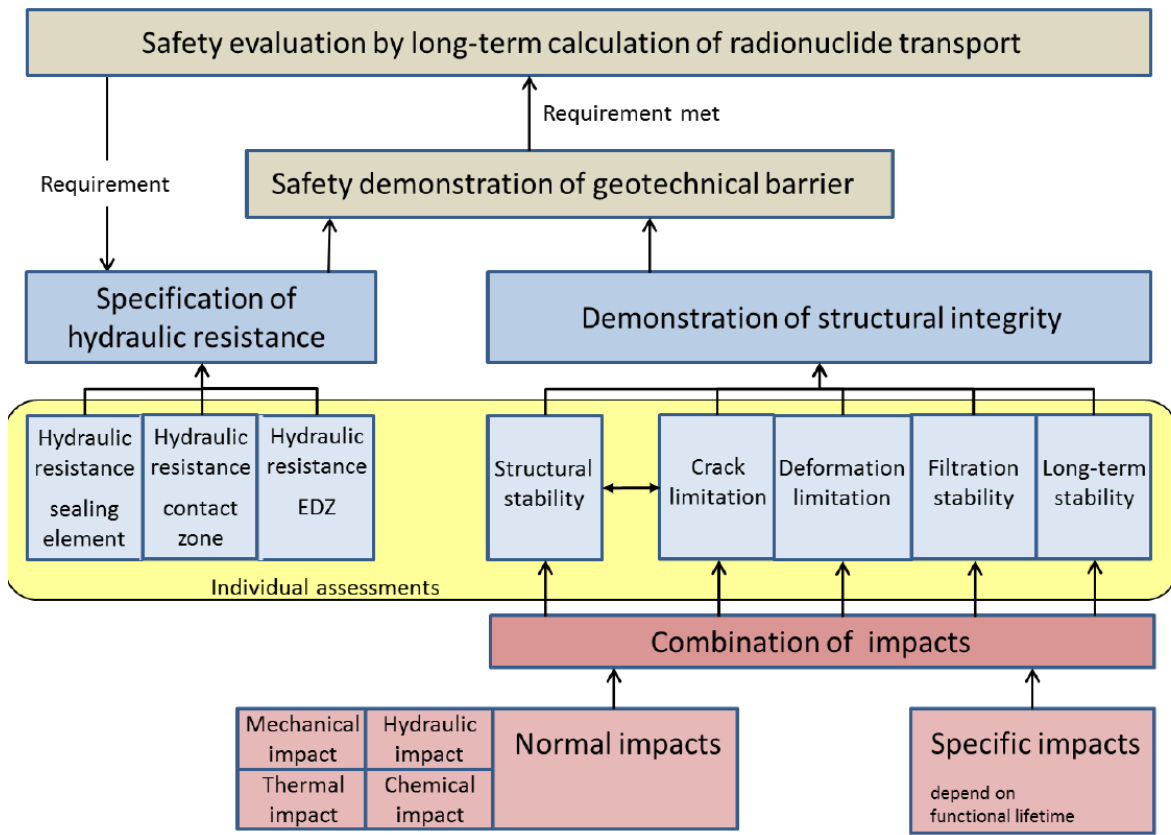


Figure 2-23: Connection of hydraulic long-term calculations in a long-term safety assessment with the individual function-related assessments using the example of a shaft seal (Müller-Hoepp et al., 2012)

The design values for the individual assessments are derived from the characteristic values of the actions on and the properties of the barrier combined with the related partial factors. When applying the method of partial factors, actions, and resistances, the parameters of the targeted relation are allocated partial factors. The effects of actions (E_d) are multiplied by partial safety factors and, thus, increased, whereas resistances (R_d) are divided by partial factors and, thus, decreased. This method and the application of partial factors generally account for uncertainties in the representative values of the actions and uncertainties in the properties of the structure. Depending on model generation, any uncertainties in the model regarding actions and resistances are accounted for by the choice of specific model parameters, if necessary. Model parameters covering the uncertainties are not always considered, if the properties are well known (Müller-Hoepp, 2009). Thus, the initial requirement

$$E_d \leq R_d \quad [1]$$

is divided into specific calculations for both terms. For the effects of actions, E_d , the following applies:

$$E_d = y_{Ed} * E(F_{di}; a_{di}; X_{di}) \quad [2]$$

With:

- y_{Ed} partial factor for model uncertainty in the actions model,
- F_{di} design values for actions,
- a_{di} design values for the geometric parameters, and
- X_{di} design values for the construction material properties.

The design values for the action F_d are calculated by multiplying the characteristic individual value (F_c) by the partial factor of the (y_f) action.

$$F_d = y_f * F_c \quad [3]$$

In accordance with the above, the following applies for the design values of the construction material properties X_d :

$$X_d = (\eta * X_c) / y_m \quad [4]$$

With:

- η conversion factor for duration of loading, moisture, etc.
- X_c characteristic value for the building material properties
- y_m partial factor of the construction material property

In contrast to actions, there is no partial factor assigned to geometric parameters. The design value of a geometric parameter (a_d) is calculated by adding the nominal value (a_{nom}) and the deviation from the nominal value (Δa) that has been considered. Taking the deviation (Δa) into account is particularly important for geometric parameters that react sensitively. The deviation is determined from the expected changes in the respective parameter. An example is the effective length (buckling length) of a steeply inclined rock layer. Changes in length directly affect the buckling behavior. Thus, a deviation Δa needs to be considered as well.

$$a_d = a_{nom} + \Delta a \quad [5]$$

The design value for the resistance is calculated as follows:

$$R_d = \frac{1}{y_{Rd}} * R(a_{di}; X_{di}) \quad [6]$$

- y_{Rd} partial factor for model uncertainty in the resistance model

The various factors influencing the system can be determined by both deterministic and probabilistic methods. For example, the geometry of the structure is a result of the design draft and the stress model. Actions can be determined based on statistics and on limit value assessments and building material properties can also be determined based on statistics (Müller-Hoeppe & Krone, 1999). If the applicable standards and regulations do not contain suitable partial factors, the latter can also be determined by means of probabilistic methods or calibration (Kreienmeyer et al., 2008). Figure 2-24 illustrates the methods for determining partial factors.

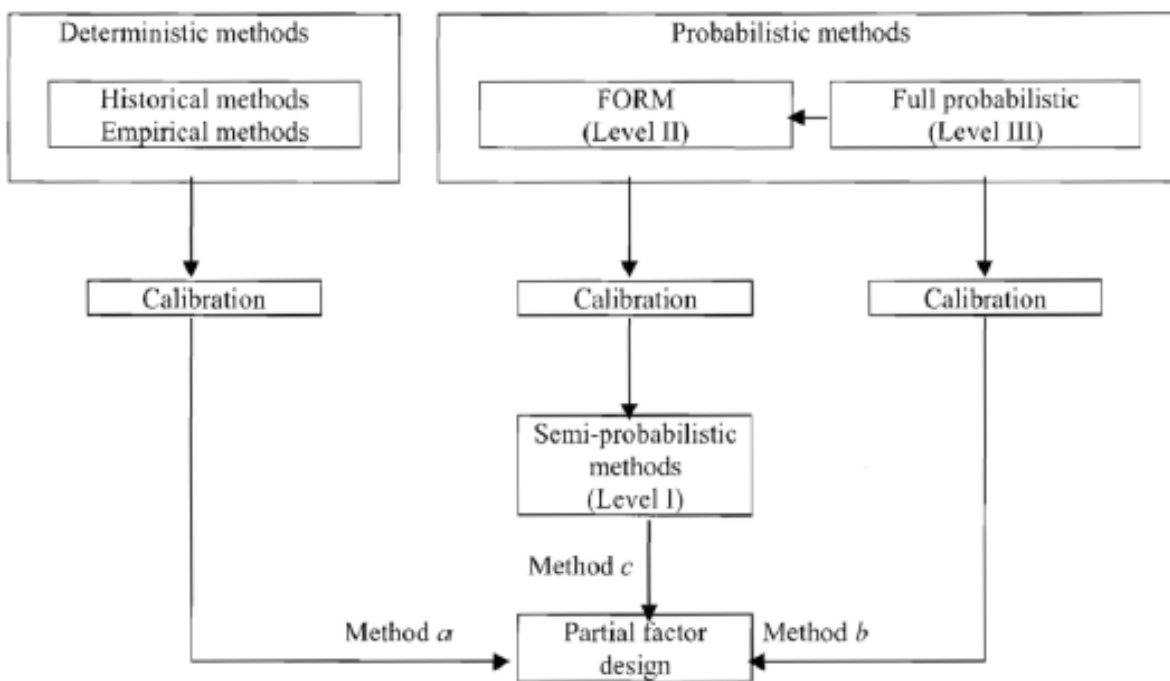


Figure 2-24. Reliability methods for determining partial factors (DIN EN, 1990)

The individual assessments of the limit states are to be carried out “at the level of ultimate limit state verifications”, i.e., they must have the same reliability level as a verification of ultimate limit states. This safety concept is necessary to ensure that the design complies with the requirements. In the structures considered, the demonstration of tightness is thus to be considered at the level of a verification of ultimate limit states, because a loss of tightness would result in “danger to life and limb” (DAfStb, 1997). Unlike in the Eurocodes, the term “resistance” includes more than just mechanical stability. The term is synonymous with the prevention of a danger to life and limb and can also mean the hydraulic resistance. Compliance with the reliability level for resistance in the corresponding assessment ensures the functional integrity of the structure.

As mentioned above, the assessments give information on the reliability of a structure. To demonstrate reliability, a corresponding confidence level or failure probability needs to be met. In an ultimate limit state verification, a failure probability p_f of 10^{-4} for the intended lifetime of the structure is sufficient (Müller-Hoeppe & Krone, 1999). Thus, the verification of the effectiveness of the safety function indicates that the probability that a barrier does not fail prematurely during its expected lifetime is $p_s = 1 - 10^{-4}$, i.e., the survival probability p_s of the barrier is $p_s = 1 - p_f$ (Müller-Hoeppe & Krone, 1999).

2.3 ISIBEL

The ISIBEL project was performed in two phases between 2005 and 2010 and represents a link between early suitability assessments of the salt dome in Gorleben prepared in the 1990s and the VSG project (see previous sections). Developing methods and tools to demonstrate the safety and refined considering advanced international experience was main scope of the project. The results contributed significantly to the further advancement of the state of the art in science and technology about the final disposal of HLW/SF in salt formations. The following sections summarizes the outcome of the project as outlined in (Krone et al., 2008).

The design of a geological disposal facility requires knowledge about three important pillars:

- geological environment and the geological properties of the site;
- repository concept including the regulatory frame and the inventory to be disposed; and
- safety and safety demonstration concept.

The safety concept describes the idea how to achieve safety in consideration of the actual geological environment or site and the repository concept including all mine cavities and opening. In this regard, safety must be demonstrated for both the geological barrier and the engineering system (including the mine openings and EBS system). The safety demonstration concept describes this. The integrity of the geologic main barrier can be demonstrated by the dilatancy and hydrofracture criteria. The mine openings must be located at sufficient depth and at a suitable distance away from potential fault zones or strata boundaries. In combination with the inventory and the host rock, a temperature criterion is an essential boundary condition, which requires site-specific evidence. The integrity of the EBS, especially the geotechnical components such as shaft and drift sealing, follows a separate safety demonstration concept. This includes the evidence of sufficient hydraulic resistance, mechanical stability, resistance against erosion, long term stability and as well as technical feasibility.

Krone et al. (2008) states the safety concept for GDF in rock salt includes backfilling

“... the entire void volume of all mine workings [...] with crushed salt which will be compacted by convergence. During compaction, the porosity and permeability of the crushed salt decreases until, in the long run, it exhibits the same barrier properties as rock salt.”

“The drifts and the access areas to the emplacement sites will be sealed by means of shaft and drift seals. These geotechnical barriers must be placed and – as regards their hydraulic resistance and long-term stability – designed in such a way that brine intrusion to the waste via the shaft and the drifts that are backfilled with crushed salt and a subsequent forcing out of contaminated solutions via the same pathway as a result of decreasing convergence need not be feared in the case of undisturbed repository evolution.”

“Taking into account the gradually decreasing porosity and permeability of the compacting crushed salt over time, the requirements concerning the long-term stability and the hydraulic resistance of the geotechnical barriers have to be set such that a de facto zero emission can be demonstrated. In turn, the compliance with these

requirements has to be demonstrated by the engineering-based assessments of the barrier integrity", see Figure 2-25.

The goal of "zero emission" as named in Krone et al. (2008) represents the base for the further development to the concept of containment providing rock zone (CRZ). At the outer boundary of this CRZ the discharge of radionuclides results in a radiological load below the required level. Thus, the radiological load at surface and biosphere is lower as well. The boundary of the CRZ can be represented by the boundary of the rock formation or an internal virtual boundary.

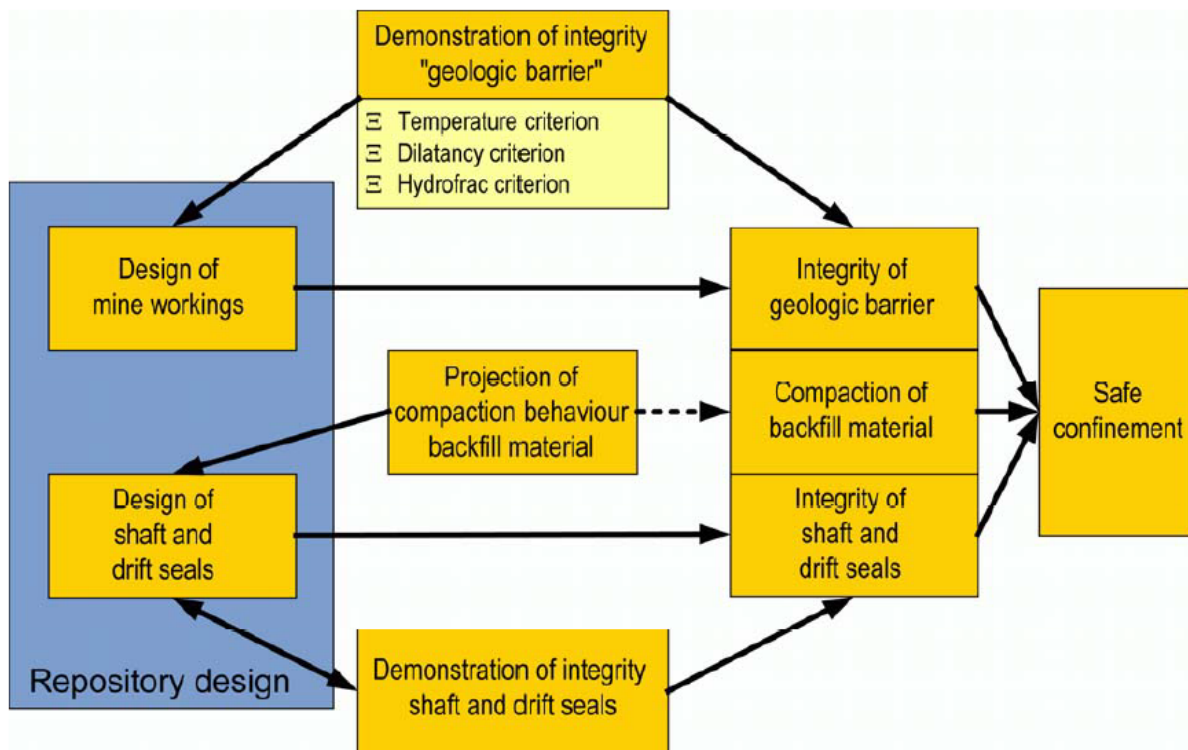


Figure 2-25: Safety concept "Safe Confinement", (Krone et al., 2008)

The safety concept of Krone et al. (2008) puts all long-term relevant safety function to the geotechnical barriers (including backfill) and the geological barrier.

"In contrast to this, no special requirements are made on the integrity of the containers during the post-closure phase. The same applies to possible additional measures for the retention of radionuclides in the event of brines reaching the waste. For the mobilisation of radionuclides from the waste and for their retention in the near field, the parameters specific to the waste, the waste packages, and the backfill and sealing materials are assumed."

"The assessment of the long-term radiological safety is based on the consideration of possible developments of the final repository system. This also includes scenarios that describe the migration of radioactive nuclides from the waste packages into the biosphere. The migration may occur in liquid or gaseous phase. In order to determine

all repository evolutions that are conceivable within the limits of human intellect, it is necessary to elaborate a comprehensive set of scenarios."

"Taking into consideration the recent progress in the demonstration of the integrity of the geological barrier and of the geotechnical barriers, a safety assessment concept was developed in this R&D project that takes full account of the advantages of rock salt and of the safety concept concerning the safe confinement of waste:

- *The main focus of the long-term safety assessment is the demonstration of the long-term safe confinement of the waste through the demonstration of the integrity of the geotechnical barriers and of the geologic main barrier.*
- *The evaluation of releases is done for those developments of the final repository system for which an impairment of the barrier integrity and therefore the development of a continuous pathway for radionuclides cannot be ruled out. Whether these developments are considered to be likely or unlikely or can be excluded is the result of the scenario analysis. In this project, several release scenarios were selected as examples and considered without assessing their respective probability of occurrence."*

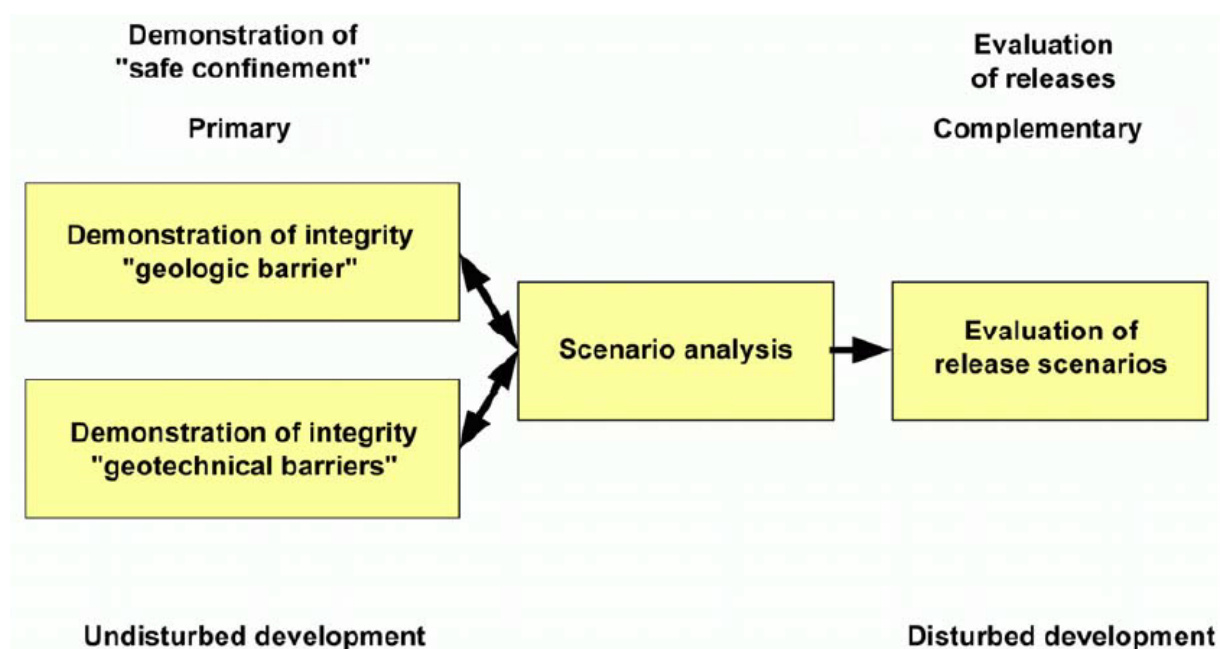


Figure 2-26: Methodical approach to assess long-term radiological safety (Krone et al., 2008)

2.4 Waste Isolation Pilot Plant

2.4.1 Cement Seal Experiments

The United States and Germany have both identified cement-based materials as prime candidates for the sealing and isolation of nuclear fuel wastes in the subsurface. The purpose of the cement-based seals is to produce immediately strong and low-permeability seals to isolate parts of a repository from the environment and biosphere. A successful seal must be: (1) at acceptably low permeability, (2) able to penetrate very fine fractures within the host rock, and (3) be physically and chemically compatible with the host environment. As part of the investigations for the Waste Isolation Pilot Plant (WIPP), the United States has made a considerable effort to study and improve upon cement-based seals. This section highlights some of the major studies that have contributed to the current state-of-the-art for cementitious geotechnical barriers for the safe disposal of nuclear waste.

2.4.1.1 Borehole Plugging Program

Development studies of cementing materials for the Borehole Plugging Program were carried out at the US Army Engineer Waterways Experiment Station (WES) Structures Laboratory starting in 1975, before the first excavations were made at the WIPP site. The purpose of the program was to: (1) develop techniques for plugging boreholes through and adjacent to underground disposal facilities, (2) seal boreholes with plugs which will prevent movement of fluids and gases through the borehole, potentially impacting the stability of salt beds, and (3) provide plugs which will maintain their integrity for time periods comparable to the life of the rock formations in which they are used.

ERDA-10

In 1977, exploratory well ERDA-10 was plugged to investigate quality control and quality assurance for plugging boreholes under field conditions. The initial ERDA-10 borehole had a diameter of 20 cm [7.825"] and a total depth of 1162.8 m [3815']. In August 1977, several modifications were made, and cores were taken from the ERDA-10 borehole to increase the diameter of the wellbore at the surface, addition of an annulus, and increasing the depth of the borehole to 1351 m [4431']. Two cores were taken from the Bell Canyon Formation (a hydrocarbon-bearing formation below the Salado Formation). Figure 2-27 shows the plugging plan, locations of drilling and coring, and approximate depths for the major geologic features (Gulick, 1979). The four different plugs were emplaced in two different formations (Castille and Salado), varied by composition (salt vs. fresh water), and cured at different temperatures and pressures (Table 2-4).

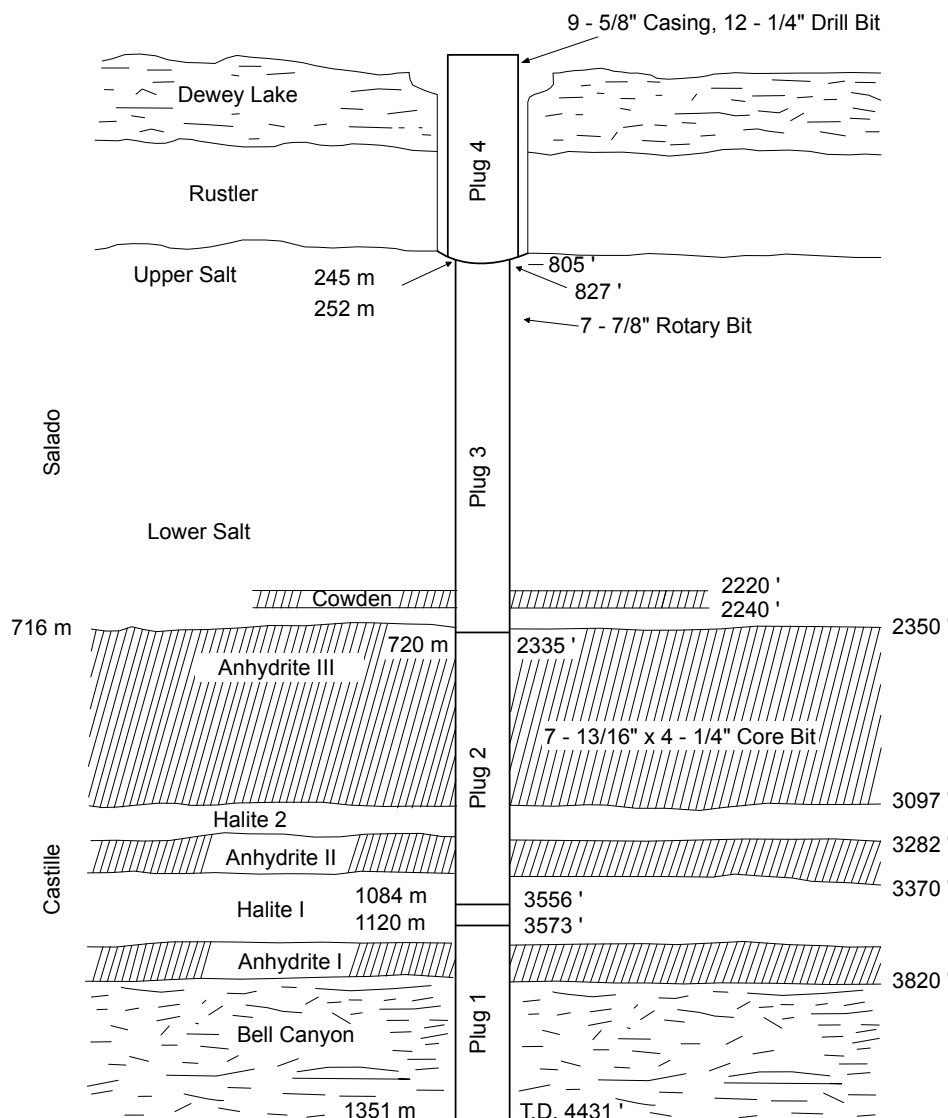


Figure 2-27: Schematic of the ERDA-10 borehole and planned plugging program. (Modified from Gulick (1979)).

Table 2-4: Plugging plan for the four plugs with grout mixtures and curing conditions. For additional details on mixtures, see Table 1 in Gulick (1979).

Plug No.	Depth (m)	Length (m)	Weight % salt	Curing T (°C)	Curing P (MPa)
1*	1351 - 1137	214	30	52.7	16.8
2*	1137 - 701	436	36	51.6	14.5
3*	701 - 244	457	36	51.6	14.5
4†	244 - GL	244	0	26.7	3.1

* Additional additives include calcium chloride (2%), salt gel (attapulgite, 2%), dispersant (0.1%), and silica sand (0.5%).

† Added 2% Bentonite gel and a fresh water turbulent inducer compound.

The plugs were emplaced on Oct 1, 1977, and allowed to cure for 48 hours, coring operations began on Oct 3, 1977. The cores were shipped to the WES Laboratory in Vicksburg, Mississippi for analysis. These early emplacement experiments show that the quality control

procedures presented in Gulick (1979), were adequate and provided a uniform cement slurry which hardened and gained strength like tests conducted in the laboratory.

In addition to testing the 4 plugs from the ERDA-10 borehole, five other grout mixtures were created and tested (Gulick et al., 1980). The analyses performed by WES occurred over the course of a two-year period. The analyses included: bulk density, compressional wave velocity, dynamic modulus, static unconfined compressive strength, porosity, water permeability, gas permeability and porosity, and petrographic and chemical characterizations (Tables 3-2 to 4-3 in Gulick et al., 1980). The results for the 5 grout mixtures created in the lab in Gulick et al. (1980) highlight: (1) there is no evidence of deterioration of any of the samples after 2 years, (2) push-out bond strengths were higher for the mixtures containing brine, (3) no clear trend in porosity or density change, and (4) after 30 days no sample had a permeability higher than 0.9 microdarcy. The testing of the field samples from the ERDA-10 field-plugging operation show the three grout mixtures as stable and durable materials. After 1 year of aging, analyses of the ERDA plugs showed: (1) little variation in bulk density, (2) compressional wave velocities revealed strong, competent grouts, (3) 5 to 15% reduction in dynamic modulus for the brine mixed grouts, (4) strengths of *in-situ* for plugs are in excess of 1.7 MPa [250 psi], (5) the fresh-water plug had a strength > 41 MPa [6,000 psi] at 28 days, and (6) water-permeability data shows significant reduction at later ages from initial values. The testing of the ERDA-10 plugs presented in Gulick et al. (1980) illustrates the durability and soundness of the grout mixtures from Gulick (1979).

AEC-7

AEC-7 was an exploratory borehole drilled by Oak Ridge National Laboratory (ORNL) in 1974 as part of the WIPP siting process (Statler, 1980). The AEC-7 borehole is located ~11 km northeast of WIPP (near the initially proposed WIPP site). Due to its location and it being abandoned, the AEC-7 borehole was selected for the Bell Canyon Test (BCT). On March 19, 1979, reentry began, the wellbore was cleared, and total depth extended to 1435 m to intersect a high-pressure aquifer within the Bell Canyon Formation (Figure 2-28). The intended plug location was at 1370 m depth and the fluid pressure within the Bell Canyon aquifer was established at 12.4 MPa. Two plugs 2 m long and 20 cm diameter were created with two different grouts; BCT-1F (6.5% NaCl) and BCT-1FF (no NaCl) (See Table 1, Christensen and Peterson, 1981). The saltwater grout showed poor bonding to anhydrite in lab tests, thus the freshwater plug BCT-1FF was chosen for the field test. The plug was installed to isolate the upper regions of the borehole from the Bell Canyon Aquifer (capable of producing 38,160 liters [240 standard barrels] per day). The plug was left in for 4 months, over which time fluid pressure, inflow rates, flow path permeability, fluid buildup, and tracer tests were conducted (Results presented in Tables 2 – 5 and Figures 5 – 8 of Christensen and Peterson, 1981). The results indicated that the freshwater grout BCT-1FF had a higher strength, was more expansive, the grout adhered more tightly than the saltwater grout BCT-1F, as well as showing no observable leakage at the interface. However, both freshwater and brine-based grouts are deemed suitable for emplacement and they both far exceeded the safety assessments for the WIPP (Christensen and Peterson, 1981).

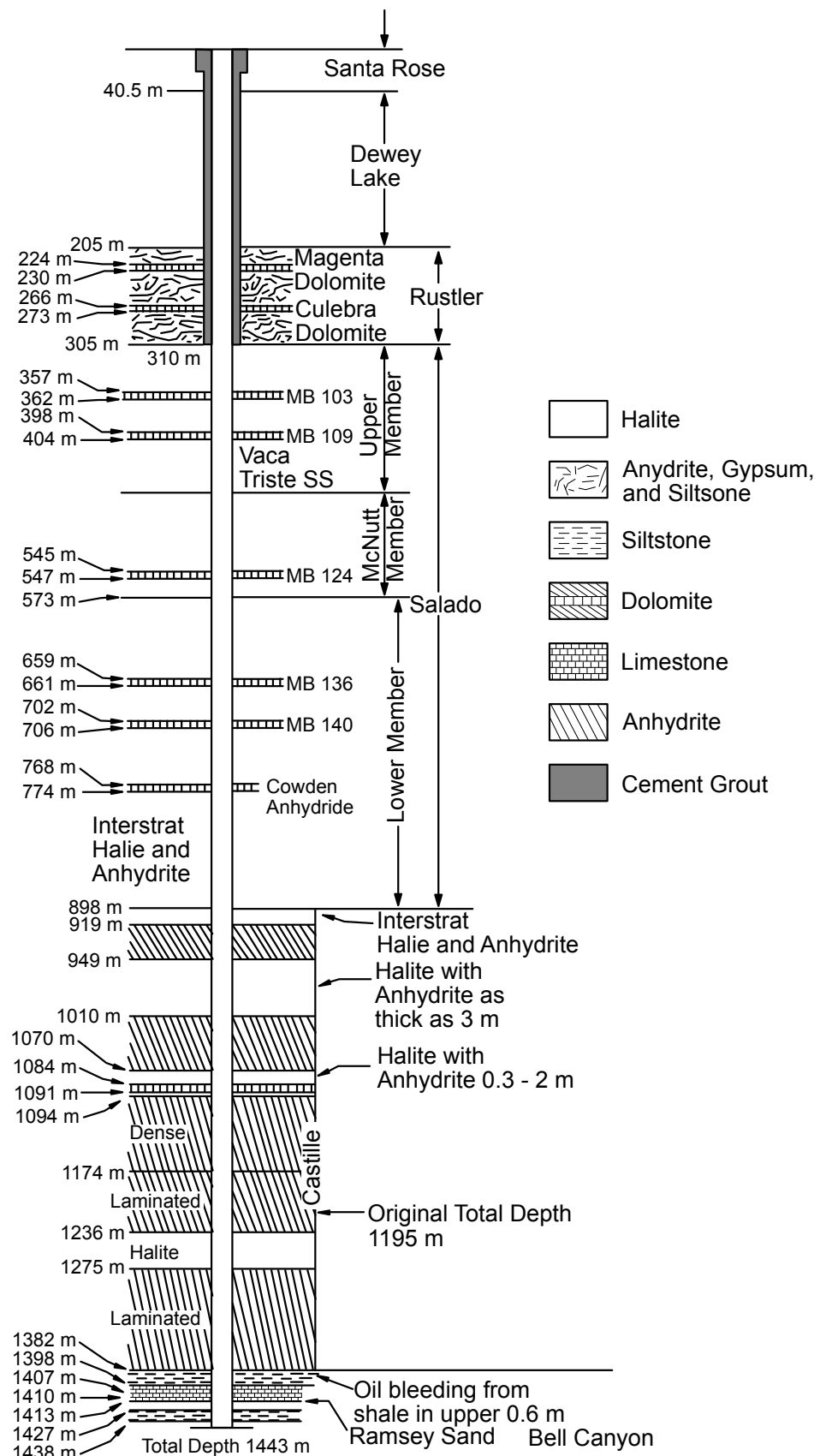


Figure 2-28: Schematic of AEC-7 borehole. The cementitious plug was emplaced from 1368 to 1370 m, just above the Belly Canyon aquifer (Modified from Christensen and Peterson, 1981).

2.4.1.2 Small-Scale Seal Performance Test (SSSPT)

In the late 1980s and early 1990s, the WIPP underground experimental program had three main components: PSP (Plugging and Sealing Program), TSI (Thermal/Structural Interactions), and WPP (Waste Package Performance). The Small-Scale Seal Performance Test (SSSPT) was a series of experiments in the PSP program (Table 2-5) using a variety of sealing materials (Table 2-4). Tyler et al. (1988) summarizes PSP with historical introduction through 1988.

Table 2-5: Small Scale Seal Performance Tests: (Knowles and Howard, 1996).

Series	No. of Seals	Material	Orientation	Diameter (cm)	Length (cm)	Construction Date
A	6	Salt-based concrete	Vertical	15 – 91	95	Jul-85
B	3	Salt-based concrete	Horizontal	91	91	Feb-86
C/1	6	Salt blocks and 50/50 salt/bentonite blocks	Horizontal	91	91	Sep-86
C/2		Bentonite Blocks	Horizontal			Dec-90
D/1	3	Salt blocks	Vertical	97	300	Jan-88
D/2	2	Bentonite block core	Vertical	97	91	Sep-89
F	18	Ultrafine grout injected into fractured anhydrite layer through 18 vertical boreholes	Vertical			Feb-93 to Mar-93

Table 2-6: Seal Material Descriptions (Knowles and Howard, 1996).

Seal Material	Material Description
Salt-Saturated Concrete	Salt saturated concrete, slightly expansive
Crushed Salt	Salt block density relative to intact salt was 82%
50/50 Salt/Bentonite Blocks	Salt/Bentonite Blocks were a mixture of 50% salt and 50% bentonite by weight. Density ~78% intact materials
Bentonite Block Core	Core of one seal was 1.8 g/cc dry density. Core of second seal was 2.0 g/cc dry density.

The goal of the SSSPT experiments was to conduct a series of *in-situ* performance tests of concrete seals, while taking measurements of temperature, strain, stress, and displacement near different sized seals emplaced in the underground at WIPP. The SSSPTs emplaced candidate seal materials in underground boreholes of various configurations. Several tests were carried out from 1985 to 1990 (Stormont, 1987; Torres et al., 1992). Test F (Ahrens & Dale, 1996 – related to Test E in earlier documents, which was not conducted) later injected grout into the fractured anhydrite bed Marker Bed 139 (MB-139), an approximately 1-m thick horizontal anhydrite and clay layer located approximately 1 m below the floor of the repository horizon. The main objectives of SSSPT were (Stormont, 1987):

1. Determine *in-situ* fluid flow performance for various seal systems
2. Determine *in-situ* structural performance of host rock and seal materials
3. Assess seal emplacement techniques
4. Support the development of numerical predictive capabilities

Test Series A emplaced salt-water-based concrete seals in vertical boreholes in Room M of the WIPP Facility. The general test configuration of each borehole is illustrated in Table 2-5. The seals had imbedded strain gages, pressure and strain gages, and thermocouples.

Based on these and previous studies (Buck, 1985; Wakeley et al., 1986; Comes et al., 1986) a new expansive salt-saturated concrete (ESC) mixture was developed (Table 2-7).

Table 2-7: ESC Mixture Used in SSSPT Test Series A (Stormont, 1987).

Material	kg to make 1 m ³
Class H Cement	216
Chem. Comp. III (Type K) cement	144
Fly Ash	122
Plaster	43.3
Aggregate, 3/4" max	828
Concrete Sand	817
Fine salt (NaCl)	59.3
Sodium Citrate	2.56
De-Air #1	5.13
Water	170

After 180 days the first results were published in Stormont (1987) with the main conclusions:

1. Thermal/structural response of Test Series A were consistent, and the data collected are reasonable.
2. Temperature measurements are consistent with heat conduction from the concrete to the adjacent rock.
 - a. Peak temperatures reached are a function of the size of the concrete seals (Larger volumes lead to higher temperatures).
3. Two temperature peaks are evident while the concrete seals are curing, associated with two different hydration reactions in the concrete.
4. Creep of adjacent salt is the main contributor to stress and strain on the seal.
5. Thermal strains show no appreciable change to the strain trends.
6. Strain and pressures are continually decreasing after emplacement suggesting they may eventually stabilize.
7. Results suggest that the concrete/salt interface has substantial strength.

SSSPT-F involved injection of grout into the disturbed rock zone in an anhydrite layer (MB-139) below the floor of the repository. It was designed to demonstrate:

- (1) the ability the ability to practically and consistently produce ultrafine cementitious grout at the grouting site;
- (2) successful, consistent, and efficient injection and permeation of the grout into fractured rock at the repository horizon;
- (3) the ability of the grout to penetrate and seal microfractures;
- (4) procedures and equipment used to inject the grout.

SSSPT-F was conducted in WIPP Room L3, which was chosen based in its position stratigraphically in the salt (See Figure 1-3 in Ahrens and Dale, 1996), time since excavation (>5 years) and room width (10 m) providing significant time for the DRZ to develop (Ahrens and Dale, 1996).

The Test Plan (Ahrens, 1992b) called for the emplacement of a concrete slab on the floor of Room L3 at the experiment site. Figure 2-29 illustrates the staging area for the experiment with a cement slab with 18 core holes drilled for gas-flow and tracer-gas tests. Grouting activities began with the drilling and grouting of eight primary and eight secondary grout holes. After completion of grouting activities, 24 post-grout core holes were drilled. The cores were examined for evidence of grout, and the holes were tested for gas transmissivity.

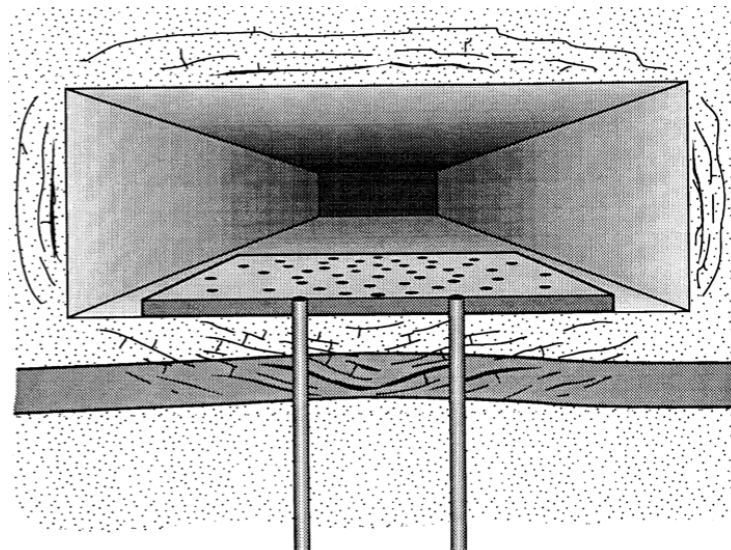


Figure 2-29: Staging area in WIPP Room L for SSSTP-F (Ahrens and Dale, 1996). MB-139 is the gray layer below the floor of the drift, intersected by the disturbed rock zone (illustrated with fractures).

The ability to produce ultrafine cementitious grout practically and consistently at the grouting site was demonstrated in SSSPT by the success of 18 separate grouting events. Consistency is evidenced by the less than 1 μm variation in particle size throughout. Overall, SSSPD-F was successful in meeting all objectives set prior experiment. For more detailed explanations of the experimental setup and results, the reader is referred to Ahrens and Dale, 1996.

2.4.2 WIPP Salt Backfill Reconsolidation Research

Granular or crushed salt has been widely investigated as backfill material and a seal system component within salt disposal research. With regards to the US programs, granular salt has been included in a variety of laboratory experimental testing initiatives along with field demonstrations performed in the WIPP underground. Many of these field tests were conducted from 1984 to 1995 to validate the storage and disposal of transuranic nuclear waste in salt (Kuhlman et al., 2012; Kuhlman & Sevoulian, 2013). Figure 2-30 shows the north experimental part of the WIPP underground, in relation to the first waste disposal panel (the only existing panel in 1997). A handful of the field tests included the use of granular run-of-mine (ROM) WIPP salt as backfill material; however, in-situ measurements and collection/characterization of post-samples were irregularly documented. The laboratory

testing utilizing specifically granular ROM WIPP salt have been conducted under various conditions (i.e., stress, moisture, temperature) with multiple objectives. In the following sections, an overview and summary of the field tests and laboratory experiments using granular WIPP salt as backfill is provided.

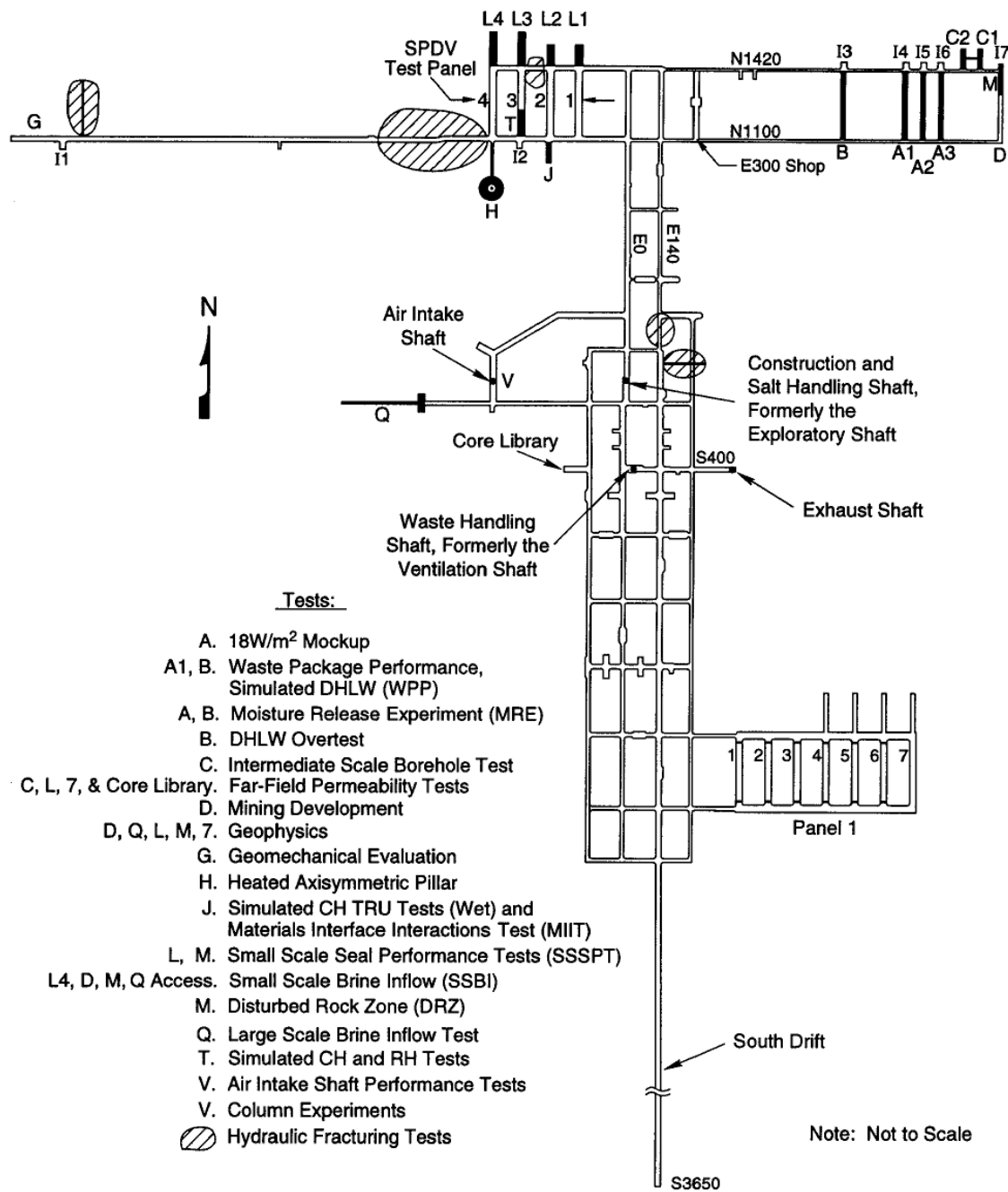


Figure 2-30: Underground WIPP field test layout before emplacement of waste (Munson et al., 1997).

2.4.2.1 Field Tests

2.4.2.1.1 Thermal/Structural Interactions (TSI) Tests

From 1984 to 1990, the Thermal/Structural Interactions (TSI) tests in the underground at WIPP were designed to identify the stability of excavated rooms and response of host rock with respect to emplaced heat-generating waste, which included Rooms A1-A3, B, H, and J. Although the WIPP mission (transuranic defense waste) did not include heat-generating high-level waste, the TSI tests were conducted at WIPP to benefit a different bedded salt site being developed at the time in Texas. In Rooms A1-A3 and B, which utilized granular salt, the goal was to simulate defense high level waste (DHLW) canisters by installing vertical heaters into boreholes in the floor (Figure 2-31). In Rooms A1 and A3, all heaters were backfilled with crushed salt, while only a select few in Room A2 were backfilled. The surface temperature between the heater wall and the annular crushed salt for the 1.4 kW guard heaters in Room A2, and. The guard heaters in Room A3 never did reach a steady state but the temperature range represents an average at the end of the test, approximately 1950 days (Matalucci 1988; Munson, 1988). Unfortunately, in Rooms A1-A3, in-situ measurements of the crushed salt backfill around the heaters were not conducted and they were never sampled for post-characterization. Many of the heaters/canisters are currently in place, although the rooms are no longer accessible (Brady et al., 2013).

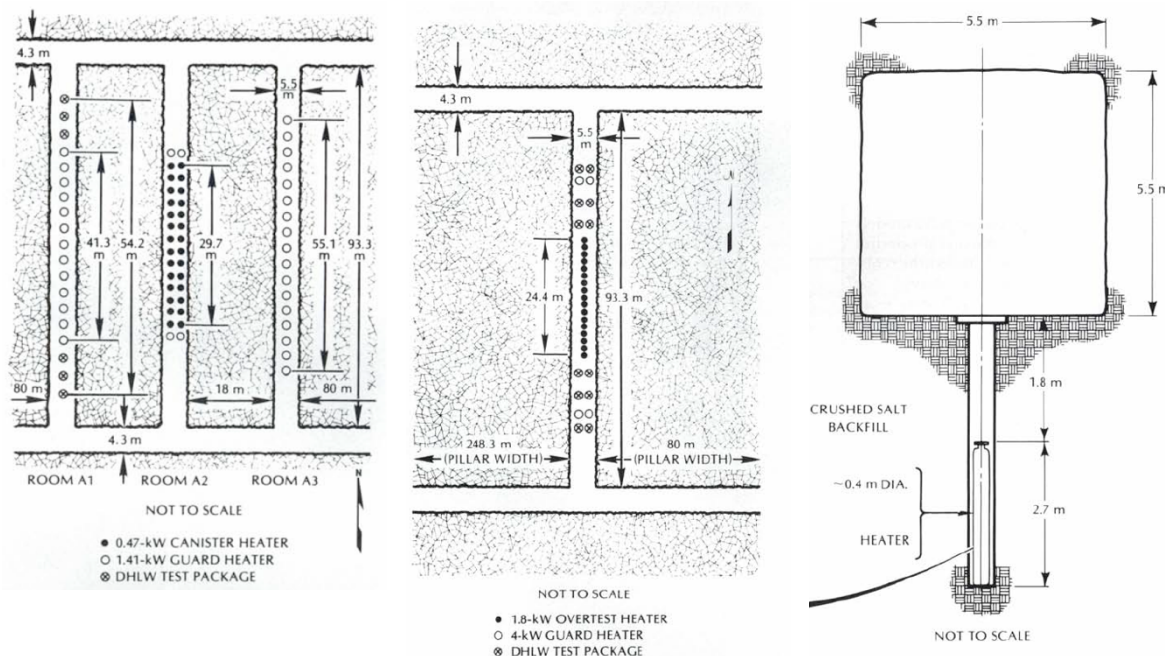


Figure 2-31: Layout of WIPP Rooms A1-A3 with heaters, and layout of Room B along with cross-sectional view

Testing in Room B aimed at accelerating heat effects to determine room closure rates and increased deformation due to creep. There were several types of backfill placed on top of canisters including bentonite/sand mixtures, vermiculite, and crushed salt (Krumhansl et al. 1991b). Most DHLW canisters were removed in 1988 for laboratory testing and post-characterization (Molecke and Sorensen, 1989; Brady et al., 2013).

For canisters emplaced with granular salt, many had a “rind” of compacted backfill and/or salt about 2 to 20 cm [0.8 to 8.0 inches] thick and was removed intact with the container. Hydrogen Chloride (HCl) vapors of approximately 10 ppm were recorded during the over-coring process. The presence of HCl was attributed to the thermally induced breakdown of magnesium chloride minerals in the host rock salt (Kuhlman et al., 2017). Sample cores of the backfill materials were recovered for analysis of density, moisture changes, and geochemical alterations. The crushed salt backfill had an initial emplaced density of approximately 1290 kg/m³, where post-test samples of this material had a measured density of up to 2160 kg/m³, almost equal to the density of the host rock. This crushed salt had been highly compacted by salt creep through borehole closure. The crushed salt originally occupied a 5.7 cm-wide annulus around the canister and reduced to a width of about 2.5 to 3.0 cm. Creep borehole closure and brine migration led to significantly lower permeability and lower porosity backfill materials.

2.4.2.1.2 Waste Package Performance (WPP) Tests

The Waste Package Performance (WPP) tests in the underground at WIPP focused on determining the durability and integrity of various waste packages, along with investigated effective engineered barriers for waste confinement. While there were several rooms in the underground that included portions of these tests, Room J and Room T mainly incorporated crushed salt backfill investigations.

Room J (Figure 2-32) was known as the Materials Interface Interactions Test (MIIT), which included experiments on the effects of a salt/brine environment on a wide range of waste package material (metals, glass, etc.). Seven other countries participated with the US in the experiment by providing multiple samples of canister materials and waste forms.

Crushed salt backfill was used in Room J; the toe of pile (i.e., the base layer) was in contact with a brine pool. The granular salt wicked up the brine and led to what was considered “moist” crushed salt. Backfill material samples and brine specimens were collected at 0.5, 1, 2, 2.5, 3, and 3.75 years. Crushed salt and mixed salt/bentonite backfill had higher water content in samples collected near the brine pool (6 to 12%). Mixed backfill away from the brine pool only had water contents of 0.5 to 4%, despite the high humidity of Room J. After 3.75 years, brine had wicked 60 to 100 cm into the crushed salt backfill pile. Areas where the backfill had higher moisture content were associated with increased corrosion in metal waste packages. Removal of drums from damp backfill was difficult, requiring shovels and jackhammers. Drums sitting in the brine pool had their paint coating flaked off but were not rusted after 12 months of exposure. By the end of the test (3.75 years), all drums had pronounced corrosion – especially at the air/brine interface (Molecke and Wicks, 1993).

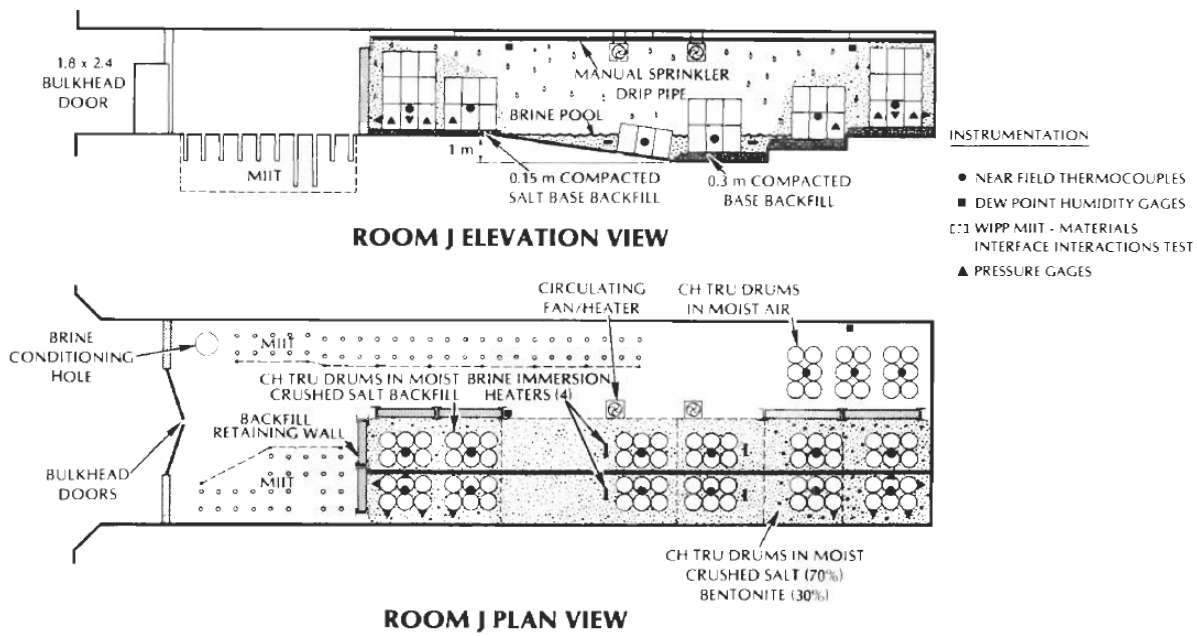


Figure 2-32: Elevation and plan view of WIPP Room J.

Room T evaluated emplacement effectiveness, techniques, and tailored backfill materials. Most of the room consisted of emplaced remote handled (RH) canisters in horizontal boreholes in the wall, but the back portion of the room involved the stacked sets of 240 empty steel drums (i.e., standard contact handled transuranic waste containers). Half of the drums were covered or mostly surrounded with crushed salt and the other half with tailored backfill of 70 mass-% crushed salt and 30 mass-% bentonite (Figure 2-33). Pressures and room closure were monitored for five years to study any drum deformation; however, post-sample collection of the backfill material never took place, likely due to safety concerns of reentry with danger of roof collapse (Tyler et al., 1988; Molecke, 1992).

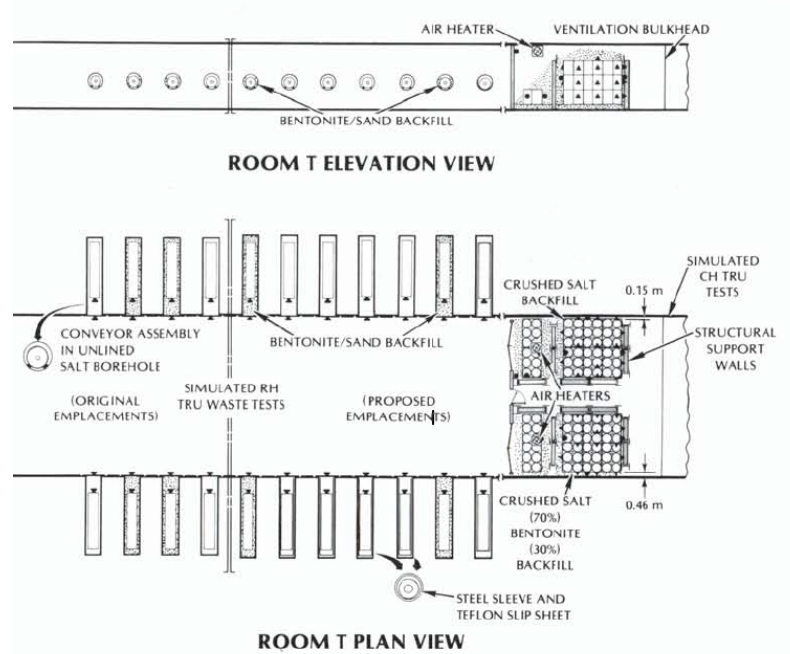


Figure 2-33: Elevation and plan view of WIPP Room T.

2.4.2.1.3 Crushed Salt Blocks in SSSPT

As mentioned in section 2.4.1.2, the SSSPT, conducted in the underground at WIPP, included many material types for testing seal effectiveness conducted in Room M. Series C-Phase 1 and Series D-Phase 1 (Table 3), involved seals of pure crushed salt blocks, emplaced horizontally and vertically (Figure 2-34). In test series C, two salt seal systems were instrumented to measure deformation and pressure, while two were left un-instrumented to perform permeability and fluid flow testing. The crushed salt seals of Series D-Phase 1 did not reach a desirable reconsolidated intact density for an effective fluid seal at the time of test termination. The structural measurements indicated the crushed salt seals provided little resistance to closure and flow and would need to have achieved 90 to 95% density of the host rock to do so (Knowles and Howard, 1996).

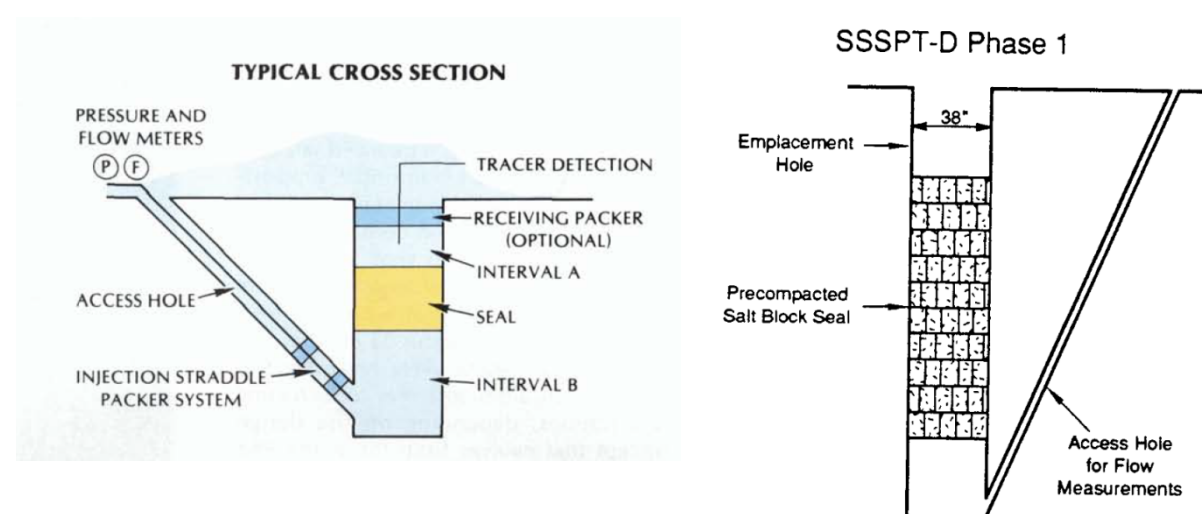


Figure 2-34: Diagram of typical seal borehole setup for SSSTP in WIPP Room M and salt block seal in Series D-Phase 1.

2.4.2.1.4 Demonstration of WIPP Shaft Seal with Crushed Salt

An intermediate-scale and large-scale dynamic compaction demonstration using run-of-mine WIPP salt established possible initial conditions of a compacted salt seal component, while confirming the viability of using crushed salt as a major component in the construction of the proposed WIPP shaft seals (Hansen et al., 1995; Hansen and Ahrens, 1996). The selection of deep dynamic compaction as a construction technique was because it provided the greatest energy application to the crushed salt given available techniques. Dynamic compaction was also relatively easy to apply and had an effective depth of compaction influence far greater than lift thickness (approximately 2 m). The basic construction technique was demonstrated above ground; however, the concept was noted to be readily adaptable to existing shaft backfilling procedures by transporting granular salt to the working level in a shaft by dropping it down a slickline and, if desired, applying a small mist of additional water onto the crushed salt when placed at the shaft working horizon.

To show feasibility of the concept, the intermediate-scale compaction tests were conducted by dropping a cylindrical tamper weighing 890 kg into a chamber container (1.2 m diameter and 1.8 m height) of crushed WIPP salt with the pattern shown in Figure 2-35a. Two different tests

were completed, where the first contained 0.26 mass-% water and the second 1 mass-% water, with produced fractional densities of 0.87 and 0.9, respectively, after compaction. Post-test blocks were also cut to perform gas permeability, density, and moisture content measurements. While no appreciable difference in permeability was found between the two tests (average of $4.16 \times 10^{-13} \text{ m}^2$), the success of implementation led to the large-scale test.

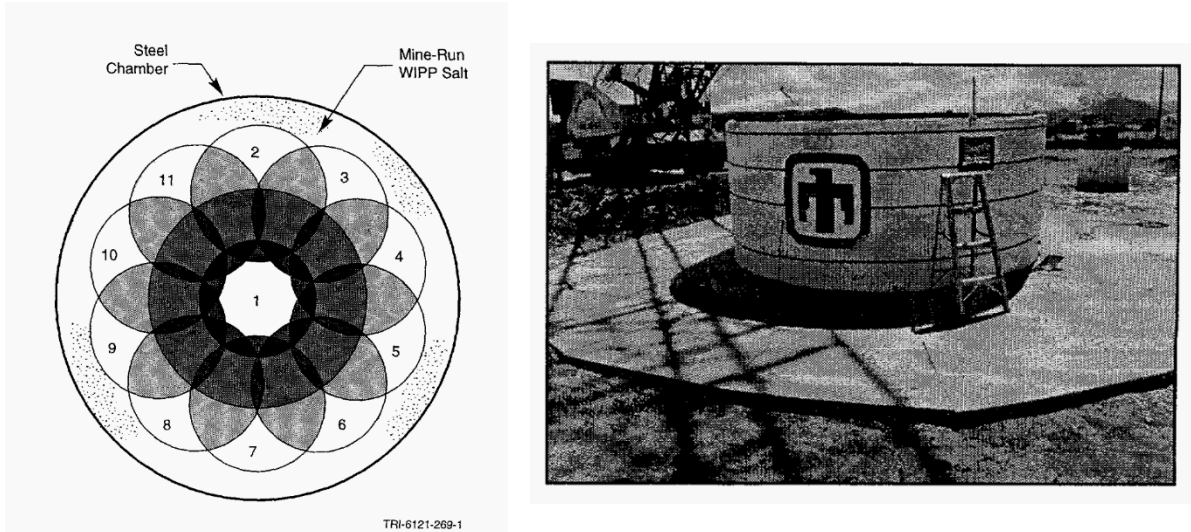


Figure 2-35: WIPP Large-Scale Salt Compaction Tests: a. Weight drop pattern b. Chamber used

The large-scale compaction consisted of a chamber with dimensions of 3.6 m diameter and 3.6 m height (Figure 2-35b). About 40 m^3 of ROM WIPP salt was sprayed with water to achieve 1.0 mass-% moisture while loading into the chamber. During the test, a new tamper weighing 9,144 kg was dropped from 15 m high for a total of 495 drops (same pattern shown in Figure 2-35a) to reach 3 Modified Procter Energy (3 MPE = 8.07 MJ/m^3 [$168,600 \text{ ft-lb/ft}^3$]). The demonstration included some environmental controls (dome cover, blanket, and space heaters, etc.) and lasted about 3 months. From post-test analysis, it was found the moisture added was subsequently lost due to imperfect insulation and having the constant temperature of 25 °C. Difficulties arose when retrieving core for post-permeability measurements in the lab, with only one sample being long enough. Large blocks (0.1 m^3) were eventually cut out and then subcored. Final average fractional density was estimated to be 0.9, where in situ nitrogen permeabilities averaged $9 \times 10^{-14} \text{ m}^2$.

2.4.2.2 Laboratory Tests

Laboratory experiments on natural granular rock salt consolidation have been ongoing since the late 1970s at many institutions around the world. The US has primarily conducted these investigations relating to the WIPP site, largely connected with room or shaft sealing studies. Some were performed for model validation and enhancement, while others more so for material behavior parameters. Though there have been many other studies, Table 2-8 provides a handful of projects that utilized crushed or ROM salt from WIPP, along with their conditions and range of final fractional densities reached in samples. Most were performed under hydrostatic pressures, low confining stresses, and relatively low temperatures, until recently. There are many possible experimental approaches to reach high fractional densities, but most authors of the studies concluded that moisture content, and its availability, plays a large role

in consolidation. The limited emphasis on pressure solution processes and pore structure parameters (e.g., specific surface area, pore size, tortuosity, etc.) in the past, as well as the advancement of modeling capabilities and analytical tools, has driven the need for additional laboratory experiments to take place.

Table 2-8: Summary of test conditions of key WIPP salt consolidation projects (not inclusive).

Report	Type of Test(s)	Conditions					Final Fractional Densities
		Stress (MPa)	Temperature (°C)	Added Moisture Content	Time (days)		
Pfeifle (1985)	Unconfined compression	5 to 20	20	Natural	0.04	N/A	
Holcomb and Shields (1987)	Hydrostatic	0.69 to 3.44	Ambient	0.5 to 3 mass-%	10 to 52	0.78-0.94	
Holcomb and Zeuch (1988)	a. Quasistatic b. Creep	a. Up to 21 b. 1.72 to 10.1	a. & b. 21 to 100	Natural	2.5 to 3.5	a. 0.78-0.85 b. 0.67-0.81	
Zeuch et al. (1991)	a. Hydrostatic b. Shear	a. 1.72 to 0.34 b. 3.45	20	a. Brine Saturated b. Dry	a. 115 to 330 b. 48	a. 0.88-0.95 b. 0.88-0.92	
Brodsky (1994)	a. Hydrostatic b. Shear	a. 1.72 to 6.9 b. 3.45 to 6.9	All at 25	a. & b. Brine Saturated and 3 mass-%	a. 30 to 100 b. 35 to 75	a. 0.90-1.0 b. 0.95-1.0	
Bauer et al. (2012)	Hydrostatic/ Shear	Up to 20	100, 175, 250	Natural	0.25 to 12.5	0.73-0.97	
Stormont et al. (2017)	Hydrostatic	19 to 40	90, 175, 250	Natural and 1 mass-%	2 to 112	0.80-0.99	

3 Case study: Asse II (Germany)

Significant experience in constructing the EBS with salt concrete and Sorel concrete was obtained at the Asse II mine under realistic in-situ conditions (e.g., in size and depths). The sealing of a rock salt drift with salt concrete was part of a larger planned sealing test that was only partially realized. Sorel concrete has extensively been used to construct flow barriers to control (delay and direct) an inflow of brine into disposal chambers in a carnallitic (i.e., magnesia-rich) environment. Based on the practical experience an operational plan on how to realize an engineered barrier is given.

3.1 Introduction

Asse II mine is in the Asse hill range in Germany about 30 km north of the Harz Mountains or 80 km southeast of the city Hanover. It was founded as an underground potash and rock salt mine with initially one shaft called shaft Asse 2 created at the beginning of the 20th century. The shaft was sunk between 1906 and 1908 and reached the Stassfurt potash layer at a depth of 631 m. In 1909 the production started at the levels 700 m and 750 m at the northern flank of the salt diapir. The additional ventilation shaft Asse 3 drowned during its construction phase at a depth of 400 m and was not replaced. Still a total of 2 M t of carnallite had been produced by the end of 1925 when potash mining stopped. Ninety percent of the mined cavities were backfilled with processing residue during operation (Kokorsch, Ausgabe 01/2010 Heft 5). In addition, a total of 6.7 M t of halite were mined between 1916 and 1964 dominantly from the Stassfurt formation at the southern flank and a minority from the Leine formation in the central part. These operations left 3.35 M m³ and respectively 0.45 M m³ open volume or a total of 131 and 20 open stopes (Deisenroth & Kokorsch, Ausgabe 01/2011 Heft 7) which remained unfilled for 29 to 75 years (Lautsch, 2021). An overview of the mining activities is given in Figure 3-1.

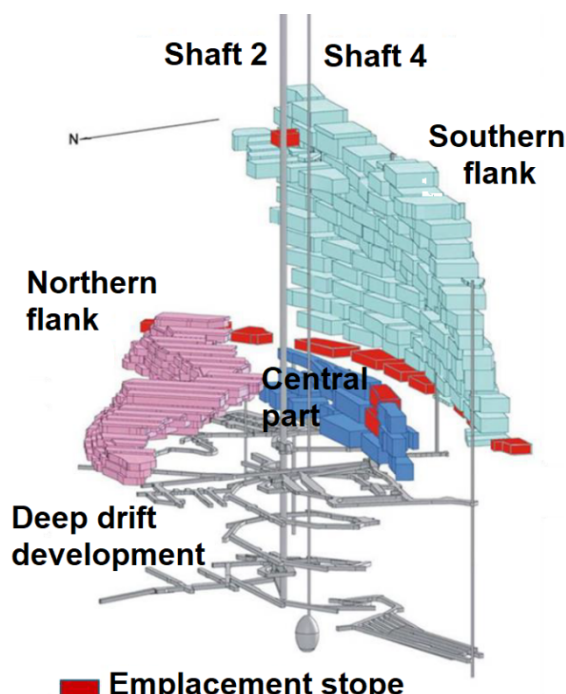


Figure 3-1: 3D model of the mining areas within Asse 2 including the stopes with radioactive waste after (Lautsch, 2021)

On behalf of the federal government, the Society for Radiation Research (in German: Gesellschaft für Strahlenforschung GSF) acquired the mine in 1965 and started research on the disposal of radioactive waste. This included “trial” emplacement of low-level waste (LLW) from 1967 and intermediate-level waste (ILW) from 1972. Until the end of this phase in 1978, a total of 125,000 barrels of LLW and 1,300 barrels of ILW (about 47,000 m³ of waste) had been emplaced in 13 stopes (Kokorsch, Ausgabe 02/2010 Heft 6). Ten emplacement stopes are in the southern flank on level 750 m and one on level 511 m. Two additional emplacement stopes are in the central part between levels 725 m and 750 m (Asse GmbH, 2017). After 1979 the shaft Asse 2 and the drift system were both extended down to 975 m and the ventilation shaft Asse 4 was sunk. The focus of research switched to High Level Waste (HLW) until 1992 (Kokorsch, Ausgabe 02/2010 Heft 6).

Research on the disposal of HLW was carried out, including the construction of a sealing element out of salt concrete and a corresponding investigation of its permeability about 10 years later. In 1988, a brine inflow of several cubic meters per day was documented that stepwise increased over the years to a maximum of around 14 m³/d (BGE, 2020). Stabilization measures to protect the hanging wall layers and sealing measures to avoid exchange of fluids with emplacement stopes commenced to prepare the underground drift system for a planned closure. Although a corresponding concept had been worked out the retrieval of all waste before closure became statutory order in 2013. Measures are still being implemented to extend the service life of the underground drift system to enable safe retrieval over the next few decades and to minimize fluid exchange in disposal chambers in an emergency brine inflow.

Sealing experiences at Asse II mine can therefore be divided into two categories. The long-term sealing in rock salt with salt concrete was investigated for the application in other HLW repositories. Additionally, flow barriers are being constructed from Sorel concrete to delay and reduce the exchange of fluids for a possible beyond-design brine inflow at the Asse II mine. While both types of constructions differ in their application and their constituents, both must be mechanically stable, stiff enough to build up radial stresses against the creeping rock mass to close micro cracks of the EDZ and they need to be chemically stable against a fluid. The applications have not only led to in-situ experiences (e.g., the processing of the materials in the underground in an adequate time and quality), in addition to that the almost serial construction of flow barriers has established a suitable quality control system.

3.2 Salt concrete to test long-term sealing of horizontal drifts in rock salt

Fischer (1990) suggested a symmetrical multilayer EBS in rock salt to perform long-term sealing of horizontal drifts in both directions. The concept distinguishes components of the construction regarding their function. The three main components are:

- **a hydraulic sealing system** of multiple layers on the outside of the EBS assures instant sealing after completion – to be composed of asphalt
- **a long-term sealing** at the inner side of the hydraulic seal that develops its sealing function over time as the surrounding rock mass creeps onto it and compresses it – to be composed of salt briquettes
- **the central abutment** that carries and guides the load coming from the creeping rock mass and keeps the sealing in place – to be composed of salt concrete

While the central abutment and the long-term sealing are only composed of salt concrete and salt briquettes respectively, the hydraulic sealing with instant tightness is more complex. Figure 3-2 shows the major functioning elements of the hydraulic seal. The design includes a chamber and the above located blind raise in the center of the component, both containing bitumen with filler. Via a declining borehole the raise is connected to the open drift outside the barrier. Due to this connection a pressure increase in the drift should push the bitumen into potentially existing gaps or joints within and around the seal. The larger density of the bitumen ensures that it remains below the pressurized fluid coming from the drift. The advancing abutment (called pre-dam, in German: Vordamm) made from salt concrete keeps the bitumen chamber and raise in position, while its face towards the drift is protected by poured asphalt.

Under pressure, the salt concrete element between the chamber and the deeper positioned sand-asphalt element shall remain intact but at the same time it should glide along the contour to compact the compressible sand-asphalt, poured asphalt, and long-term sealing elements. The sand asphalt separates the filled bitumen from the long-term sealing due to the shape of the contour and its higher specific gravity. The poured asphalt finally prevents the sand-asphalt being squeezed towards the long-term sealing. Additional supporting walls are required to construct the EBS with its different types of asphalt seals in a retreating operation.

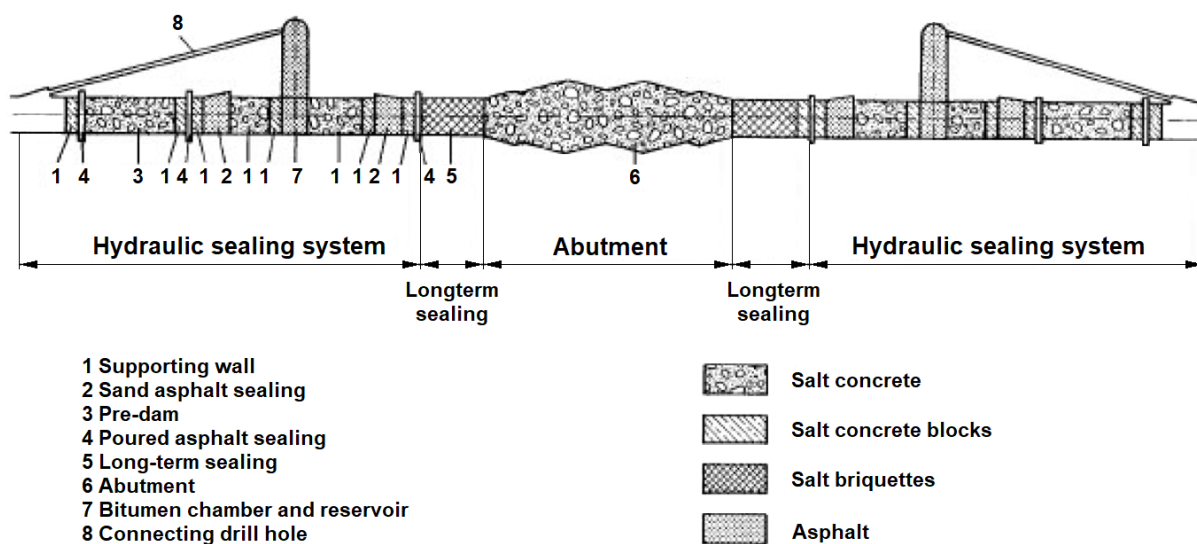


Figure 3-2: Side view of a symmetrical EBS concept for fluid pressure from both sides, after (Fischer, 1990)

The execution of one half of this EBS concept and an additional pressure chamber at the backside were planned at Asse II mine to test the tightness and technical feasibility of the concept, but only the advancing salt concrete abutment was realized (Kreienmeyer et al., 2008, p. 47ff). This salt concrete element is 8 m long, about 5.5 m wide and up to 3.4 m high with a volume of 128 m³. Each cubic meter of the mixture contains 380 kg of cement, 169 liters of NaCl-saturated brine and 1496 kg crushed salt. The construction was split into 4 concreting sections in the first phase, followed by further 3 sections in the second phase. Towards the roof a 0.1 m high gap was left in the first place, that was later filled with salt concrete by hand.

Finally additional cementitious injections were placed into the hand filled material (Gläß et al., 2005).

10 years after its construction the permeability of the abutment regarding gas and brine was overall sufficiently low in the salt concrete body, in the contact zone with the walls and the floor, and inside the former EDZ (see Table 3-1). However, the filled roof gap did not perform as well and showed a permeability between approximately 10^{-12} m^2 and 10^{-19} m^2 so that construction measures need to be changed. Additionally, the EDZ showed its maximal permeability near the roof, which underlines the negative effect of the low-quality filling. Furthermore, it is believed that the two orders of magnitude higher saline permeability is due to secondary leaching.

Table 3-1: Permeabilities to gas and brine in the Asse seal (Gläß et al., 2005)

	Gas permeability (m^2)	Brine permeability (m^2)
Salt concrete body	$6.0 \cdot 10^{-19} - 4.4 \cdot 10^{-24}$	$4.1 \cdot 10^{-20} - 9.0 \cdot 10^{-21}$
Contact zones with the walls and the floor	$6.0 \cdot 10^{-23} - 1.0 \cdot 10^{-24}$	$8.0 \cdot 10^{-20} - 1.4 \cdot 10^{-21}$
Contact zone with the roof	$2.1 \cdot 10^{-13} - 6.5 \cdot 10^{-19}$	-
Rock salt contour (former EDZ)	$6.5 \cdot 10^{-21} - 2.0 \cdot 10^{-24}$	-

The middle section of the filled roof gap showed the smallest compressive stress, indicating the incomplete connection to the rock mass despite the injections made. Hydraulic fracturing tests showed that the contact zone and the former EDZ were the weakest areas of the sealing, whereas no fracture occurred inside the salt concrete body. Ultrasonic measurements located the porous material and the incomplete connection in the roof accordingly. While the walls did not reflect any signals, some local heterogeneities were identified in the floor, which had no negative effect. Ground penetrating radar additionally recorded a disturbed zone between the face and up to 1.6 m into the seal, which was also reflected in lower compressive stresses that were reached here. Core samples confirmed earlier observations. Despite these deficiencies, a permeability $< 10^{-18} \text{ m}^2$ was achieved over the whole in situ seal. Still additional attention should be spent on the improvement of the roof filling (Gläß et al., 2005). Further improvements on the concreting process and deformation of the contour could also be based on the “pilot study” which was carried out prior to the Asse seal (Mauke et al., 2007).

3.3 Sorel concrete for the construction of flow barriers

In 2013 the retrieval of the LLW and ILW from Asse II mine became statutory order. To allow the time-consuming retrieval operation from the underground, “emergency planning” was started to minimize the probability of a beyond-design-brine-inflow and to minimize the radiological consequences of such an event. The emergency planning comprises two parts:

- Preventive measures executed to allow a safe operation and to be prepared for an emergency. These include the filling of remaining cavities, construction of sealing structures (i.e., “flow barriers”), improvement of brine management, and planning of emergency measures.

- Emergency measures that will only come into operation if an emergency arises. For example, the retreat from the underground, the filling of emplacement stopes with fluids, artificial flooding against the natural flow, and sealing of the shafts.

Flow barriers at the Asse II mine are geotechnical constructions made of Sorel concrete that seal parts of the underground workings from each other to prevent circulation of liquids. During retrieval they ensure that any contaminated liquid will remain inside the emplacement stopes so that the operation can continue safely. In a post-operational phase they additionally delay and reduce the mobilization and transportation of radionuclides (HelmholtzZentrum münchen, 2008) by guiding the rising fluid around the emplacement stopes (Heydorn, 2006), see Figure 3-3. As the underground mine works are connected to carnallitic salt layers that bear magnesia, the expected solution in the former underground mine drift system will contain magnesia as well. Thus, Sorel concrete was chosen to construct the flow barriers due to its chemical and mechanical stability in the presence of magnesium brine and good sealing properties.

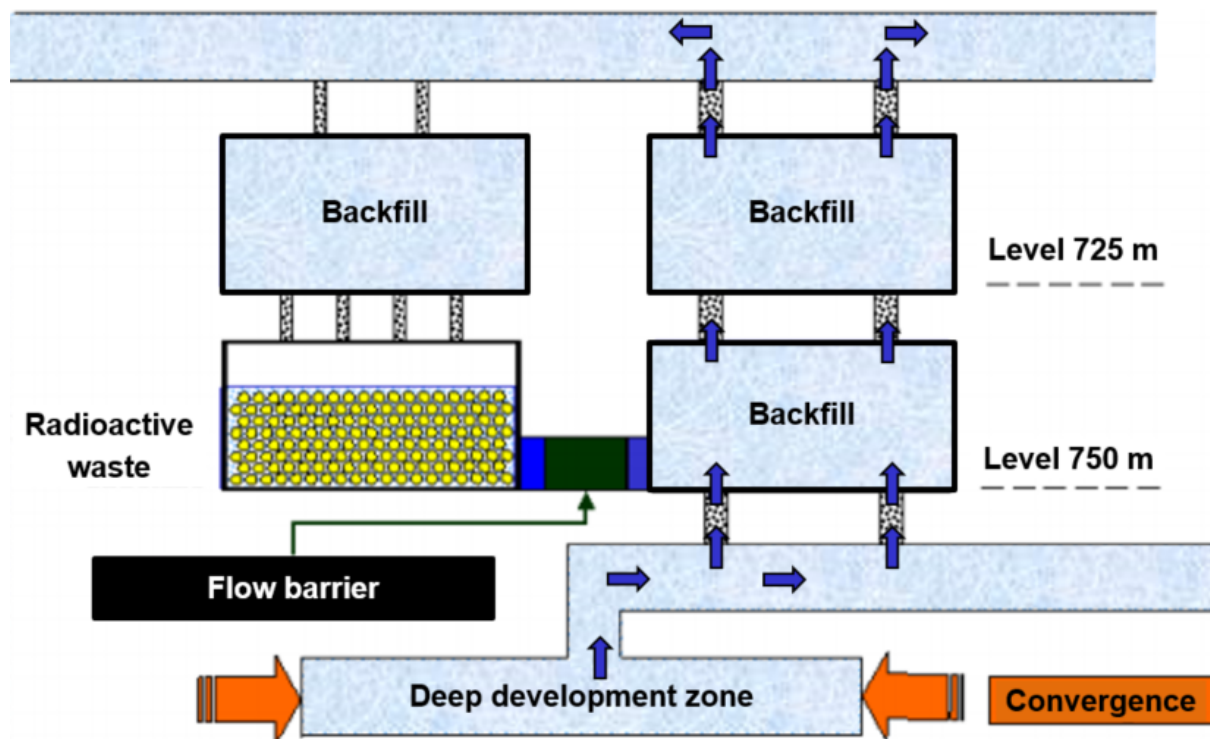


Figure 3-3: Schematic position and purpose of a flow barrier between stopes, after (Heydorn, 2006)

Determination of hydraulic requirements

In a pre-study the location of flow barriers and their geometries were planned based on existing surveying data. A structural model of the underground drift system was set up to simulate the radionuclide migration in case of a beyond-design brine inflow. With this model the locations and resistances of the sealings were determined (Köhler et al., 2019; No. 5). The hydraulic requirements are a prerequisite to start planning flow barriers at the right locations (Heydorn et al., 2018).

Each flow barrier consists of a core barrier constrained by an abutment on each end (see Figure 3-4). To stabilize the abutments additional stowing material can be used to back up the

free faces (Köhler et al., 2019; No. 5). As flow barriers are located at access points towards emplacement stopes, their shapes and sizes can differ, although simple shapes are preferred. The length of the abutment is at least equal to the largest diameter at its position. For a typical drift profile with a 20 m² cross section, a length of around 5 m is therefore required. The core barrier in turn has a length of about 30 m. Such a flow barrier is therefore built with 800 m³ of Sorel concrete (Heydorn, 2006).

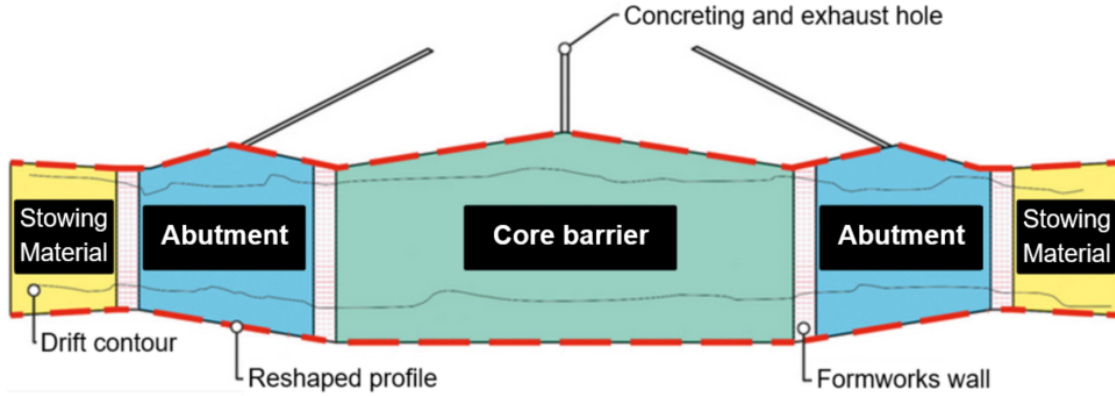


Figure 3-4: Basic concept for a horizontal flow barrier at Schachtanlage Asse II (Köhler et al., 2019; No. 5)

The fabrication of each flow barrier follows a defined order that is summarized in Figure 3-5 and explained below.

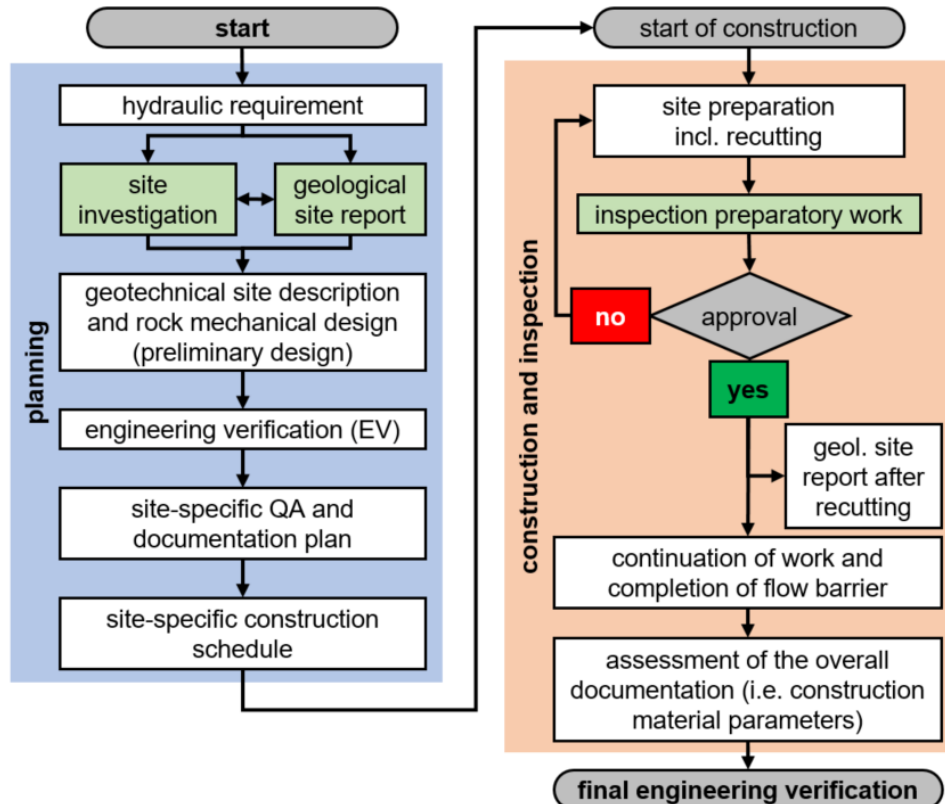


Figure 3-5: Scheme of the flow barrier building process sequence after (Köhler et al., 2019; No. 5)

Site characterization: To build a high-quality seal the building conditions need to be characterized before construction can commence. This incorporates surveying the drift

geometry and position, documentation of existing boreholes, as well as detailed long-term convergence monitoring and up-to-date depth and permeability measurements in the EDZ. Any drilled hole in the sealing section or nearby will be backfilled in line with quality requirements to prevent any short circuit for migration paths (Heydorn, 2006).

Planning: Based on the site characterization the specific dimensions of the flow barrier and the required profile cut of the contour are planned. These will ensure a minimum hydraulic resistance according to the pre-study with the structural model as well as gradual transitions between roof, side walls and floor. The final design typically aims for a hydraulic resistance which is one order of magnitude above that required. A design verification against the pre-study is the foundation for a site-specific quality assurance (QA) and documentation plan. Additionally, a schedule is prepared for all mandatory tasks during construction to document the process and thresholds to be reached. All relevant documents are handed over to the nuclear and mining authorities for approval (Köhler et al., 2019; No. 5).

Construction execution: Prior to the construction some preparation work is needed. At first holes are drilled from a higher level to each section of the barrier. They are used to pour in concrete and to let air escape. Subsequently a road-heading machine will execute the profile cut, to remove parts of the EDZ and reshape the profile. For a gradual transition between the sections the EDZ around the abutments is removed in a cone shape, starting with a minimum size at the free face and increasing towards the core barrier up to its dimensions. This shape fixes the position of the abutment geometrically. Although a simple profile is preferred, the roof will be dome shaped for a maximum filling degree without roof gap (Köhler et al., 2019; No. 5). The construction itself starts with strip foundations out of Sorel concrete at the end of each section. On top of that formwork walls are build out of pre casted Sorel concrete bricks and mortar (Asse GmbH, 2016). They constrain each section and allow concreting in place, which begins with the abutments and is followed by the core barrier including the above located concreting drillings. The high position of the concrete inflow increases the setting pressure from installation onward. It will therefore reduce the time until radial stresses built up and reduce hydraulic pressure differences, minimizing further development of an EDZ. Depending on accessibility additional stowing material can be used to back up the free faces of the abutments before or after building the barrier (Heydorn, 2006).

The selection of Sorel concrete as the construction material follows the same considerations as for long-term sealings. At first mechanical and chemical long-term stability against fluids are required. At Asse II mine these are especially $MgCl_2$ -rich solutions. Furthermore, the low permeability of the material will deliver high hydraulic resistance. Additional stiffness accelerates the build-up of radial stresses and by that reduces the development of any future EDZ. The material then must provide high strength to redistribute these stresses from the rock mass. Eventually the processing of the material in adequate time and quality, as well as its transportation underground are of utmost importance. The selected mixture "A1" is composed of 25% $MgCl_2$ solution as a mixing fluid, 63.7% crushed rock salt with a defined size distribution and 11.3% MgO as binder (BfS, 2009a). Its fluid permeability is approximately 10^{-20} to $1.6 \cdot 10^{-19} \text{ m}^2$ (Heydorn, 2006). This composition reached a higher stiffness compared to its predecessor "R 29.6 A2" that was compressed in a pilot test (Köhler et al., 2019; No. 5). The

A1 mixture shows a majority of the 3-1-8 phase and a minor quantity of the 5-1-8 phase (Freyer, 2015).

To start concreting a flow barrier, strict production planning is required. Each component of the Sorel concrete is separately transported from the surface to the construction material station underground, where the rock salt aggregates and the MgO are mixed to a dry pre-product. From here the mixture is pneumatically transported to a semi-mobile mixing unit where a $MgCl_2$ -solution is added to produce the concrete. The ready-mix is pumped into the borehole. To ensure Sorel concreting follows the plan, the constituents can be inspected on arrival, formulation can be checked, temperatures measured, and samples tested (e.g., uniaxial compressive strength).

Assessment: Following the construction a final engineering verification is used to confirm the quality of the flow barrier based on a QA audit, supervision reports, and any geotechnical measurements.

The flow barriers at Asse II mine show strong similarities with long-term sealings for final waste disposals regarding the preparation work, size, and applied materials. Moreover, the applied quality control and analysis of the actual hydraulic resistance have now established ways to proof the integrity of such barriers. A total of 32 flow barriers were constructed between 2006 and mid-2019. Up to the end of that phase 16 of them already received final engineering verification, to prove they achieve the required hydraulic resistance. On average each flow barrier required around 1,630 m³ Sorel concrete with approximately 30% in the core barrier and 70% for the abutments. The work continues for around 20 more of them (Köhler et al., 2019; No. 5). Based on these numbers the construction of flow barriers has become a standard procedure on an industrial scale that can be adapted to long-term sealings in other repositories.

The current procedure goes back to a long history at Asse II mine including multiple test barriers (Köhler et al., 2019; No. 5). Four of them can be summarized as follows:

- The first test barrier PSB A2 was built in 2003 at 775 m depth in the Leine rock salt. It is 40 m long with a 30 m core barrier and two 5 m long abutments. The barrier was not stiff enough as radial stresses did not increase up to the expected level. In the long-term this could lead to the exceedance of the fluid pressure criterion in the EDZ and consequently open migration paths. Although the permeability requirements were met the stiffer recipe A1 was favored for a new trial. Furthermore, it was decided to pump with a larger height-difference and with larger volumes, which in turn led to new processing equipment.
- The second barrier PSB A1 was built in 2006 at the 950 m level in the Stassfurt rock salt layer. It has a total length of 30 m and is composed of a core barrier of about 15 m between two abutments. The mix unit was located 60 m above the barrier to create additional setting pressure at the end of the concreting process by filling the borehole, too. The filling inside the borehole and the constant convergence of 0.3 to 0.4% per year over preceding years led to a fast built up of radial pressure. In 2019 it reached

around 13 to 14 MPa and confirmed the stiffness of A1. During hydration, temperature up to 105 °C was reached. The barrier is still under 2 MPa fluid pressure from the pressure chamber behind it. This large-scale experiment showed that the Sorel concrete could be produced, transported, and processed on an industrial scale. Good filling of the cavity, integral tightness, and hence a sufficient low permeability were reached. Recipe A1 was used for further sealings at Asse.

- In a third test called K2C-750-1 the A1 mixture was applied in a carnallitite layer with similar outcome. Therefore, this Sorel concrete mixture has been considered suitable for carnallitite, too.
- A fourth test was carried out in staple shaft 4. Here the mixture A1 proved to be suitable for vertical sealing. The more than 100 m long Sorel concrete column between levels 750 m and 850 m showed high settlement stability. Because the removal of the EDZ over a long shaft was difficult, an injection technique and a corresponding testing procedure for permeability resistance were developed.

In general, the Sorel concrete proved its suitability for horizontal and vertical seals. In comparison to a long-term seal here the requirements are challenging as well but not as rigorous.

3.4 Selected further learnings

3.4.1 Well installation for monitoring

Some flow barriers at Asse II mine cover sumps that have monitored brine inflow over a long period. To continue monitoring these inaccessible areas after concreting, the sumps are prepared accordingly. At first drainage holes are drilled from a higher level. Initially a large diameter is drilled with raise boring equipment and then sealed with Sorel concrete. In a next step, the smaller drainage holes are drilled inside the Sorel column to the final diameter. At the lower end of the hole, circular Sorel concrete support rings are installed between roof and floor to secure the future bottom of the sump located inside the barrier. These rings are stacked onto each other and sealed against roof and bottom of the drift. The whole procedure is carefully tracked with frequent in-hole camera surveys. Finally, the flow barrier can be constructed around the readily prepared sumps (Asse GmbH, 2016).

3.4.2 Crushed salt as backfill

In many concepts crushed salt is an integral part of the multi-barrier system. The material is anticipated to reach a similar permeability compared to the natural rock mass on a long-term basis. As it is material from the host rock or very similar to it, crushed salt remains chemically stable. Because of that, the crushed salt will be able to take over the sealing function over time. Besides that, it reduces the maximum deformation of the surrounding rock mass, leading to a quicker equilibrium of the differential stresses and therefore protection of the natural barrier. The denser the material, the less time is required until these positive effects become effective. This density or initial filling degree of the drift depends on factors like grain size distribution, backfilling technology including compaction, and the remaining roof gap after filling. Backfilling carried out with slinger trucks in combination with material from the

roadheading process at Asse II mine resulted in an initial density of 1.46 g/cm³ and a corresponding porosity of 33%. In contrast, pneumatic backfilling with material from other mines only delivered a density of 1.27 g/cm³ and a porosity of 41%. The time dependent self-compaction of the crushed salt accelerates with both a higher water content and more heat (Droste et al., 1998).

The TSDE (Thermal simulation of drift emplacement) at the Asse II mine was an accelerated drift closure experiment under heated conditions, in which six mock-up casks for radioactive waste were used to heat the surrounding crushed salt backfill and rock mass over eight years. The closure rates were observed to be below the expected values. In heated zones the porosity decreased from 35 to 23%, whereas non-heated areas only reached 30%. Settling of the backfill started in its upper zone and continued towards the lower zones. Two-thirds of the vertical drift closure (contour deformation) in heated drifts originated in the uplift of the floor (Droste et al., 2001).

As most of the experiments with crushed salt in Germany were made with rock salt that originated from the roadheading process at Asse II mine (including a subsequent sieving process to remove large grains), it can be referred to as a reference material. Although the specifications were not always the same, a maximum grain size of 31.5 mm and a natural moisture content of 0.1 mass-% were typical (Müller-Lyda, 1999). For example, a relative humidity of 75% will increase the moisture content of the rock salt to 1 mass-% (Fröhlich & Conen, 1998), which in turn reduces the mechanical resistance of the crushed salt backfill by 50%.

The projects BAMBUS (Bechthold et al., 1999) and BAMBUS II (Bechthold et al., 2004) focused on the understanding of the backfill behavior, on the increase of the related data base and on improvements of the numerical modelling codes in combination with the corresponding material laws to predict the behavior. The initial experiments covered the dependencies between backfill porosity, permeability, and thermal conductivity. The second project continued after the completion of the TSDE experiment at the Asse II mine. The retrieval of two mock-up casks was accompanied by physical, mechanical, and hydrological experiments at samples of the backfill and the surrounding rock that were in various compaction and deformation stages. These investigations quantified parameter values for simulation models in the backfill and in the surrounding rock including the EDZ. By that they extended the basis for repository design optimization and long-term performance prediction of barriers in salt repositories for radioactive waste.

3.4.3 EDZ size and healing

The following information are dominantly summarized and translated from GSF-Report-247 (Brasser & Droste, 2008). The disturbance of the three-dimensional compression state of the rock mass by excavations like drifts and chambers leads to the development of deviatoric stresses. The corresponding deformation in turn triggers micro-cracking of the rock mass, especially at the drift contour over longer periods. The permeability of this excavation damaged zone (EDZ) at Asse II mine was investigated in the projects ALOHA (Wieczorek & Zimmer, 1998) and ALOHA2 (Wieczorek & Schwarzianek, 2004). Many permeability measurements were carried out at four locations in the Asse II mine, which showed an EDZ thickness in all

open drifts of not more than 0.5 m in the sidewalls and up to 1.5 m in the floor. This zone around the cavity showed an increased permeability from 10^{-16} to 10^{-15} m² compared to the natural permeability of rock salt of 10^{-21} m². Continued research on the compaction of crushed salt near a heat source executed at the Asse II mine in the project BAMBUS II showed that previously heated zones after cooling down showed even higher permeability (Rothfuchs et al., 2003).

With a permeability between 10^{-20} and 10^{-18} m² a 25 m long supported drift section on the 700 m level showed considerably lower values compared to unsupported drifts. The circular steel support including concrete backfill was installed 90 years before. As the support was able to carry a high load, the surrounding rock mass was under high compressive and reduced deviatoric stress. This resulted in compressed micro cracks and reduced permeability. Although the cracks were compressed, they did not heal. As they still existed, the permeability remained higher compared to undisturbed rock (Wieczorek & Schwarzianeck, 2004, p. 57). Regarding the importance of the EDZ for long term safety, Wieczorek and Schwarzianeck (2004) concluded that:

- creep properties of the rock salt will eventually lead to compressive stresses in a repository, which will lead to a reduced permeability. The EDZ will therefore only affect the area immediately around sealings
- proof is needed if the permeability reduction in the proximity of sealings is sufficient or if profiling of the contour is required just before the construction of the seal and if profiling is suitable to reduce the EDZ

The development of the EDZ over time was investigated in ADDIGAS (Jockwer & Wieczorek, 2008). Here the permeability of the EDZ in 800 m depth remained almost constant over a year, after the floor had been re-mined down by 1 m. Based on this, it was concluded that the time would be sufficient to prevent the development of a new EDZ during construction of seals.

3.4.4 Shaft sealing

According to a conceptual planning of backfill and sealing the shafts 2 and 4 at Asse II mine were planned to be fully filled from their bottom up to earth's surface. The deepest part of shaft 4 has already been backfilled with diabase aggregates. During the future closure they will both be filled (Figure 3-6) from their current bottoms as follows (DBE, 2006):

- Starting from the bottom the shafts will be backfilled with Sorel concrete or Sorel grout up to the 490-m-level to minimize water and radionuclide transportation. Additionally, it will act as an abutment for the layers above.
- Above this, sealings made of 8 m Sorel concrete & bitumen, 30 m Sorel concrete, 10 m salt clay and 10 m bentonite will be used in the water-tight rock salt layer around 450 m below surface to seal the underground structure. This arrangement is long-term stable in contact to MgCl₂-rich brine from below and NaCl-rich brine from above (TUBAF, 2005). The bitumen furthermore provides instant sealing capabilities.
- At a depth of around 400 m, a 20 m thick layer of magnesite rock aggregates and MgCl₂-rich safety fluid will be used.
- The upper part of several hundred meters combines hard rock aggregates and NaCl-rich brine. A concrete plug finalizes the column.

The concept uses findings from the large-scale test for waterproof sealing at Salzdetfurth Mine (Breidung, 2002). According to that an integral permeability of the sealing and its surrounding rock mass of less than $5 \cdot 10^{-16} \text{ m}^2$ and an air-entry pressure of 600 kPa (Buhmann et al., 2005) are required, as well as the stability of the construction's position and chemical long-term resistance are needed. In that case, safe, long-term stability is even assured if the actual permeability is one order of magnitude larger. The compliance with the requirements is examined during dimensioning planning and a proof of function is made after erection of the structure. The position stability is assured by abutments and the brine column above. The function of the sealings can be investigated through pneumatic pressure tests (GRS, 2006).

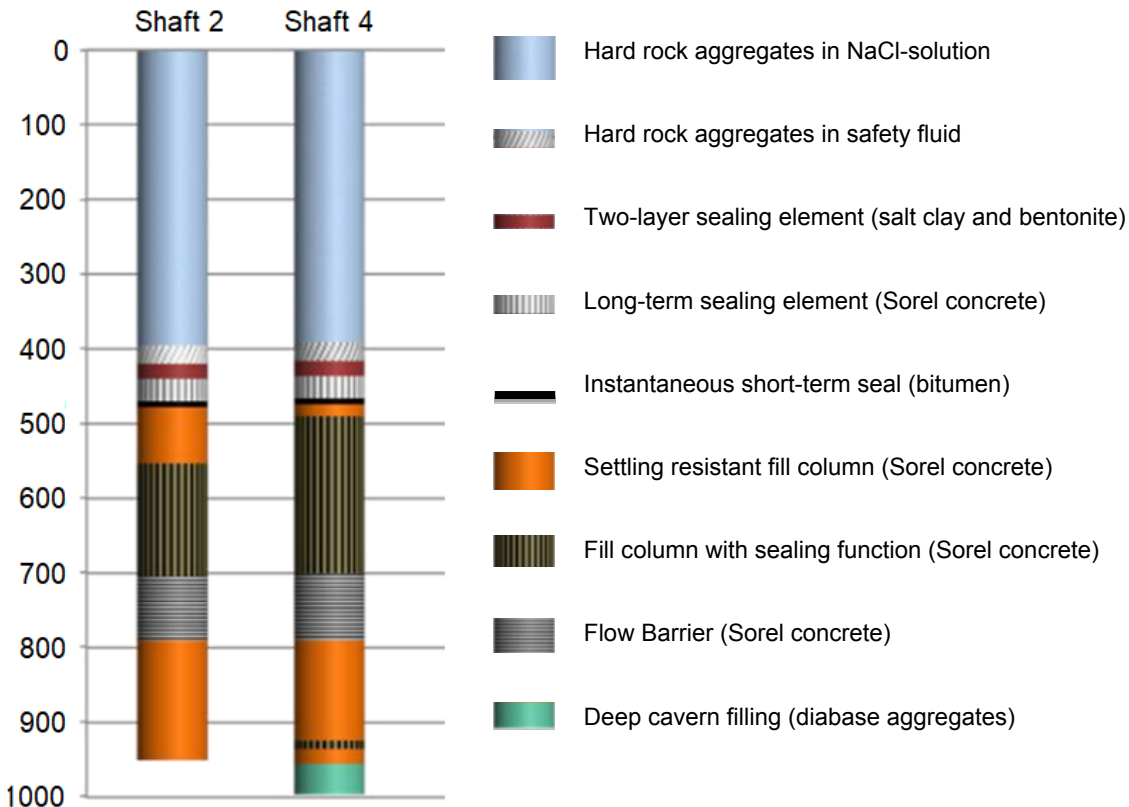


Figure 3-6: Asse shaft 2 and 4 sealings (Kudla et al., 2013; pp. 19-21)

4 Case study: Morsleben

The Morsleben repository has a long history in rock salt and potash mining. Major challenges are induced by the exposed carnallitite and hard salt, the close vicinity to the salt table (i.e., the salt-caprock interface) and the complex structure of large cavities (BfS, 2016c). The case study illustrates large scale backfill with salt concrete, learnings from test sealing structures in rock salt and anhydrite, planned sealing measures to isolate decentral parts of the repository in the east, west and south from the remaining openings as well as a shaft sealing to prevent an inflow of brine.

4.1 Introduction and Project Description

The *Repository for Radioactive Waste Morsleben* (German abbreviation: ERAM) is located close to the former inner German border at the west side of the state of Saxony-Anhalt. In 1971, the abandoned potash and rock salt mine was selected from the existing salt mines of the German Democratic Republic as its central repository for LLW and ILW. The state operated the repository until 1991 when the German Reunion caused an interruption. From 1994 the Federal Republic of Germany continued the operation until 1998. In both periods together a total volume of around 37,000 m³ LLW and ILW was emplaced (BGE mbH, 2018). The former mining activity had left more than 8 Mm³ of open volume that over the years led to a disintegration of the rock mass in parts of the mine workings (BfS, 2016d). Additional measures are necessary to close the repository safely.

“The former salt mine Morsleben does not meet today’s criteria for a repository, but it can be safely closed in accordance with current legal regulations:” (BGE mbH, 2021)

The closure of the repository is planned with all the waste remaining in place under fulfillment of the protection goals for the environment, public and personnel such as long-term containment and limited subsidence. As the closure has not been approved yet, the focus at ERAM is to monitor and maintain the repository to ensure its safety and its ability of being closed adequately according to both mining and nuclear law (BGE mbH, 2018).

4.2 Geology and mine openings

The Morsleben repository is in a Permian salt structure that belongs to the Zechstein group. The rock mass was dominantly shaped by tectonics rather than rising upwards through halokinesis. It is therefore not a classic diapir. On top of a carbonatic base rock all evaporite formations from Werra (z1) over Stassfurt (z2), Leine (z3) and Aller (z4) exist. While the Werra formation has a relatively constant thickness and is locally lifted upward along faults, the latter three formations have been heavily folded. The folding in the west is very strong with layers that undulate several hundred meters in height over short distances. Towards the east the folding becomes less intense. Above -140 m (relative to mean sea level) the salt has been eroded, with only caprock and anhydrite remaining under the quaternary top layer (see Figure 4-1) (Behlau et al., 2000).

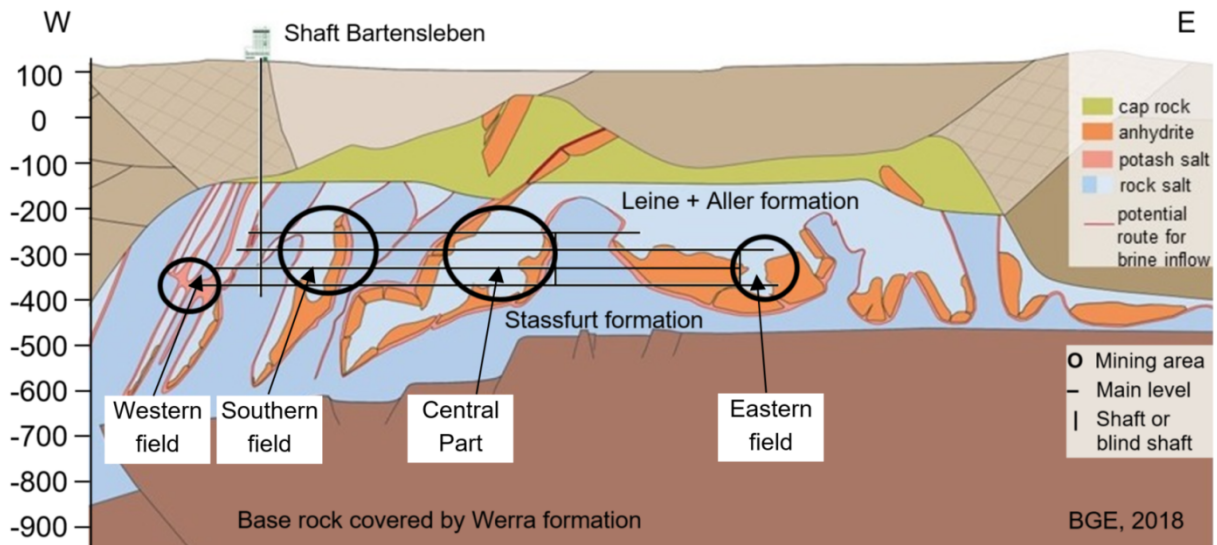


Figure 4-1: Geological east-west cross-section through ERAM close to shaft Bartensleben after BGE, 2018

ERAM can be reached from the surface via the two shafts Marie and Bartensleben. The underground mine works stretch over a maximum length and width of 5.6 km (NW-SE) by 1.7 km (W-E) and account for a cavity volume of around 5.4 M m³. More than 80% of that volume belongs to the Bartensleben mining area where LLW/ILW emplacement took place. The area has been developed by four main levels with the first one being on -253 m (relative to mean sea level) or 380 m below land surface level (bsl). The remaining levels continue with a spacing of about 40 m to the total depth (BfS, 2009b).

The Bartensleben mining area is divided into the Central Part and several satellite fields (east, north, west, south). In the western part of the Bartensleben mine, the Zechstein salt formation is about 580 m thick, whereas it is only 380 m in the east (Behlau et al., 2000). As mining focused on the Stassfurt and Leine formations the mining parts are separated by unmined zones that are only intersected by connecting drifts. While most of these drifts are surrounded by salt, at least one was driven through anhydrite. Depending on the mined mineral the stopes and their alignment vary. Whereas the steep potash layers that were mined earlier led to narrow and high cavities that were stacked on each other in the southern part, the rock salt in the Central Part was exploited in large stopes of up to around 30 m in height and width, and 100 m in length, a few times even longer. Depending on its quantity and type, the waste was separately emplaced in a dedicated part of the mine, mostly on the 4th level (incl. 4a and 5a) (compare Figure 4-2).

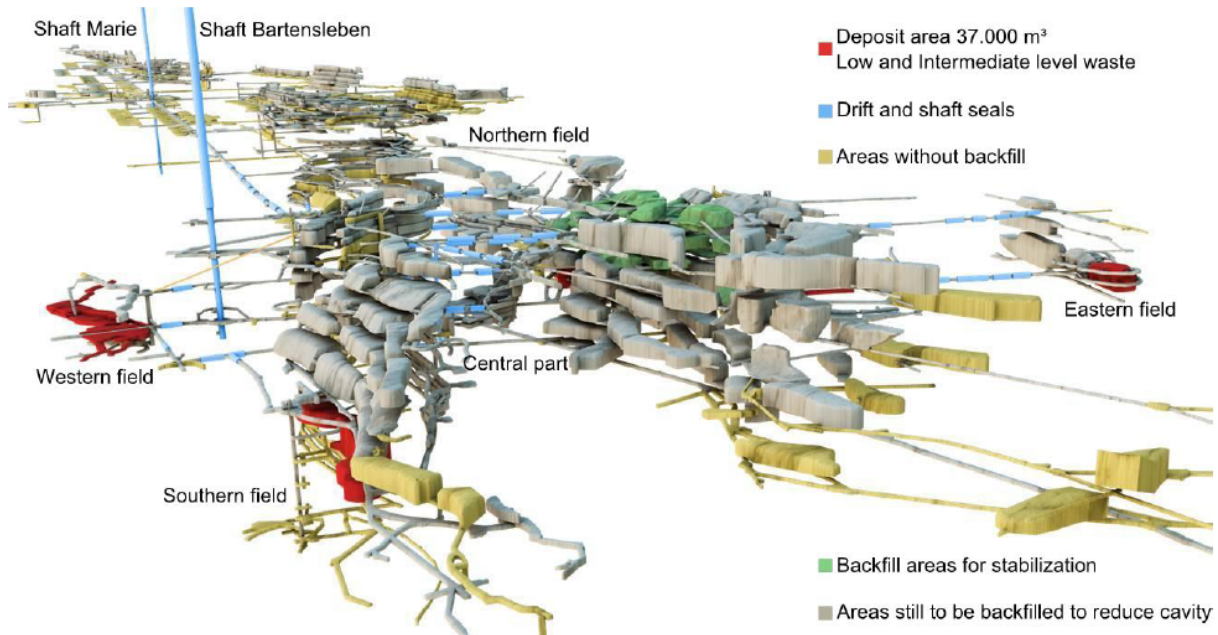


Figure 4-2: ERAM mine workings of shaft Bartensleben in the foreground and shaft Marie in the background (Mauke & Herbert, 2013)

4.3 Geotechnical Barriers within the Safety Concept

The common goal for the different types of waste that have been separately disposed of in different parts of the mine, is to contain their nuclear inventory in place and to seal it from the biosphere. According to the current closing concept (BfS, 2009c) following geotechnical barriers are required. To restore the natural barrier and to keep liquids outside the repository the shafts need to be sealed. In addition to that 75% of the remaining cavities are to be backfilled for long-term stability, to limit void volume for leaching processes and to seal the emplacement areas. The closing concept is currently being reviewed, which may lead to future changes (BGE mbH, 2018). It is planned to submit the updated version in 2026. So far four backfilling categories are planned of which one is assigned to each underground working. The categories after (Preuss et al., 2002) are:

- Category I (drifts with high requirements) are sealings close to the emplacement areas or between the workings of shaft Bartensleben and shaft Marie to lock fluids and gases inside their current location and that serve as a barrier for solutions that could potentially penetrate the repository drift system. Around 20 horizontal sealing structures made of salt concrete are required in rock salt, one horizontal sealing made of magnesia concrete in anhydrite and one vertical sealing in a raise that will be sealed with bitumen. These constructions make up 1% of the salt concrete backfill.
- Category II is assigned to workings that need geo-mechanical stabilization to protect the natural barrier against ruptures from high stresses. This includes the already backfilled central part and workings that are potentially endangered for an inflow of solutions. In total, 23% of the salt concrete will be used here to fill between 95 and 100% of the voids and to reach widespread contact between filling and the roof.
- Category III workings will primarily be backfilled to reduce the cavity volume to delay and to minimize impacts of a solution inflow and corresponding dissolution. Secondly,

the backfill improves their geomechanical stability. This category requires around 58% of the salt concrete if stopes are filled at a required 65% of their volume.

- Category IV comprises all workings that expose carnallite layers. To significantly reduce the possibility for dissolution, these locations are targeted for total backfill. Here the remaining 18% of the salt concrete backfill will be used. As many areas are inaccessible, the filling degree cannot be verified and is therefore assumed to be 50% during calculations, to be conservative.
- The remaining open space will serve as a storage for gas that will develop over time from waste (BfS, 2016b).

For category I the salt concrete mixture “M2” is planned, while for categories II through IV mixture “M3” is planned (Mauke et al., 2012). The mixtures have been designed according to the requirements of the categories. As M3 mixture has less cement it will develop less heat during hydration and therefore induce less stress compared to M2 mixture (Table 4-1).

Table 4-1: Recipes of the salt concretes M2 (for stabilization of Central Part and for sealings) and M3 (for main backfilling volumes) (Engelhardt et al., 2003)

	M2 (mass-%)	M3 (mass-%)
Rock salt (NaCl) maximum grain size 20 mm	53.8	54.5
Water	13.4	12.6
High slag sulfate resistant cement (CEM III)	16.4	9.9
Coal fly ash (DIN EN 450)	16.4	23.0

Even fillings that are not planned as a sealing will over time experience compressive loads that result from convergence of the surrounding rock salt. This will in turn reduce gaps as well as the adjacent EDZ and therefore increase the overall resistance of the repository against fluids (BGE mbH, 2018). Hence, all backfilled mine works will support the safety goal to contain the nuclear inventory and to keep liquids away from them. As opposed to loose backfill (e.g., crushed salt), the salt concrete itself contains less porosity, will not deform as much, and will sooner carry loads from the rock mass.

Before seals can be constructed the suitability of the technique has to be demonstrated in a series of investigations. Starting with a concept design of the sealing, at first model calculations as well as laboratory trials, technical trials and in-situ trials will be made. If all of these are successful a prototype can be built. Only if this works according to the requirements the sealing can be constructed (Carstensen, 2019). In the following only large-scale activities will be summarized.

4.4 Salt concrete for horizontal sealings in rock salt layers – category I

A typical sealing structure in rock salt consists of multiple rigid segments, about 25 to 30 m length each. The segments are separated by 1-m long joints with a plastic behavior, created by materials such as salt briquettes (see Figure 4-3). The segments are preferably built in-drift with a simple shape, a constant cross-section and rounded edges (BfS, 2016c). To create such a favorable shape and to reduce the EDZ, typical drift contours are recut by a thickness of 0.2 to 0.5 m before concreting them. Therefore, the salt concrete segment has a larger diameter than the original drift. At the transition towards the unchanged drift the sealing is therefore shaped as a truncated cone with a length of about 1 m (BfS, 2009b). As initial sealing is required, the contact zone of at least one segment of the structure will be post-treated with a cementitious injection. The injection is applied through several ring lines that are placed along the circumference of the drift seal. Rock salt creeps under differential mechanical load, especially evident over long periods. In such host rocks even sealing segments without post-treatment injections are therefore completely enclosed with time, resulting in a reduction of the permeability in the contact zone and EDZ over the whole length of the sealing structure (BfS, 2016c). To inject multiple times in each position, the ring lines incorporate one feeding line for injection material and one flushing line for cleaning. Due to the spacing of about 0.75 m between the ring lines a 25 m long segment requires approximately 30 ring lines, which are collected in a central tube towards the “air side” of the seal. This central tube with a diameter of about 20 cm is removed by over-drilling and is then sealed again (IGH, 2009).

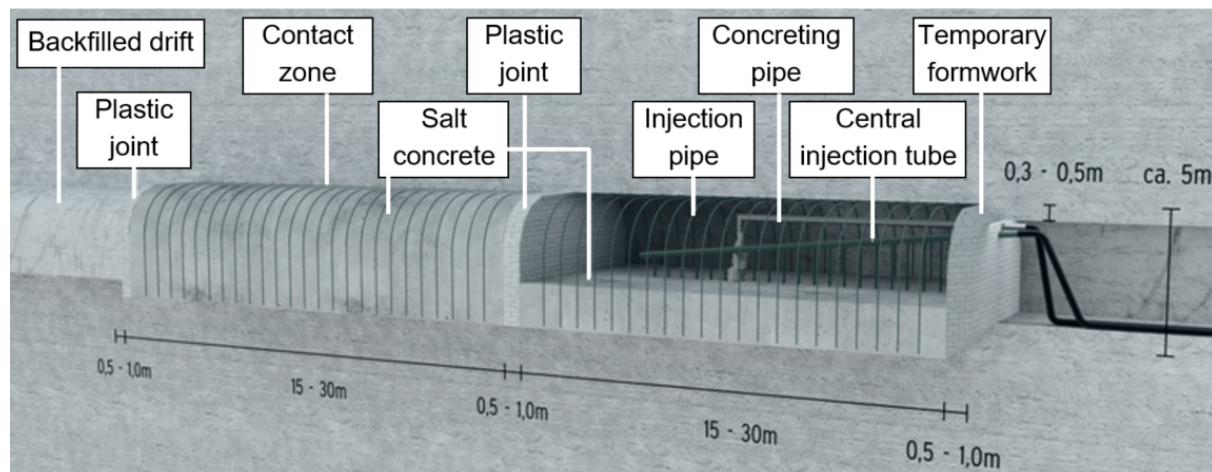


Figure 4-3: Schematic drawing of a horizontal sealing after (BfS, 2016c)

Due to geometrical constraints at ERAM some of the salt concrete seals in rock salt must combine the abutment and the sealing function into a single segment. Consequently, the single segment must demonstrate a minimal hydraulic resistance, remain in its position, include limited fractures, and ensure long-term stability (Laske, 2010). To uncouple effects between chemical corrosion and the hydro-mechanical effects, Müller-Hoeppel defined a maximum permeability of 10^{-18} m^2 at the contact zone (Müller-Hoeppel & Polster, 2004).

4.4.1 ERAM in situ Test Seal - main Hydraulic Test at 2nd Level

To demonstrate the properties of a salt concrete seal according to the planned closure concept the *ERAM in situ Test Seal* was built in a blind (i.e., dead-end) drift in rock salt. The requirements included a permeability of less than 10^{-18} m^2 , a lifetime of at least 20,000 years, stability against a fluid pressure up to 6 MPa, and resistance against NaCl and IP21 brine solutions (Mauke, 2011).

Approximately 6 months after the initial construction of the 20 m² cross-section drift for the in-situ Test Seal, its roof was recut with a taper angle of 3 degrees towards the blind end and with rounded edges to reduce the EDZ (Mauke, 2013). Before filling the void, a site investigation was carried out. and multiple sets of sensors were installed in several positions within the seal, but also in the vicinity of the drift and in an adjacent drift. This included sensors for temperature, shrinking and strain, fluid and pore pressure, stress monitoring, and convergence (compare Table 4-2). Their tasks were to monitor the seal and its near-field and to compare real data with predictions. In addition, two large metal plates were positioned perpendicular to the axis of the drift at approximately 1/3rd and 2/3rd of the length as predetermined breaking planes for the shrinking sealing body but without an effect on the effective sealing length (see Figure 4-4). Furthermore, pipelines for concreting, injecting, and air evacuation were installed.

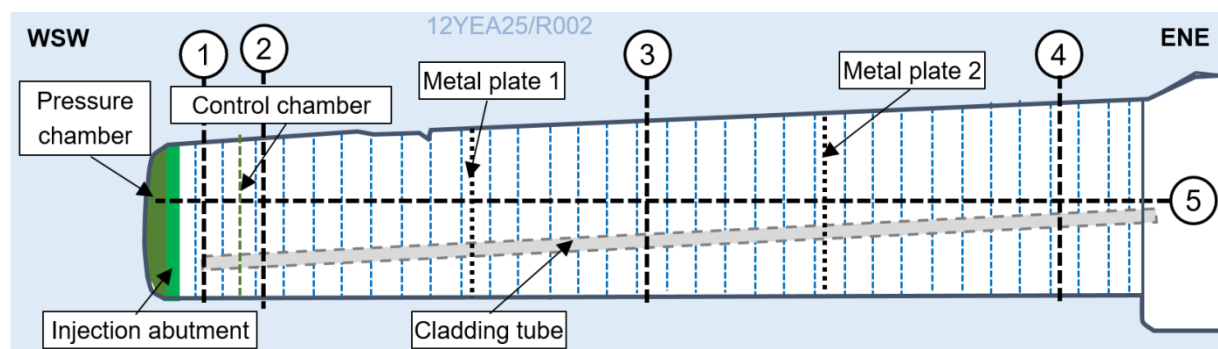


Figure 4-4: Section view of the ERAM in situ Test Seal with cross-sections 1 to 5, predetermined breaking planes (metal plates) and the fluid-pressure-chamber on the left side after (Niederleithinger et al., 2019).

Table 4-2: Measuring devices at ERAM Test Seal, cross-sections 1 to 5 (Stahlmann et al., 2013)

Cross-section	Measuring devices for
1	strain, temperature, pore-pressure
2	strain, deformation, temperature, pore-pressure
3/4	strain, deformation, temperature
5	deformation, temperature

December 2010 the approximately 25 m long sealing was constructed with concrete mixture M2 "wet in wet" over 20 hours. After a few days the temperature of the concrete had reached its maximum (about 64 °C); the cooling concrete shrunk by 0.5 to 0.7 mm/m. The expected widening gap to the edge of the drift was partially compensated for by the convergence of the rock mass (Mauke, 2011). The material is affected by two time-dependent processes: the seal

shrinks while it cures, while it also creeps under a constant load. The calcium-silicate hydrate (CSH) and calcium aluminate hydrate (CAH) phases, which would strengthen the salt concrete, do not exist or are present in the semi crystalline form of gels (Herbert et al., 2010).

Initial hydraulic pretests were carried out approximately 60 days after deconstruction of the formwork. The measurements verified the prediction that a joint would develop between the sealing and the rock mass (Jautze et al., 2012; 2013).

Shrinkage stopped approximately 2.5 months after concreting. In February 2011, when displacement of the drift/seal contour had stopped, the contact zone of the seal was additionally injected in four steps to reduce its permeability. In the first and second step *Ultrafin 12* (diameter $d_{95} = 12 \mu\text{m}$) was mixed with 90% NaCl-solution, while in the third and fourth step it was mixed with 30% NaCl-Solution. During the injections 1.15 m^3 of suspension were used in addition to the 484 m^3 of salt concrete were filled the void initially. Due to its construction, the in-situ Test Seal incorporated beneficial conditions for a high resistance of the salt concrete body, the contact zone and the surrounding EDZ (Mauke, 2011). Sections of core samples from the roof contour demonstrated the dominant filling of joints with the grout. Only isolated micro-fractures appeared (Mauke, 2013).

The removal of the cladding tube including all injection tubes inside was carried out in two steps. At first a step-type drag bit removed the plastic injection tubes inside. Drilling out the steel cladding tube proved to be more demanding. Out of four drill bit types, only one option was able to remove all 16.4 m of tubing. Afterwards it was concluded that no steel tube should be used or it should only be used temporarily during the installation of the injection lines. The hole was sealed with a modified salt concrete that included barite powder to avoid autogenous shrinkage. The concrete was pumped through a pipe at 6 bar overpressure to the end of the borehole and then pulled out in steps by initially 1.5 m and later 3.0 m (Mauke, 2013).

Continued hydraulic tests from 2014 to 2018 showed decreasing permeability over time. In November 2015 the value fell below the target of 10^{-18} m^2 and decreased further, reaching $1.4 \cdot 10^{-19} \text{ m}^2$ in March 2018 (Wollrath et al., 2018). Although the in-situ Test Seal proved the required permeability, it contained cracks. There are cracks at the edges of the seal that are limited in range and that can be explained with existing theories. These do not affect the seal performance. An additional horizontal crack was observed to have formed, which was not explained by prior theoretical models. As no clear guarantee of crack limitation can be made, additional large-scale experiments are planned (BGE mbH, 2018). It is assumed that the high heat of the chemical reaction and the shrinkage behavior of the salt concrete have led to these ruptures. These have not affected the tightness but may have reduced the resistance against dissolution. In the future the salt concrete will be cast in place in multiple steps to reduce the heat load and to allow cooling of each section on its own (BGE mbH, 2018).

4.4.2 Destruction free quality measuring of seals

The Large Aperture Ultrasonic System (LAUS) was used to inspect the in-situ Test Seal for fracture planes (Niederleithinger et al., 2021). The authors report about an adapted interpretation software (InterSAFT, K. Mayer, University of Karlsruhe) that enabled them to detect the planes and to differentiate the reflectors (air gap or metal) up to 7 m from the face.

These were confirmed by drillings. Based on the data, a 3D reconstruction of the seal was made. They report a further improvement by using the Reverse Time Migration (RTM) imaging method (Büttner et al., 2021). Using this method, a separation wall at 8 m was localized. The non-destructive ultrasonic methods are therefore capable to inspect the quality of a seal up to several meters. The LAUS technique is adapted to borehole investigations that could detect joints with alternative orientations (e.g., between contour and seal), and that could be used to measure deeper inside the seal but more limited in its penetration depth.

4.5 Sorel concrete for horizontal seals in anhydrite – category I

Between the eastern part and the central part of the ERAM one drift on the 4th level is in anhydrite. To permanently separate the two parts of the mine from each other a seal is necessary. In contrast to salt, the brittle rock does not creep and therefore drifts do not show convergence. As a result of that, the seal cannot take advantage of an improving connection with the host rock over time. Instead, it needs to be tight at construction. As laboratory tests had shown a swelling pressure of Sorel concrete type DBM2¹ ("Damm-Bau-Mörtel 2" by K-UTEC AG) the material was considered for this purpose.

4.5.1 Conceptual seal in anhydrite at ERAM

The concept seal from 2008 (Krauke & Fliß, 2008) combines two inner core barriers of 30 m length and two outer core barriers of 25 m length with 10 m long pre-seals on both ends. The core barriers are made of Sorel concrete type DBM2 with a planned permeability less than 10^{-18} m^2 while the pre-seals are cement-based with a permeability less than 10^{-16} m^2 . The segments will be separated by Sorel concrete abutments with a length of about 5 m (see Figure 4-5).

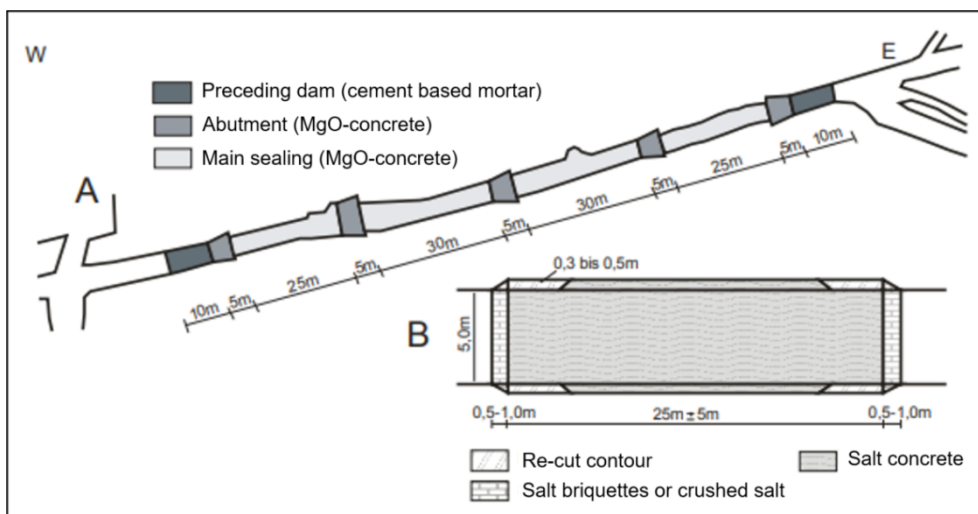


Figure 4-5: Conceptual seal in anhydrite at ERAM with a total length of about 150 m after (Orzechowski, 2017), (Krauke & Fliß, 2008) and (Polster, 2010)

While the inner part of the seal would remain stable against MgCl-rich solutions that could potentially reach the seal in the long-term, a preceding Na-rich solution could already be

¹ DBM2 components (weight-%): MgO (10.5), quartz sand (34.4), anhydrite powder (29.4), micro silica (4.5), MgCl₂-solution 390 – 430 g/l (20.8), soldering flux (0.4)

stopped by the pre-seals. The diverse structure creates a robustness against infiltrating solutions. Within calculations the pre-seals are neglected as a conservative assumption. The MgO-seal elements were planned to combine the sealing function by a pore pressure of at least 1 MPa and the abutment function to carry the load of the surrounding rock mass. Under these circumstances, thermodynamic calculations show an acceptable stability against Na-rich solutions. Because the adjacent potash formation would increase the MgCl-content over time, the seal would eventually be long-term stable. Within the calculations a 20 cm thick EDZ in the anhydrite with a permeability 10^{-17} to 10^{-18} m² was anticipated. The material was to be installed from a higher level to ensure a hydraulic pressure and to increase the initial resistance without injections. Injections were therefore only required to seal the cement-based pre-dams. These were planned to be made of epoxy resin or acrylate (Krauke & Fliß, 2008).

The anhydrite rock mass itself shows a varying permeability from $> 10^{-15}$ m² in jointed zones to $< 10^{-20}$ m² in competent rock. As there is no connection to groundwater bearing layers the rock mass is thought to be chemically stable. This accounts for reasonably imaginable liquids that could access the drift through the mine, as they would be saturated. Therefore, an engineered barrier system should be able to delay the transport of nuclides by sealing any liquids between the east and the central part. Adjacent measures also incorporate backfilling of drifts, the filling of boreholes, and a seal on the second level in rock salt. The engineered barrier is required to have a permeability $\leq 10^{-18}$ m² over a period of at least 20,000 years. Therefore, it must be stiff enough to keep its shape, must have a low permeability, and must be constructible under real conditions. Additionally, it will only be accepted if proof of long-term stability is shown. This includes either the limitation of joints or chemical stability (Carstensen, 2019).

4.5.2 Sorel concrete seals – cast in situ – test site Bleicherode

A large-scale pilot seal was constructed at Bleicherode Mine in 2010 to illustrate the processing of larger quantities of the Sorel concrete DBM2 and show the material can sustain a swelling pressure above 1 MPa. At first a blind drift with a cross-section of about 3.1 by 2.6 m was excavated by smooth blasting technology. It was not possible to recut the contour with a roadheading machine. The construction was followed by measurements to examine and describe the initial state of the test site. The approximately 8.7-m long seal was built between two brick wall abutments left a gap towards the blind end, which could afterwards be used as a pressure chamber (see Figure 4-6) (Mauke & Herbert, 2013). The seal was concreted in 34 hours without interruption (Mauke, 2015). The temperature reached a maximum of 110 °C inside the seal and 65 to 85 °C at the side walls. The swelling pressure decreased concurrently with the temperature decline. In a second swelling phase, at a concrete temperature of around 40 to 45 °C, the swelling pressure reached again 1 MPa but decayed away over the next few weeks. The swelling pressure was therefore not sustainable. Investigators concluded that heating the DBM2 above 65 °C destroyed its swelling tendency. It did not seem feasible to keep with temperatures below this threshold. As a result, a relatively high permeability occurred in the contact zone between the seal and the anhydrite, with the primary leakage occurring through the floor (Mauke & Herbert, 2013).

As the trial failed, the whole concept to prove tightness was reconsidered. The test led to creation of additional requirements related to the preparation of the contour (Carstensen, 2019).

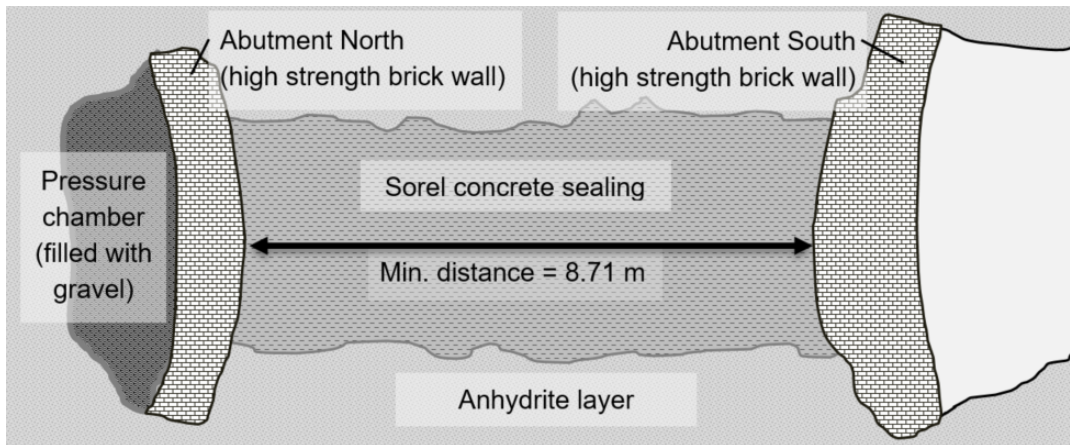


Figure 4-6: Schematic profile of the large scale test in anhydrite after (BfS, 2016c)

In 2012 a 40-m long test drift with a cross-section of 4.5 by 5 m was prepared by drilling and blasting at ERAM for a cast-in-place concrete seal. Strength and permeability tests of the contour followed in the years 2012/13 and 2015/16 respectively. There are still no further results published (Carstensen, 2019).

4.5.3 Sorel concrete seals – shotcrete and bitumen

Shotcreting in combination with bitumen/asphalt is a planned alternative approach to seal in anhydrite. Using shotcrete will reduce the heat input while the bitumen/asphalt guarantees instant sealing. Chemically, the MgO shotcrete will be like the large-scale experiment GV2 in the R&D projects CARLA (Priestel et al., 2010) and MgO-SEAL (Gruner et al., 2017). The EBS will be composed of multiple shotcrete sections, each several meters length, that are divided by air-filled gaps across the whole cross-section. In a second step these gaps will be filled with bitumen/asphalt material and pressurized from the second level of the mine through boreholes. To improve the tightness of the contact zone between the shotcrete and the contour, injections will be made (see Figure 4-7). Before a prototype will be constructed, tests will be done in the laboratory in small and larger scale as well as in-situ. Based on the results the EBS-design will be assessed in model calculations. If these show reasonably good results the prototype can be constructed to proof the concept and to prepare for the actual EBS on 4th level of ERAM in anhydrite (Carstensen, 2019).

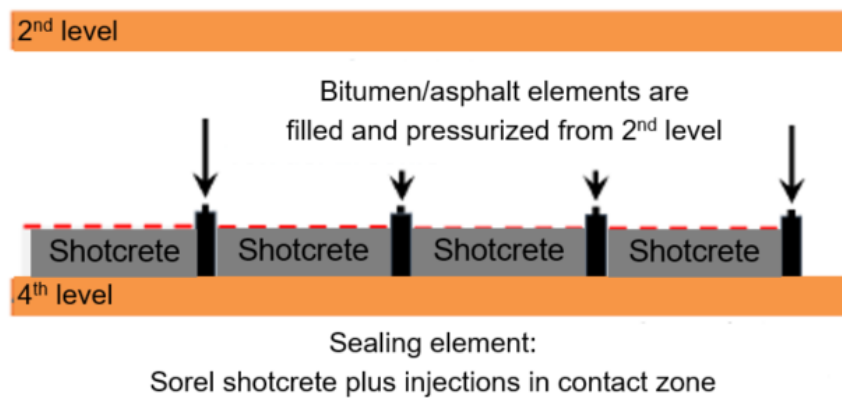


Figure 4-7: Scheme of a shotcrete - bitumen EBS in anhydrite rock at ERAM (Carstensen, 2019)

4.6 Salt concrete as backfill for large cavities to maintain the integrity of the impermeable barrier in the hanging wall of the repository (category II)

Due to the history of the Bartensleben mine as a salt producer, in its Central Part many rock salt stopes were excavated in a comparatively small area without being backfilled afterwards. As these cavities have remained open for a long time, stresses increased and have induced local failures of roofs. In 2001 a large caving event on the second level of the Central Part then triggered the planning and realization of *Mining Hazard Prevention Measures in the Central Part* (in German: bGZ). Thus, 27 stopes were backfilled with 935,000 m³ salt concrete between 2003 and 2011. The goal was to stabilize the overlaying natural barrier as well as to minimize subsidence to ensure permanent decommissioning capability. These measures refer to category II. Without them, the progressive deformation of the hanging wall could have damaged the impermeable caprock between the repository and the overburden in the long term (BfS, 2016e).

The production system for the backfill comprised a surface-based mixing plant and a pumping unit near shaft Bartensleben as well as pipelines through the shaft down to the cavity in the underground. The dry components of the hydraulic backfill namely high slag cement, fly ash and salt aggregates as well as the mixing salt solution were stored in silos and tanks on the surface (see Figure 4-8). After mixing the concrete it was delivered to the surface pumping unit that forwarded the material to its destination underground. Initially it conveyed at a rate of 300 m³/d, with a largest grain size of 4 mm. After upgrading the pumping unit and pipelines, the system achieved approximately 580 m³/d with a maximum grain size of 20 mm. A pumping distance of 425 m vertically and 1,200 m horizontally were covered. At the end of the pipeline the concrete was poured into the stopes through boreholes close to the roof (Fischer et al., 2004). To avoid the migration of solution to deeper levels either seals were started on the lowest level and backfilling continued towards the higher ones or temporary seals proved to be effective (BfS, 2009c).



Figure 4-8: Mixing plant for salt concrete on surface (A: silos for the storage of cement and fly ash, B: shaft Bartensleben, C: concrete batch mixer, D: tank for salination of the mixing solution, E:container for quality control) (Fischer et al., 2004)

Because concreting large volumes in-place produces heat and therefore induces stresses in the surrounding rock mass, several safety demonstrations were carried out. These included limits of subsidence, temperature increases, and the chemical stability of the concrete. An initial inspection prior to the concreting assured that adequate materials, equipment, personnel, and quality control processes were in place. To keep the performance requirements (e.g., heat input, viscosity, “bleed water,” and strength) within the limits the concrete mixture was adjusted for each batch. To guarantee a continuous quality of the cement and fly ash, their producers had to follow German Industrial Standards, controlled by independent approved agencies for material testing. The quality of the salt aggregates derived in the potash processing was constantly monitored to match requirements on grain size distribution and mineralogical composition. For each delivery of components to the site the documents were reviewed, the material visually inspected for impurities and samples were taken. Before pumping the concrete underground its temperature and its slump according to guidelines for self-compacting concrete were determined to estimate the pressure required for pumping and the flow angle of the suspension (Fischer et al., 2004).

“In addition to the in-house quality control, an accredited quality control inspection agency reviews plant records to verify that the required records are being maintained in a complete and accurate fashion and a specified number of concrete specimens has been tested and complies with the established quality control requirements (external control). All data of the mixing process are documented, recorded electronically, and stored in a database for evaluation. Further to that, appropriate procedure and work instructions are established for all activities and production steps relevant for achieving and assuring product quality.” (Fischer et al., 2004)

According to numerical analysis the large volumes of cast in place concrete were to increase the temperature of the filled cavern by a maximum change of 60 K. Temperature measurements in 2004 showed a temperature in the hydrating concrete of 60°C with a slightly decreasing value. The thermal tension in the near field of the cavern created acoustic emissions that could be monitored (Fischer et al., 2004).

The stopes were generally backfilled beginning with the more distant ones and continuing towards the shaft in a retreating manner. The filling went from low levels to the higher ones in order to rule out drainage into empty lower levels. Temporary dams were used to keep backfilling material or excess solution in place (BfS, 2009b).

5 Case study: WIPP Site

5.1 Introduction

The Waste Isolation Pilot Plant (WIPP) is located 659 m below the surface in Permian bedded salt deposits 42 km southeast of Carlsbad, New Mexico, USA. WIPP is currently a licensed and operating repository for defense-generated transuranic (TRU) waste. WIPP has been disposing of TRU waste since 1999. It was an active research location for in situ testing of both TRU and defense high-level (DHLW) wastes until 1987, when the possibility of defense DHLW ultimately going to a bedded salt location was ruled out in favor of Yucca Mountain. A large-scale underground testing program resulted in a great deal of data and many reports, leading to a new understanding regarding the behavior of bedded salt under repository conditions.

5.2 Project Description

There are several historical accounts of the events and science associated with WIPP. Kuhlman et al. (2012) is a recent summary of the aspects of WIPP testing relevant to heat-generating waste. Rechard (2000) gives a brief timeline of WIPP developments and regulatory milestones. Mora (1999) is a longer documentary of WIPP history up to licensing and opening (1974-1999). The National Research Council (1996) has prepared a book that described the research used in WIPP to a wider audience. Matalucci (1988) is a color pamphlet with photos describing the larger WIPP in situ tests, while SNL (1987) is a pamphlet about WIPP science activities prepared for a stakeholder audience.

Many in-situ salt experiments were conducted in the underground at WIPP from 1983-1995 (Matalucci et al., 1982; SNL, 1987; Munson et al., 1997). Kuhlman & Sevoujian (2013) provide a summary of major US and international field and laboratory tests in salt, while placing the tests in the context of the safety function being investigated. Some of these tests were conducted to provide information immediately relevant to the TRU waste WIPP design (e.g., plugging and sealing), while other tests were only relevant to the DHLW mission, and were conducted in WIPP because of the site's availability, with the intention of the data being useful for a DHLW site in salt elsewhere. Summaries of underground in situ testing at WIPP can be found in Matalucci (1988), Tyler et al. (1988), and Munson et al. (1997).

5.3 Geology

The WIPP site is located in the approximately 600 m thick Permian Salado Formation (Figure 5-1). The Salado is a bedded salt deposit found uniformly across the Delaware Basin. Powers et al. (1978) describes the site geology at the time of site selection.

The detailed (i.e., m-scale) stratigraphy of the salt near the WIPP disposal level is shown in Figure 5-2. Map units 0-4 are found at the elevation of many of the excavations in the WIPP underground. Some excavations (e.g., the WIPP north experimental area) are at a higher stratigraphic elevation, so that boreholes in the floor would extend down to the same map units. The detailed local stratigraphy (i.e., the presence of any anhydrite or clay layers) has strong effects on the stability of the local salt.

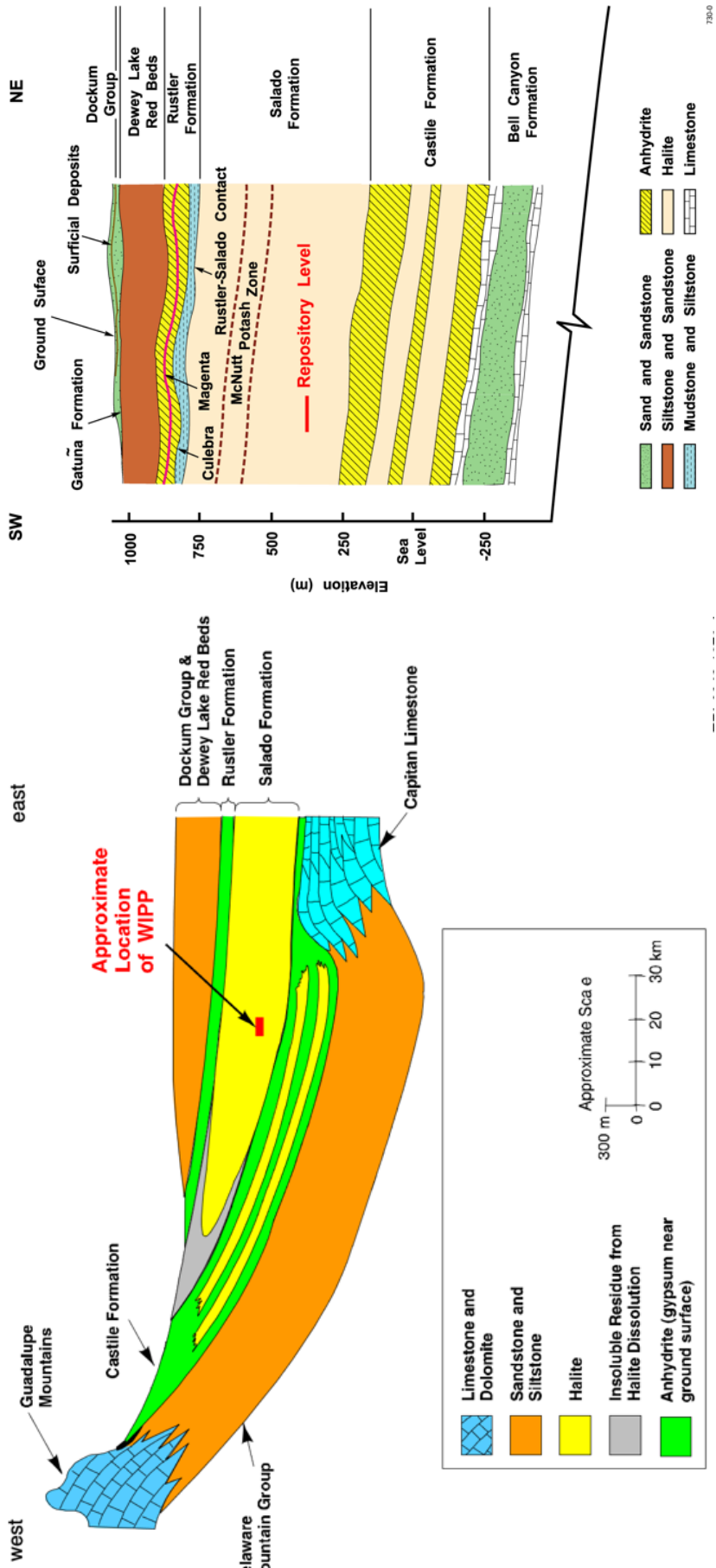


Figure 5-1: WIPP Generalized Regional (left) and Site (right) Geologic Cross Sections

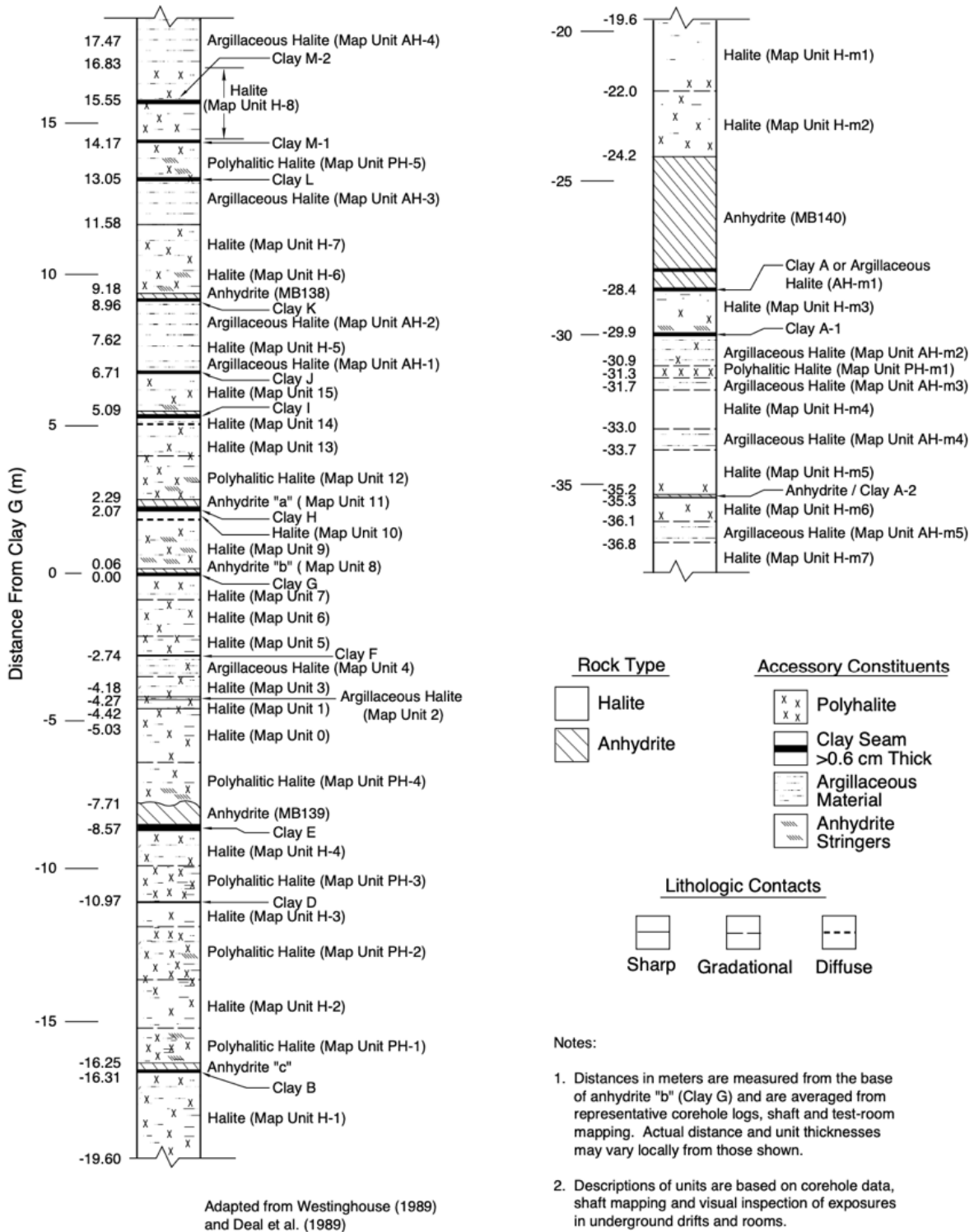


Figure 5-2: Detailed stratigraphy near the WIPP underground facility (Roberts et al., 1999)

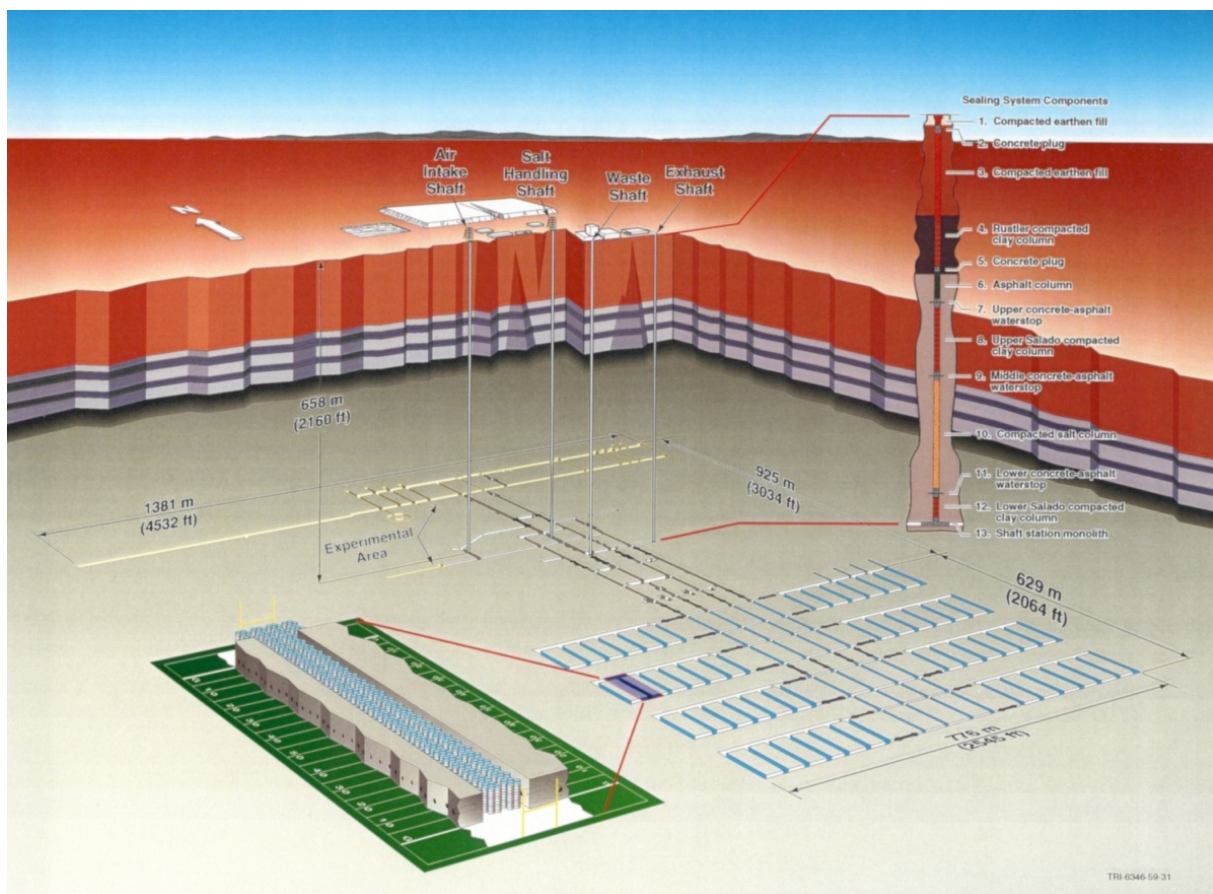


Figure 5-3: WIPP repository layout and Shaft Seals

5.4 Geotechnical Barrier

WIPP's design consists of eight primary disposal panels, which each consist of seven disposal rooms. The geotechnical barrier at WIPP does not include additional backfill in the disposal rooms, aside from the waste itself and bags of powdered MgO added as a chemical buffer.

Shaft seals (Figure 5-3 and Figure 5-4) were designed to limit groundwater entry and release of contaminants through the sealing system (SNL, 1996; Hansen & Knowles, 2000). The design approach applies redundancy to functional elements and specifies multiple, common, low-permeability materials to reduce uncertainty in performance. The system is made of 13 elements with high-density and low-permeability. Hydrologic, mechanical, thermal, and physical features were considered in the design.

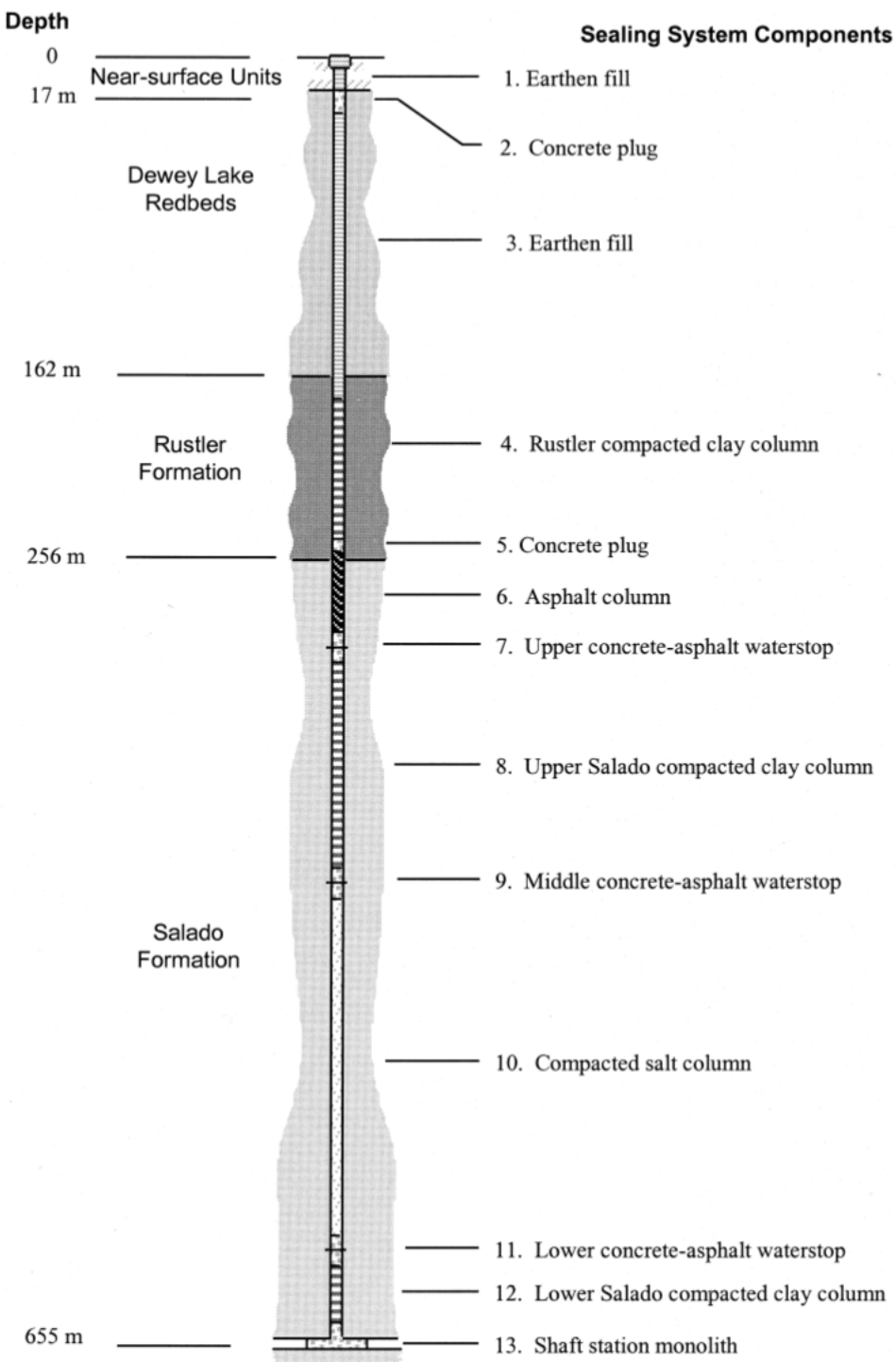


Figure 5-4: WIPP Shaft Seals (Hansen & Knowles, 2000).

Drift seals were previously planned to be installed at the entrance to every disposal panel, and at key connecting drifts (Figure 5-3). These seals were initially planned to be a multipart closure termed “Option D”. This seal involved a concrete block explosion isolation wall, removal of the majority of the DRZ around the closure, and emplacement of a large Salado Mass Concrete (SMC) monolith (Figure 5-5). Salado Mass Concrete was a specially designed salt-saturated expansive Portland cement-based concrete (Wakeley et al., 1994; Wakeley et al., 1995). Due to issues related to the constructability of the Option D panel closures, the US Department of Energy has worked with the WIPP regulator (the Environmental Protection Agency, EPA) to

change the law applicable to WIPP. The panel closures are now comprised a 30.5-m (100 ft) section of drift filled with run-of-mine salt between two metal bulkheads.

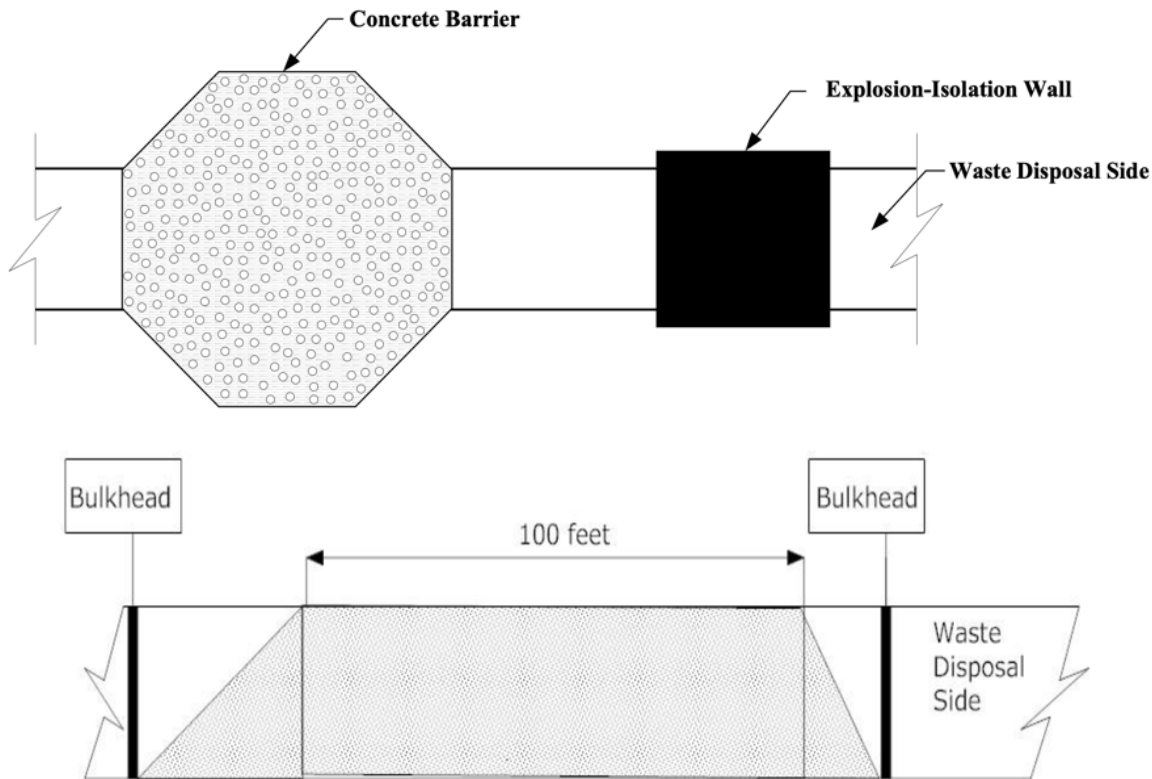


Figure 5-5: WIPP panel closures: Previous Salado Mass Concrete monolith design (top) and new run-of-mine salt (bottom) (from DOE, 2011)

The run-of-mine salt panel closures are considered simpler and more constructable, but once the salt reconsolidates the panel closures should still evolve to be as low permeability as the native salt. A demonstration of the run-of-mine panel closure was constructed in a blind drift in the WIPP underground, to illustrate the process (Gadbury & Hansen, 2015).

6 Closure of Industrial Rock Salt and Potash Mines in Germany

A major concern at rock salt and potash mines is the unintended infiltration of unsaturated water into the mine workings. As this industry developed, many shafts drowned as early as during construction, while other mines faced such challenges in a later stage of their business. To protect their investment, the natural resource, the health of employees, third parties, buildings, and to protect the environment, many trials were done to seal mine sites against water, brine, other solutions, and to a lesser extent against gases. These experiences have been the basis for latter efforts to create long-term seals for repositories with much higher requirements.

It has been concluded from the assessed dams in German rock salt and potash mines, that the functional ones were constructed in rock salt and initial seals were only achieved through use of a long dam. Shorter dams had to be injected to seal properly (Müller-Hoepppe & Krone, 1999).

During the early 20th century, the efforts were based on empirical experience and followed a trial-and-error approach. In Germany four drift seals demonstrated good sealing capabilities. These are dam Leopoldshall I/II – III, built in 1903 (Stassfurt), dam Leopoldshall III – IV, built in 1922, dam Bismarckshall (Thomas Münzer, Bischofferode) built in 1916 and improved in 1923, and dam Sachsen-Weimar built in 1929, which achieved tightness after injection of silica grout. These were used to seal operational parts of the mine from brine inflow as a precautionary measure or as emergency actions (Müller-Hoepppe & Wieczorek, 2017).

One of the first documented dams in a German rock salt or potash mine was constructed at the Leopoldshall mine near Stassfurt. The original dam was cone-shaped and acted as an abutment due to its shape. It was made of clinker bricks and cement-based mortar. This dam was extended by two cylindrical elements, one in each direction. The dam extensions started with cement-based brick walls at the older dam and then continued with MgCl-saturated bricks and magnesia mortar. At the infiltration side a wooden element and another magnesia brick wall were added. Low viscosity asphalt was applied on both sides of the wooden element, and between the magnesia brick wall and the clinker brick wall. The dam remained functional during the 20 operational years of the mine (Orzechowski, 2017).

The dam of the Sachsen-Weimar mine was built to seal a solution containing a fault. Beginning from the fault, sealing was accomplished through use of a clay element, followed by a brick wall, wood, and a special concrete element in cylindrical shape. The seal was supported by an abutment of clinker bricks in the shape of multiple cones. Through multiple pipes inside the dam, solutions were drained to produce mortar, and injections were made (Orzechowski, 2017).

At the end of the 20th century dams had to be built to separate mine panels before their controlled flooding in the following facilities (Müller-Hoepppe & Wieczorek, 2017):

- The dam “Abschlussbauwerk Hope” was built in 1983 before the adjacent mine panel was flooded. It is composed of a cone shaped salt concrete element which is covered on the pressurized side and divided in the middle by an asphalt element. The installed

measuring devices failed and therefore the data cannot be used verify the function (Fischle & Schiweger, 1987).

- The dam Dammbauwerk Rocanville is made from MgO-concrete, bentonite, and a material called "Dowell Chemical Seal". It was built in 1984 as an emergency action against brine intrusion and appears to have maintained adequate tightness (Handke, 2002). A 19 m² cross-section was sealed on a length of 28 m with magnesia binder and silicate aggregates against a solution reservoir in the underground. In addition to the abutment function, bentonite and Dowell Seal were used to seal the dam. In addition, swelling cement with an increase of 15% volume was injected into the contact zone. The calculated maximum acceptable pressure was 9.8 MPa (Krauke & Fliß, 2008).
- Dammbauwerk Immenrode is a symmetrical seal with both an instantaneous and a long-term seal element on each side. These are respectively made of salt concrete and bentonite bricks. The seal was built in 1998/99 as a precautionary measure to separate the drowning Immenrode mine from the operating mine in Sondershausen (Handke, 2002).
- Since 2000 the Bischofferode potash mine is being closed by a stepwise flooding process. Dams guide the solution, which is made with halite with a special gravity of 1.28 to 1.30 g/cm³ within the mine. These dams (like Roßleben) are made of bitumen and shotcrete on each end that protects the inner seal. (Krauke & Fliß, 2008).

Systematic in-situ investigations on the construction of seals and plugs for radioactive waste repositories are recognized by Müller-Hoeppel and Wieczorek after 1998. One approach focusses on the seal body with bentonite as the first choice, the other one draws the attention to the surrounding EDZ which has historically often been a migration path. After re-mining the drift and shaft contour, the following seals were outfitted with measuring devices and constructed following the first approach (Müller-Hoeppel & Wieczorek, 2017):

- Shaft seal at Salzdetfurth mine is made of bentonite and was built and instrumented between 1998 and 2000 (Breidung 2002; Gruner et al. 2003; Sitz et al. 2003).
- Dammbauwerk EU-1 at Sondershausen mine is made of custom-shaped bentonite bricks on the pressurized side, which are then followed by a poured asphalt seal and a salt concrete abutment, built in 1999. The seal withstands a pressure of 8 MPa (Handke, 2002).

The experiment Shaft Seal Salzdetfurth was conducted to verify function and constructability of a long-term shaft seal in accordance with national administrative regulation for (non-radioactive) underground disposal sites in salt formations (TA Abfall). This incorporated a seal against liquids and required long-term stability of the seal's position. A blind raise 2.5 m in diameter was drilled between the 744 and 774 m levels that showed similar geological conditions compared to the day shaft 2 that should be sealed after a successful test. The test construction concentrated on vertical seals and their stability while the transition towards horizontal drifts was investigated in another project. On a retractable steel support specifically sized hard rock aggregates were installed as a settling-resistant column. A filter layer against wash out and a bentonite seal followed. The bentonite was a mix of granular pressed and loose material with a combined density of 1.7 to 1.75 g/cm³. In the center of the column a permeable layer out of gravel and sand was installed. Above it the upper seal followed. The column was

then closed by a sand and concrete layer on top of it (see Figure 6-1). This setup provided two sealing elements that could be tested at once, one laying above and one below the pressure chamber out of highly permeable materials. For the experiment, fluid was injected with 4 MPa and later with 7 MPa into the permeable layer. Conservative estimates reached at least 1 MPa of swelling pressure. The experiment showed fluid paths along cables and at the shaft contour, but whenever bentonite and salt had direct contact without flushed-in sand grains, the contact was intense. At constant fluid pressure the seal function improved over time up to an equilibrium. Therefore, this type of seal proved its function for all shaft seals in salt geology.

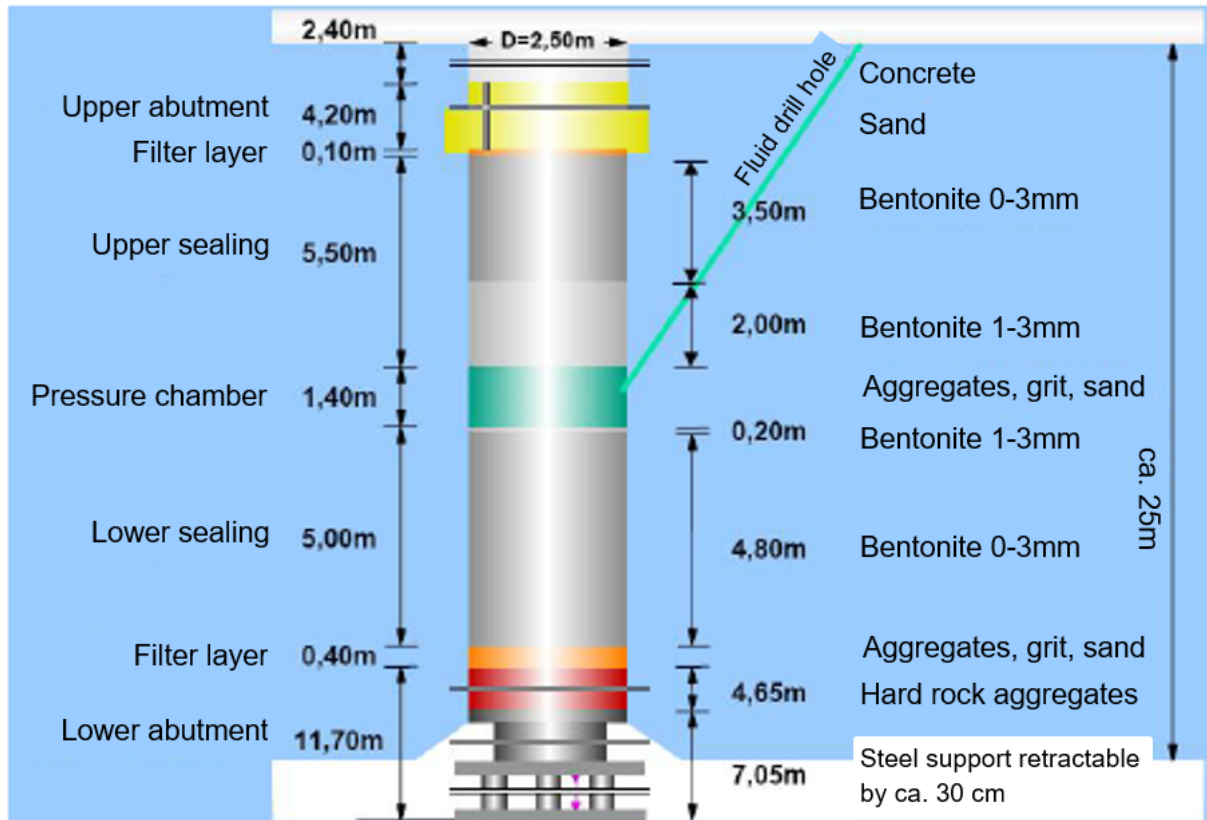


Figure 6-1: Experiment set-up in blind raise and used materials after (Breidung, 2002)

Shaft seal Salzdetfurth as well as Dammbauwerk EU-1 Sondershausen demonstrated the functionality of the seals in principle; however, problems associated with piping effects and bypasses became evident.

7 Summary and Next Steps

This state-of-the-art report from the RANGERS project summarizes a significant amount of history related to the development of robust engineered barrier system for deep geological repositories in salt formations. The report presents a high-level summary of some active and historical research projects, including ELSA, VSG, ISIBEL, and WIPP. The report then presented three case studies of the Asse II, Morsleben, and WIPP sites, focusing on historical developments related to engineered barrier systems. Lastly the report presented a discussion on the closure of industrial rock salt and potash mines in Germany.

The goal of this state-of-the-art report has been to summarize key historical and ongoing activities and research on the topic of engineered barriers. This report sets the stage for our next analysis planned on emerging and promising future approaches related to engineered barriers in salt that may be the topic of future investigation for deep geologic repositories in salt.

This report has been a collaborative effort between BGE TEC and Sandia, and the co-authors would like to add that they have learned from one another as part of the report preparation process, and as part of the process of advancing the RANGERS project.

8 References

- AG Morsleben, 2007. Planfeststellungsverfahren zur Stilllegung des Endlagers für radioaktive Abfälle Morsleben - Prüfkomplex: Schachtverschlussystem der Schächte Bartensleben und Marie, Magdeburg: Ministerium für Landwirtschaft und Umwelt des Landes Sachsen-Anhalt.
- Ahrens, E. & Dale, T., 1996. Data Report on the Waste Isolation Pilot Plant Small-Scale Seal Performance Test, Series F Grouting Experiment. Sandia National Laboratories, Albuquerque, NM.
- Asse GmbH, 2016. Schachtanlage Asse II - Sonderbetriebsplan Nr. 1/2016 "Erstellung geotechnischer Bauwerke in der 2. südlichen Richtstrecke nach Westen auf der 750-m-Sohle (SV-750-21, WL-750-55a, SV-750-18)", Remlingen.
- Asse GmbH, 2017. Radioaktives Inventar. [Online] Available at: https://archiv.bge.de/archiv/www.asse-gmbh.de/die_schachtanlage_asse_ii/radioaktives_inventar.html [Accessed 05 02 2021].
- BBergG, 2020. Bundesberggesetz vom 13. August 1980 (BGBl. I S. 1310), das zuletzt durch Artikel 237 der Verordnung vom 19. Juni 2020 (BGBl. I S. 1328) geändert worden ist. English: German Federal Mining Act.
- Bauer, S.J., Broome, S.T., Hansen, F.D., & Callahan, G.D., (2012). Couple thermal-hydrological-mechanical processes in salt: Hot granular salt consolidation, constitutive model and micromechanics. SAND2012-9893P
- Bechthold, W., Rothfuchs, T., Poley, A., Ghoreychi, M., Heusermann, S., Gens, A., Olivella, S., 1999. Backfilling and Sealing of Underground Repositories for Radioactive Waste in Salt (BAMBUS Project). - Final Report, Luxembourg: European Commission, Nuclear Science and Technology.
- Bechthold, W., Heusermann, S., Smailos, E., 2004. Backfilling and Sealing of Underground Repositories for Radioactive Waste in Salt (BAMBUS II Project) - Final Report, Luxembourg: European Commission Nuclear Science and Technology.
- Behlau, H., Mingerzahn, G. & Bornemann, O., 2000. ERA Morsleben: Erarbeitung eines geologischen Lagerstättenmodells Morsleben - Abschlussbericht AP 9M 2124601100 (Teil 1 von 2). In: Planfeststellungsverfahren zur Stilllegung des Endlagers für radioaktive Abfälle Morsleben - Verfahrensunterlage. Salzgitter: BfS, p. 100.
- BMU, 2010. Safety Requirements Governing the Final Disposal of Heat-Generating Radioactive Waste as at 30 September 2010, Berlin: Bundesministerium für Umwelt, Naturschutz und Reaktorsicherheit.
- Bollingerfehr, W., Bertrams, N., Minkley, W., Buhmann, D., Mönig, J., Eickemeier, R., Popp, T., Fahland, S., Prignitz, S., Filbert, W., Reinhold, K., Hammer, J., Simo, E., Kindlein, J., Thiemeyer, T., Knauth, M., Völkner, E., Liu, W. & Wolf, J., 2018. Concept developments for a generic repository for heat-generating waste in bedded salt formations in Germany – KOSINA, synthesis report, BGE TEC 2018-03, Peine.
- Brady, P., C. Herrick, K. Kuhlman, B. Malama, M. Schuhens & B. Stenson, 2013. Sandia Experimental Programs Background and Proposed Activities for Forensic Investigation of Rooms B and A1. Albuquerque, NM: Sandia National Laboratories.

- Brasser, T. & Droste, J., 2008. Endlagerung wärmeentwickelnder radioaktiver Abfälle in Deutschland - Anhang Untertagelabore: Aufgabe und Zielsetzung von Untertagelaboren, Braunschweig/Darmstadt: Gesellschaft für Anlagen- und Reaktorsicherheit (GRS).
- Breidung, K., 2002. Schachtverschlüsse für untertägige Deponien in Salzbergwerken - Forschungsvorhaben Schachtverschluss Salzdethfurth des BMBF, Abschlussbericht FKZ: 02C0516, Kassel: K+S AG.
- Bundesamt für Strahlenschutz (BfS), 2009a. Beschreibung der zur Verfüllung der Firstspalten und Resthohlräume in der Südflanke der Schachtanlage Asse ausgewählten Baustoffe Sorelbeton A1 und A1-560. BfS-KZL 9A/44215100/GHR/TV/0001/00, Remlingen: Asse GmbH and DBE TECHNOLOGY GmbH.
- Bundesamt für Strahlenschutz (BfS), 2009b. Kurzbeschreibung der Stilllegung des Endlagers für radioaktive Abfälle Morsleben. In: Stilllegung ERA Morsleben. Salzgitter: Bundesamt für Strahlenschutz, p. 65.
- Bundesamt für Strahlenschutz (BfS), 2009c. Stilllegung ERA Morsleben - Kurzbeschreibung der Stilllegung des Endlagers für radioaktive Abfälle Morsleben, Salzgitter: Bundesamt für Strahlenschutz.
- Bundesamt für Strahlenschutz (BfS), 2010. Untersuchung der Kontaktzone am Asse-Vordamm – Zusammenfassung und Interpretation der Messergebnisse BfS-KZL 9M/22310131/GH/RB/0130/00, Remlingen: DBE TECHNOLOGY GmbH.
- Bundesamt für Strahlenschutz (BfS), 2016a. Morsleben - Großversuch vertikales Dichtelement. [Online] Available at: <https://archiv.bge.de/archiv/www.endlager-morsleben.de/SharedDocs/AktuelleArbeiten/Morsleben/DE/2015/grossversuch-dichtelement.html> [Accessed 11 03 2021].
- Bundesamt für Strahlenschutz (BfS), 2016b. Morsleben - Stilllegungskonzept - So soll das Endlager Morsleben stillgelegt werden. [Online] Available at: <https://archiv.bge.de/archiv/www.endlager-morsleben.de/Morsleben/DE/themen/stilllegungskonzept/ueberblick-stilllegungskonzept/ueberblick-stilllegungskonzept.html>
- Bundesamt für Strahlenschutz (BfS), 2016c. Morsleben - The sealing structures according to the decommissioning concept. [Online] Available at: https://archiv.bge.de/archiv/www.endlager-morsleben.de/Morsleben/EN/topics/decommissioning-concept/sealing-structures/sealing-structures_node.html
- Bundesamt für Strahlenschutz (BfS), 2016d. Morsleben repository at a glance. [Online] Available at: https://archiv.bge.de/archiv/www.endlager-morsleben.de/Morsleben/EN/topics/repository/repository-overview/repository-overview_node.html [Accessed 11 06 2021].
- Bundesamt für Strahlenschutz (BfS), 2016e. Projektstatusbericht - Bericht des Betreibers BfS, Salzgitter: Bundesanstalt für Strahlenschutz.
- Brodsky, N.S., 1994. Hydrostatic and shear consolidation tests with permeability measurements on Waste Isolation Pilot Plant crushed salt. SAND93-7058.

- Brodsky, N.S., Hansen, F.D. & Pfeifle, T.W., 1996. "Properties of dynamically compacted crushed WIPP salt" in Proceedings of the 4th Conference on the Mechanical Behavior of Salt. Montreal, Canada.
- Buck, A., 1985. Development of Two Candidate Concrete Mixtures (Salt, Nonsalt) for Repository Sealing Application. Miscellaneous Paper SL-85-8, US Army Engineer Waterways Experiment Station, Vicksburg, MS.
- Buhmann, D., Grupa, J. B., Hart, J., Poppei, J., Resele, G., 2005. Fluid- und Radionuklidtransport am Standort Asse. In: Projekt Langzeitsicherheit Asse - Transportmodellierung - Abschlussbericht. Petten (NL): NRG, Colenco, GRS.
- Buhmann, D., Heusermann, S., Bollingerfehr, W., et al., 2008. Überprüfung und Bewertung des Instrumentariums für eine sicherheitliche Bewertung von Endlagern für HAW - ISIBEL, Braunschweig: Gesellschaft für Anlagen- und Reaktorsicherheit (GRS) mbH.
- Bundesanstalt für Wasserbau, 2013a. Merkblatt Anwendung von Kornfiltern an Bundeswasserstraßen (MAK), 2013.
- Bundesanstalt für Wasserbau, 2013b. Merkblatt Materialtransport im Boden (MMB), 2013.
- Bundesgesellschaft für Endlagerung (BGE), 2018. BGE Einblicke: Morsleben. [Online] Available at: <https://einblicke.de/morsleben#top> [Accessed 12 03 2021].
- Bundesgesellschaft für Endlagerung (BGE), 2018. "Wir müssen noch einiges verbessern". Einblicke - Morsleben - Wo geht es hin?, Issue 3, pp. 11-12.
- Bundesgesellschaft für Endlagerung (BGE), 2020. Geotechnisches, geophysikalisches, geochemisches Monitoring und Baustoffuntersuchungen - Jahresbericht 2019 - Geomonitoring Asse, Peine: Bundesgesellschaft für Endlagerung.
- Bundesgesellschaft für Endlagerung (BGE), 2021. Short information - BGE. [Online] Available at: <https://www.bge.de/en/morsleben/short-information/> [Accessed 03 03 2021].
- Büttner, C., Niederleithinger, E., Buske, S. & Friedrich, C., 2021. Ultrasonic Echo Localization Using Seismic Migration Technique in Engineered Barriers for Nuclear Waste Storage. Journal of Nondestructive Evaluation, p. 10.
- Carstensen, A., 2019. Abdichtbauwerk im Anhydrit - Anforderungen, Entwicklung, Nachweise [Präsentation]. In: Fachforum „ERAM - Sichere Stilllegung schnellstmöglich“. Magdeburg: Bundesgesellschaft für Endlagerung (BGE), p. 22.
- Christensen, C., & Peterson, E., 1986. Field-Test Programs of Borehole Plugs in South-eastern New Mexico. Sandia National Laboratories, Albuquerque, NM.
- Comes, G., Wakeley, L., & O'Neil, E., 1987. Properties of Laboratory-Tested Specimens of Concrete from Small-Scale Seal Performance Tests at the Waste Isolation Pilot Plant, Miscellaneous Paper SL-87-9, US Army Engineer Waterways Experiment Station, Vicksburg, MS.
- Deutsche Gesellschaft zum Bau und Betrieb von Endlagern für Abfallstoffe (DBE), 2005. Planfeststellungsverfahren zur Stilllegung des Endlagers für radioaktive Abfälle Morsleben - Verfüllplan zur Stilllegung des ERAM nach vorgezogener Verfüllung von Grubenbauen des Zentralteils, Konzeptplanung - Teil 1 von 3, Braunschweig: Bundesamt für Strahlenschutz.

- Deutsche Gesellschaft zum Bau und Betrieb von Endlagern für Abfallstoffe (DBE), 2006. Konzeptplanung Verfüllung und Verschluss der Schächte 2 und 4 des Bergwerks Asse, Rev. 00. In: Bericht zum Projekt Langzeitsicherheit. Peine: DBE mbH.
- Deisenroth, N. & Kokorsch, R., 2011. Vergleich der Salzstöcke Asse und Gorleben hinsichtlich ihrer Eignung für die Endlagerung radioaktiver Abfälle. Gezähkiste, 4 (2011) No. 1, pp. 6-16.
- Department of Energy, 2011. Panel Closure System Design Planned Change Request to the EPA 40 CFR Part 194 Certification of the Waste Isolation Pilot Plant. DOE/CBFO-11-3479.
- Deutscher Ausschuss für Stahlbeton (DAfStb), 1997. Sicherheitskonzept für Bauten des Umweltschutzes, Berlin: Beuth Verlag.
- Deutsches Institut für Normung (DIN), 2007. DIN EN 1997 Eurocode 7: Entwurf, Berechnung und Bemessung in der Geotechnik – Teil 1: Allgemeine Regeln. Berlin: Beuth Verlag.
- Deutsches Institut für Normung (DIN), 2010. DIN 1054 Baugrund – Sicherheitsnachweise im Erd- und Grundbau – Ergänzende Regelungen zu DIN EN 1997-1, Berlin: Beuth Verlag.
- Deutsches Institut für Normung (DIN), 2010. DIN EN 1990 Eurocode: Grundlagen der Tragwerksplanung, Berlin: Beuth Verlag.
- Deutsches Institut für Normung (DIN), 2011. DIN EN 1992 Eurocode 2: Bemessung und Konstruktion von Stahlbeton und Spannbetontragwerken – Teil 1-1: Allgemeine Bemessungsregeln und Regeln für den Hochbau, Berlin: Beuth Verlag.
- Deutsches Institut für Normung (DIN), 2013. DIN EN 1992 NA Nationaler Anhang – National festgelegte Parameter – Eurocode 2: Bemessung und Konstruktion von Stahlbeton- und Spannbetontragwerken – Teil 1-1: Allgemeine Bemessungsregeln und Regeln für den Hochbau, Berlin: Beuth Verlag.
- Droste, J., Feddersen, H.-K. & Rothfuchs, T., 2001. Experimental Investigations on the Backfill Behavior in Disposal Drifts in Rock Salt (VVS-Project) - Final Report, Braunschweig: Gesellschaft für Anlagen- und Reaktorsicherheit (GRS) mbH.
- Droste, J., Rothfuchs, T. & Wieczorek, K., 1998. In-situ investigations on sealing of emplacement drifts and boreholes for heat generating high-level waste, Braunschweig: Gesellschaft für Anlagen- und Reaktorsicherheit (GRS) mbH.
- Dueck, A., Johannesson, L.-E., Kristensson, O. & Olsson, S., 2011. Report on hydro-mechanical and chemical-mineralogical analyses of the bentonite buffer in Canister Retrieval Test, Technical Report TR-11-07, Clay Technology, SKB, Sweden.
- Engelhardt, H.-J., Kreienmeyer, M., Müller-Hoepppe, N., Eilers, G., Köster, R., Preuss, J., 2003. A constitutive law of salt concrete used for closure of a LILW repository, 9th International Conference on RWM and Environmental Remediation, Oxford, p. 27.
- Fischer, H., 1990. Entwicklung des Versuchsbauwerkes von der Konzeption zur Berg- und bautechnischen Realisierung. Dammbau im Salzgebirge - Vorträge zur Informationsveranstaltung 05./06.12.1990.
- Fischer, H., Bergmann, U., Engelhardt, H.-J., Hund, W., 2004. Stabilization of the Central Part of the Morsleben Repository - Technical Concept, Requirements, Quality

Assurance and Operational Experience, DisTec 2004. Berlin, Bundesamt für Strahlenschutz.

Fischer-Appelt et al., 2013. Synthesebericht für die VSG. AP 13. Vorläufige Sicherheitsanalyse für den Standort Gorleben - GRS-290, Köln: Gesellschaft für Anlagen- und Reaktorsicherheit mbH (GRS), Köln.

Fischle, W. & Schiweger, K., 1987. Untersuchungen an einem Abschlußbauwerk im Kalisalzbergwerk Hope. Kali und Steinsalz 9, Heft 11, pp. 380-387.

Freyer, D., 2015. Laboruntersuchungen am Magnesiabaustoffsyste - Fragestellungen und Vorgehensweisen [Präsentation]. In: Fachgespräch "Verschlusssysteme - In-situ Bauwerke aus Magnesiabaustoff und dessen chemisch-mechanische Eigenschaften im Hinblick auf HAW Endlager". Freiberg: Projektträger Karlsruhe, pp. 105-140.

Freyer, D., Gruner, M., & Popp, T., 2015. Zusammenhang von Chemismus und mechanischen Eigenschaften des MgO-Baustoffs. Freiberger Forschungshefte. Serie E15 Naturwissenschaften. TU Bergakademie Freiberg, 2015. ISBN 978-3-86012-8.

Fröhlich, H. & Conen, O., 1998. Durchlässigkeitsverhalten von Steinsalzversatz gegenüber Laugen unter Berücksichtigung von Lösungsvorgängen. In: S. Wagner, ed. Tagungsband zum 49. Berg- und Hüttenmännischen Tag - Kolloquium 3. Freiberg: TU Bergakademie Freiberg.

Gadbury, C. & F.D. Hansen, 2015. Reconsolidated Salt as a Geotechnical Barrier 16535, 2016 Waste Management Conference. SAND2015-9936C.

Gläß, F. & Mohlfeld, M., 2002. Planfeststellungsverfahren zur Stilllegung des Endlagers für radioaktive Abfälle Morsleben - Kriterien für das Verfüllen von Bohrungen, Braunschweig: Bundesamt für Strahlenschutz.

Gläß, F., Mauke, R., Eilers, G., Preuss, J., Schmidt, H., Lerch, C., & Müller-Hoepp, N., 2005. Investigation of a salt-concrete seal in the Asse salt mine. In: WM'05 Conference 27.02.-03.03.2005. Tucson, Arizona.

Gruner, M., Freyer, D. & Popp, T., 2017. MgO-Seal - Verhalten von MgO-Spritzbeton bei Angriff von MgCl₂-Lösung [Presentation]. In: Fachgespräch "Verschlusssysteme - Konzepte, Baustoffe, Simulation, Demonstration und Anwendung". Freiberg: PTKA-WTE and TU Bergakademie Freiberg.

GRS, 2006. Gesamtbewertung der Langzeitsicherheit für den Standort Asse (Konsequenzenanalyse), Braunschweig: GSF.

GRS, 2013. Vorläufige Sicherheitsanalyse Gorleben (VSG). [Online] Available at: <https://www.grs.de/vorlaeufige-sicherheitsanalyse-gorleben-vsg> [Accessed 06 01 2020].

Gulick, C.W., 1979. Borehole Plugging Program - Plugging of the ERDA No. 10 Drill Hole, SAND79-0789, Sandia National Laboratories, Albuquerque, NM.

Gulick, C.W., Boa, J.A. & Buck, A.D., 1980. Bell Canon Test (BCT) Cement Grout Development Report. SAND80-1928. Sandia National Laboratories, Albuquerque, NM.

Handke, N. (2002). *Dammbau- und Abdichtungstechniken im Kali- und Steinsalzbergbau*. Report 2002. Mühlheim: Thyssen Schachtbau Gruppe.

- Hansen, F.D., Ahrens, E.H., Tidwell, V.C., Tillerson, J.R. & Brodsky, N.S., 1995. Dynamic compaction of salt: Initial demonstration and performance testing. SAND94-2313C.
- Hansen, F.D. & Ahrens, E.H., 1996, Large-scale Dynamic Compaction of Natural Salt. SAND96-0792C
- Hansen, F.D. & M.K. Knowles, 2000. Design and analysis of a shaft seal system for the Waste Isolation Pilot Plant, *Reliability Engineering & System Safety*, 69(1-3):87-98.
- HelmholtzZentrum münchen, 2008. ASSE: Warum Strömungsbarrieren für die Sicherheit unverzichtbar sind. [Online] Available at: <https://archiv.bge.de/archiv/www.asse-archiv.de/asse-archiv/asse-newsarchiv/news-detail/article/11094/5708/index.html> [Accessed 15 02 2021].
- Herbert, H.-J., Freyer, D., Lack, D. & Gruner, M., 2010. Nichtarteigene Materialien. In: Verschlussysteme in Endlagern für wärmeentwickelnde Abfälle in Salzformationen. Braunschweig: Gesellschaft für Anlagen- und Reaktorsicherheit (GRS) mbH.
- Heydorn, M. et al., 2018. Bau von Strömungsbarrieren im Grubengebäude der Schachtanlage Asse [Präsentation]. In: Wissenstransfer Asse. Peine: BGE, p. 23.
- Heydorn, M. et al., 2018. Industrial Planning and Construction of Drift Seals in the Asse Mine. Hannover, Federal Institute for Geosciences and Natural Resources (BGR), pp. 201-210.
- Heydorn, M., 2006. Strömungsbarrieren, ein wesentlicher Baustein des Schließungskonzeptes für die Schachtanlage Asse [Präsentation]. Remlingen, HelmholtzZentrum münchen.
- Holcomb, D.J. & Zeuch, D.H., 1988. Consolidation of Crushed Rock Salt, Part I: Experimental Results for Dry Salt Analyzed Using a Hot-pressing Model. SAND88-1469.
- Holcomb, D.J., & Shields, M., 1987. Hydrostatic creep consolidation of crushed salt with added water. SAND87-1990.
- Hurtado, L. et al., 1997. WIPP Shaft Seal System Parameters Recommended to Support Compliance Calculations, s.l.: Sandia.
- IGH, 2009. Injektion von Abdichtungssegmenten mit Feinstsuspensionen P298, Hannover: IGH Ingenieurgesellschaft Grundbauinstitut.
- IHU, 2010. Prüfbericht im Rahmen des Planfeststellungsverfahrens zur Stilllegung des ERA Morsleben - Prüfkomplex: "Verfüllen und Verschließen von Strecken" Teil 1, Stendal: IHU Geologie und Analytik GmbH.
- Jautze, T., Weißenborn, A., Hansper, F. & Einicke, O., 2012. In-situ roadway stopping in rock salt measures. Thyssen Mining Report, p. 112.
- Jobmann et al., 2017. Projekt ANSICHT, Systemanalyse für die Endlagerstandortmodelle, Methode und exemplarische Berechnungen zum Sicherheitsnachweis.
- Jockwer, N. & Wieczorek, K., 2008. Advective and Diffusive Gas Transport in Rock Salt Formations (ADDIGAS), Braunschweig: Gesellschaft für Anlagen- und Reaktorsicherheit mbH.
- Knowles, M.K. & Howard, C.L., 1996. Field and Laboratory Testing of Seal Materials Proposed for the Waste Isolation Pilot Plant. SAND95-2082C.

- Kokorsch, R. & Ausgabe, 2010. Das Bergwerk Asse - eine wechselvolle Geschichte, die noch nicht zu Ende ist - Teil I. Gezählekiste, 3 (2010) No. 1, pp. 6-12.
- Kokorsch, R. & Ausgabe, 2010. Heft 6. Das Bergwerk Asse - eine wechselvolle Geschichte, die noch nicht zu Ende ist - Teil II. Gezählekiste, 3 (2010) No. 2, pp. 6-13.
- Krauke, W. & Fliß, T., 2008. Planfeststellungsverfahren zur Stilllegung des Endlagers für radioaktive Abfälle Morsleben - Konzeptplanung und Nachweisführung für ein Abdichtbauwerk im Hauptanhydrit aus Magnesiabinder, Braunschweig: Bundesamt für Strahlenschutz.
- Kreienmeyer, M., Lerch, C., Polster, M. & Tholen, M., 2008. AP5: Nachweiskonzept zur Integrität der einschlusswirksamen technischen Barrieren. In: Überprüfung und Bewertung des Instrumentariums für eine sicherheitliche Bewertung von Endlagern für HAW - ISIBEL. Peine: DBE Technology GmbH, p. 125.
- Kreienmeyer, M., Lerch, C., Polster, M. & Tholen, M., 2008. Nachweiskonzept zur Integrität der einschlusswirksamen technischen Barrieren, Technischer Bericht zum AP 5 ISIBEL, Peine: DBE TECHNOLOGY GmbH.
- Krone, J. et al., 2008. Review and Appraisal of the Tools available for a Safety Assessment of Final Repositories for HLW - ISIBEL, Peine: DBE TECHNOLOGY GmbH.
- Krumhansl, J.L., Molecke, M.A., Papenguth, H.W. & Brush, L.H., 2000. A Historical Re-view of Waste Isolation Pilot Plant Backfill Development. SAND2000-1416C, Albuquerque, NM: Sandia National Laboratories.
- Krumhansl, J.L., Stein, C.L., Jarrell, G.D. & Kimball, K.M., 1991b. Summary of WIPP Room B Heater Test Brine and Backfill Material Data. SAND90-0626, Albuquerque, NM: Sandia National Laboratories.
- Kudla et al., 2015. Schachtverschlusskonzepte für zukünftige Endlager für hochradioaktive Abfälle für die Wirtsgesteinsoptionen Steinsalz und Ton. Mining Report 151, 55-64.
- Kudla, W., Dahlhaus, F., Glaubach, U., Gruner, M., & Haucke, J., 2009. Diversitäre und redundante Dichtelemente für langzeitstabile Verschlussbauwerke. Abschlussbericht FKZ 02C1124. TU Bergakademie Freiberg.
- Kudla, W. & Herold, P., 2021. Zusammenfassender Abschlussbericht - Schachtverschlüsse für Endlager für hochradioaktive Abfälle (ELSA - Phase 2): Konzeptentwicklung für Schachtverschlüsse und Test von Funktionselementen von Schachtverschlüssen, Freiberg: TU Bergakademie Freiberg.
- Kudla, W., Jobmann, M., Freyer, D. & Wilsack, T., 2013. Schachtverschlüsse für Endlager für hochradioaktive Abfälle, Freiberg, Peine: TU Bergakademie Freiberg, DBE TEC.
- Kuhlman, K., S. Wagner, D. Kicker, R. Kirkes, C. Herrick & D. Guerin, 2012. Review and Evaluation of Salt R&D Data for Disposal of Nuclear Waste in Salt. SAND2012-8808P.
- Kuhlman, K. & S.D. Sevoujian, 2013. Establishing the Technical Basis for Disposal of Heat-Generating Waste in Salt. SAND2013-6212P.
- Kuhlman, K.L., M.M. Mills & E.N. Matteo, 2017. Consensus on Intermediate Scale Salt Field Test Design. SAND2017-3179R.

- Köhler, J., Teichmann, L., Heydorn, M. & Wolff, P., 2019. No. 5. Einsatz von Sorelbeton für Verschlussbauwerke und Stabilisierungsmaßnahmen in der Schachtanlage Asse II. Glückauf - MINING REPORT, p. 10.
- Laske, D., 2010. Streckenverschlusskonzepte. In: Verschlussssysteme in Endlagern für wärmeentwickelnde Abfälle in Salzformationen. Braunschweig: GRS, pp. 39-48.
- Lautsch, T., 2021. Die Rückholung der radioaktiven Abfälle aus der Schachtanlage Asse II [Präsentation]. Bohr- und Sprengtechnisches Kolloquium, pp. 1-34.
- Martino et al., 2011. Enhanced Sealing Project (ESP): Seal Construction and Instrumentation Report, APM-REP-01601-0003, Atomic Energy of Canada Limited.
- Matalucci, R.V., 1988. In situ testing at the Waste Isolation Pilot Plant. SAND87-2382.
- Matalucci, R.V., Christensen, C.L., Hunter, T.O., Molecke, M.A., & Munson, D.E., 1982. Waste Isolation Pilot Plant (WIPP) Research and Development Program: in situ testing plan, March 1982. SAND81-2628.
- Mauke, R. & Herbert, H.-J., 2013. Large scale in-situ experiments on sealing constructions in underground disposal facilities for radioactive wastes - examples of recent BfS- and GRS-activities. EUROSAGE - Towards Convergence of Technical Nuclear Safety Practices in Europe. Cologne, ETSON - European Technical Safety Organisations Network.
- Mauke, R., Wollrath, J., Müller-Hoepppe, N., Becker, D., & Noseck, U., 2012. Overview of recent and future work on material development and usage of cementitious materials in salt repositories. Cementitious materials in safety cases for radioactive waste: role, evolution and interactions. Brussels, OECD/NEA.
- Mauke, R., 2011. In situ-Verification of a Drift Seal System in Rock Salt - Operating Experience and Preliminary Results [Presentation]. Peine, Sandia National Laboratories, p. 16.
- Mauke, R., 2013. In Situ Investigation of the Morsleben Drift Seal - Operating Experience and Preliminary Results. 3rd US-German Workshop on Salt Repository Research, Design, and Operation. Albuquerque, Sandia National Laboratories.
- Mauke, R., 2015. Stilllegung ERAM - In-situ-Versuch für ein Abdichtbauwerk im Anhydrit im Bergwerk Bleicherode. In: Fachgespräch "Verschlussssysteme - In-situ-Bauwerke aus Magnesiabaustoff und dessen chemisch-mechanische Eigenschaften im Hinblick auf HAW-Endlager". Freiberg: PTKA, p. 26.
- Mauke, R., Müller-Hoepppe, N. & Wollrath, J., 2007. Planning, Assessment, and Construction of a Drift Seal in a Salt Repository - Overview of Investigations. In: Engineered Barrier Systems (EBS) in the Safety Case: Design Confirmation and Demonstration - Workshop Proceedings, Tokyo, Japan, 12-15 September 2006. Paris: OECD Publishing, pp. 65-80.
- Mauke, R., Stahlmann, J. & Mohlfeld, M., 2012. In-situ verification of a drift system in rock salt – operating experience and preliminary results. The Mechanical Behavior of Salt: 7th Conference (SaltMech7). Paris, Taylor & Francis.
- Minkley, W., Wüste, U., Popp, T., Naumann, D., Wiedemann, M., J., B., et al., 2010. Beweissicherungsprogramm zum geomechanischen Verhalten von Salinarbarrieren nach starker dynamischer Beanspruchung und Entwicklung einer Dimensionierungsrichtlinie zum dauerhaften Einschluss. Abschlussbericht, IfG, Leipzig.

- Molecke, M.A., 1992. Results from Simulated Remote-handled Transuranic Waste Experiments at the Waste Isolation Pilot Plant (WIPP). SAND92-1003C.
- Molecke, M.A. & Sorensen, N.R., 1989. Retrieval and Analysis of Simulated Defense HLW Package Experiments at the WIPP. SAND88-1135C.
- Molecke, M.A. & Wicks, G.G., 1993. Details of in situ Sample Retrievals and Test Completion for the Materials Interface Interactions Test (MIIT). SAND92-2660C
- Mora, C.J., 1999. Sandia and the Waste Isolation Pilot Plant: 1974-1999. SAND99-1482.
- Munson, D.E., Hoag, D.L., Blankenship, D.A., Jones, R.L., Woerner, S.J., & Baird, G.T., 1997. Construction of the thermal/structural interactions in situ tests at the Waste Isolation Pilot Plant (WIPP). SAND87-2685.
- Munson, D.E., 1988. Summary of WIPP Thermal/Structural Interactions In Situ Tests, ASME-SES Joint Mechanics Conference. Berkeley, CA. SAND88-0172A.
- Mönig, J., Buhmann, D., Rübel, A., Wolf, J., Baltes, B., Peiffer, F.; Fischer-Appelt, K., 2012. Grundzüge des Sicherheits- und Nachweiskonzeptes - Bericht zum Arbeitspaket 4 VSG, GRS-271, Braunschweig: Gesellschaft für Anlagen-und Reaktorsicherheit (GRS) mbH.
- Müller-Hoepppe, N., Breustedt, M., Johanna Wolf, J., Czaikowski, O., & Klaus Wieczorek, K. (2012). *Integrität geotechnischer Barrieren - Teil 2 Vertiefte Nachweisführung*, Bericht zum Arbeitspaket 9.2. Vorläufige Sicherheitsanalyse für den Standort Gorleben, GRS-288. Peine, Braunschweig: DBE TECHNOLOGY GmbH, Gesellschaft für Anlagen- und Reaktorsicherheit (GRS) mbH.
- Müller-Hoepppe, N., Buhmann, D., Czaikowski, O., Engelhardt, H.-J., Herbert, H.-J., Lerch, C., Xie, M., 2012. Integrität geotechnischer Barrieren, Teil 1 Vorbemessung, Bericht zum Arbeitspaket 9.2, Vorläufige Sicherheitsanalyse für den Standort Gorleben, GRS-287, Peine, Braunschweig: DBE TECHNOLOGY GmbH, Gesellschaft für Anlagen- und Reaktorsicherheit (GRS) mbH.
- Müller-Hoepppe, N. & Krone, J., 1999. Ein neuer Ansatz zur Bewertung der Wirksamkeit von Barrieren im Endlager, Peine: DBE TECHNOLOGY GmbH.
- Müller-Hoepppe, N. & Polster, M., 2004. Verfüllen von Strecken mit hohen Anforderungen - Konzeptplanung und Nachweisführung, Peine: DBE.
- Müller-Hoepppe, N. & Wieczorek, K., 2017. Plugging and Sealing. In: Proceedings of the 7th US/German on Salt Repository Research, Design, and Operation. Washington: Sandia National Laboratories, p. 3.
- Müller-Hoepppe, N. et al., 2007. The Role of Structural Reliability of Geotechnical Barriers of an HLW/SF Repository in Salt Rock within the Safety Case, Peine: DBE TECHNOLOGY GmbH.
- Müller-Hoepppe, N. & E.S., 2009. Übertragung des Sicherheitsnachweiskonzeptes für ein Endlager im Salz auf andere Wirtsgesteine - ÜBERSICHT, Peine: DBE TECHNOLOGY GmbH.
- Müller-Lyda, I., 1999. Eigenschaften von Salzgrus als Versatzmaterial im Wirtsgestein Salz, Braunschweig: Gesellschaft für Anlagen- und Reaktorsicherheit (GRS) mbH.

- National Research Council, 1996. The Waste Isolation Pilot Plant: A potential solution for the disposal of transuranic waste. National Academy Press.
- Niederleithinger, E. et al., 2019. Qualitätssicherung von Verschlussbauwerken in Endlagern mit Ultraschall. Friedrichshafen: DGZfP, p. 11.
- Niederleithinger, E. et al., 2021. Ultraschallprüfung von Verschlussbauwerken im Salinar. Freiberg: Bundesanstalt für Materialforschung und -prüfung.
- Orzechowski, J., 2017. Entwicklung eines methodischen Ansatzes zur langeitsicheren Auslegung eines Streckenverschlussbauwerks für ein Endlager für wärmeentwickelnde radioaktive Abfälle im Salz, Clausthal: Technische Universität.
- Ottosen, 1977. A Failure Criterion for Concrete, Journal of the Engineering Mechanics Division.
- Pfeifle, T.W., 1985. Mechanical properties and consolidation of potential DHLW backfill materials: crushed salt and 70/30 bentonite/sand. SAND85-7208.
- Polster, M., 2010. Ergänzende mechanisch-hydraulisch gekoppelte Berechnungen zur Nachweisführung für Abdichtbauwerke im Steinsalz, Peine: DBE.
- Powers, D. W., Lambert, S. J., Shaffer, S. E., Hill, L. R., & Weart, W. D.[eds.], 1978. Geological characterization report, Waste Isolation Pilot Plant (WIPP) site, Southeastern New Mexico – Volumes 1 & 2. SAND78-1596.
- Preuss, J. et al., 2002. Post closure safety of the Morsleben repository. Tucson (AZ), p. 16.
- Priestel, U. et al., 2010. Entwicklung eines Grundkonzeptes für langzeitstabile Streckendämme im leichtlöslichen Salzgestein (Carnallitit) für UTD/UTV (CARLA) - Teil2: Erprobung von Funktionselementen, Freiberg: TU Bergakademie.
- Rauche, H., Sitz, P., Lukas, V., Rumphorst, K., Lippmann, G., Wagner, K., & Teichert, Th., 2003. Planfeststellungsverfahren zur Stilllegung des Endlagers für radioaktive Abfälle Morsleben, Verfahrensunterlage: Nachweisführungen zur Langzeitstabilität, zur Tragfähigkeit und zur Gebrauchstauglichkeit der Schachtverschlüsse ERA Morsleben, Unterlagen-Nr.: P 177. Erfurt: TU Bergakademie Freiberg ERCOSPLAN, K+S Consulting.
- Rauche, H., Sitz, P., Lukas, V., Rumphorst, K., Lippmann, G., Wagner, K. & Teichert, Th., 2004. Planfeststellungsverfahren zur Stilllegung des Endlagers für radioaktive Abfälle Morsleben, Verfahrensunterlage: Konzeptplanung der Schachtverschlüsse Bartensleben und Marie des ERA Morsleben, Unterlagen-Nr.: P 182, Erfurt: TU Bergakademie Freiberg, ERCOSPLAN, K+S Consulting für BfS.
- Rechard, R.P., 2000. Milestones for disposal of radioactive waste at the Waste Isolation Pilot Plant (WIPP) in the United States (Revised). SAND98-0072.
- Romero, G.R., 1988. Sandia National Laboratories Waste Management Technology Department Waste Isolation Pilot Plant Quality Assurance Program Plan – Revision M.
- Rothfuchs, T., Wieczorek, K., Bazargan, B. & Olivella, S., 2003. Final Results of the BAMBUS II Project - Experimental and Modelling Results concerning Salt Backfill Compaction and EDZ Evolution in a Spent Fuel Repository in Rock Salt Formations. The Eurosafé Forum (No.5), 25.-26 11, pp. 23-34.

Sandia National Laboratories (SNL), 1979. Waste Isolation Pilot Plant (WIPP) program plan for FY 1979. SAND79-0098.

Sandia National Laboratories (SNL), 1987. The Scientific program at the Waste Isolation Pilot Plant. SAND85-1699.

Sandia National Laboratories (SNL), 1996. Waste Isolation Pilot Plant Shaft Sealing System Compliance Submittal Design Report. SAND96-1326.

Schmitz, 2007. Dissertation. Zur hydraulischen Kontakterosion bei bindigen Basiserdstoffen. Fakultät für Bauingenieur- und Vermessungswesen, Universität der Bundeswehr München.

Schumann et al., 2009. Verschlussystem mit Äquipotenzialsegmenten für die untertägige Entsorgung (UTD und ELA) gefährlicher Abfälle zur Sicherstellung der homogenen Befeuchtung der Dichtelemente und zur Verbesserung der Langzeitstabilität, Kompetenzzentrum für Materialfeuchte CMM, Karlsruher Institut für Technologie.

Schörian, E., 1999. The Shell Bitumen hydraulic engineering handbook, London: Shell International Petroleum Company Ltd.

Sitz, P., Gruner, M. & Rumphorst, K., 2003. Bentonitdichtelemente für langzeitsichere Schachtverschlüsse im Salinar. Kali und Steinsalz, 03, pp. 6-13.

Stahlmann, J., Mauke, R., Mohlfeld, M. & Missal, C., 2013. Monitoring of Sealing Dams - Experiences from a Test Set-up at the Repository ERAM. In: Proceedings of 4th US/German Salt Repository Workshop. Berlin: SANDIA National Laboratories, p. 15.

StandAG, 2020. Gesetz zur Suche und Auswahl eines Standortes für ein Endlager für hochradioaktive Abfälle (Standortauswahlgesetz) vom 5. Mai 2017 (BGBl. I S. 1074), das zuletzt durch Artikel 1 des Gesetzes vom 7. Dezember 2020 (BGBl. I S. 2760) geändert worden ist, English: German Repository Site Selection Act.

Statler, R. D. 1980. Bell Canyon Test – Field Preparation and Operations Report. SAND-80-0458C, Sandia National Laboratories, Albuquerque, NM.

Stormont, J.C., 1987. Small-Scale Seal Performance Test Series "A" Thermal/Structural Data through the 180th Day, SAND87-0178, Sandia National Laboratories, Albuquerque, NM

Stormont, J., Lampe, B., Mills, M., Paneru, L., Lynn, T. & Piya, A., 2017. Improving the understanding of the coupled thermal-mechanical-hydrological behavior of consolidating granular salt. Final Report, NEUP13-4384.

Technische Universität Bergakademie Freiberg (TUBAF), 2005. Stellungnahme zur geochemischen Langzeitstabilität der Schachtverschlüsse, Freiberg: TU Bergakademie Freiberg.

TerraMix, 2020. https://www.terra-mix.com/uploads/media/System_Impulse_Compaction.pdf

Torres, T.M., C.L. Howard & R.E. Finley, 1992. Development, Implementation, and Early Results: Test Series D, Phase 1 of the Small-Scale Seal Performance Tests, SAND91-2001, Sandia National Laboratories, Albuquerque, NM.

- Tyler, L.D., Matalucci, R.V., Molecke, M.A., Munson, D.E., Nowak, E.J., & Stormont, J.C., 1988. Summary report for the WIPP technology development program for isolation of radioactive waste. SAND88-0844.
- Van Geet et al., 2009. RESEAL II, A large-scale in situ demonstration test for repository sealing in an argillaceous host rock – Phase II, Final report, EUROPEAN COMMISSION.
- Van de Velde, P.A., Ebbens, E.H., & Van Herpen, J.A., 1985. The use of asphalt in hydraulic engineering. Rijkswaterstaat communications Nr. 37, Den Hague: Technical advisory committee on Waterdefences.
- WHG, 2021. Gesetz zur Ordnung des Wasserhaushalts (Wasserhaushaltsgesetz - WHG) - vom 31. Juli 2009 (BGBl. I S. 2585), das zuletzt durch Artikel 3 des Gesetzes vom 9. Juni 2021 (BGBl. I S. 1699) geändert worden ist.
- Wakeley, L.D., Walley, D.M. & Buck, A.D., 1986. Development of Freshwater Grout Subsequent to the Bell Canyon Tests (BCT). Micellaneous Paper SL-86-2, U.S. Army Engineer Waterways Experiment Station, Vicksburg, MS.
- Wakeley, L.D., J.J. Ernzen, B.D. Neeley & F.D. Hansen, 1994. Salado Mass Concrete: Mixture Development and Preliminary Characterization. SAND93-7066.
- Wakeley, L.D., P.T. Harrington, & F.D. Hansen, 1995. Variability in Properties of Salado Mass Concrete. SAND94-1495.
- Wieczorek, K. & Schwarzianeck, P., 2004. Untersuchung zur Auflockerungszone im Salinar (ALOHA2), Braunschweig: Gesellschaft für Anlagen- und Reaktorsicherheit (GRS) mbH.
- Wieczorek, K. & Zimmer, U., 1998. Untersuchungen zur Auflockerungszone um Hohlräume im Steinsalzgebirge, Köln: Gesellschaft für Anlagen- und Reaktorsicherheit (GRS) mbH.
- Wollrath, J., Mauke, R., Kreienmeyer, M. & Carstensen, A., 2018. Drift Seal Systems at the Morsleben Repository - Status of the investigations and Further Procedure. 9th US-German Workshop on Salt Repository Research, Design, and Operation, Hannover: Federal Institute for Geosciences and Natural Resources (BGR), pp. 194-200.
- Zeuch, D.H., Zimmerer, D.J. & Shields, M.E.F., 1991. Interim Report on the Effects of Brine Saturation and Shear Stress on Consolidation of Crushed, Natural Rock Salt from the Waste Isolation Pilot Plant (WIPP). SAND91-0105.

List of Figures

Figure 1-1:	Schematic cross-section of potential pathways at a circular geotechnical barrier	1
Figure 2-1:	Conceptual design of the shaft sealing system (Kudla et al., 2021).....	5
Figure 2-2:	Achived total porosity based the introduced engery for the three diffrent mixtures (Kudla et al., 2021).....	7
Figure 2-3:	Achived brine permeability as a function of porosity in comparisin to other mixtures and projects (Kudla et al., 2021).....	7
Figure 2-4:	General design of the impulse compaction device and the in situ test (Kulda et al., 2020)	9
Figure 2-5.	Illustration of the different mixtures in layers with the colour code the pre-compaction process in layers (right) and colour code of the pre-compaction (left) (Kudla et al., 2021).....	9
Figure 2-6:	Pictures from the test field surface after impluse compaction at the first layer and in all four compaction points (Kudla et al., 2021).....	10
Figure 2-7:	Post-test investigation of the compacted material (Kudla et al., 2021)	11
Figure 2-8:	Achieved total porosity in four different cross sections of the first in situ test (Kudla et al., 2021)	12
Figure 2-9:	Achieved total porosity in four different cross sections of the second in situ test (Kudla et al., 2021).....	13
Figure 2-10:	Strength of retained samples from the cast-in-place-concrete C3 (Kudla et al., 2021).....	16
Figure 2-11:	Measured pressures and temperatures in MgO concrete in the first 14 days - BS2 and BS3 as contact pressures, BS1 and BS4 as axial pressures (Kudla et al., 2021)	17
Figure 2-12:	Test setup for the second in situ test (Kudla et al., 2021)	19
Figure 2-13:	Radial (S2, S4) and axial (S1, S3) pressure and pore pressure in the control chamber 2 during the large borehole test 2 (Kudla et al., 2021)	19
Figure 2-14:	Schematic illustration of the construction "Hard shell – soft core", destillation bitumen (gray) coverd by two layers of oxidiation bitumen (black) (Kudla et al., 2009)	22
Figure 2-15:	Design of the sealing system "Hard shell – soft core" as installed for the borehole test (Kudla et al., 2021)	22
Figure 2-16:	Internal design as installed for the borehole tests bitumen filled gravel column and dense stone asphalt (Kudla et al., 2021)	23
Figure 2-17:	Image of sample from the borehole edge after removal of the test (Kudla et al., 2021).....	24
Figure 2-18:	Thin sections showing penetration of the bitmen into the EDZ (Kudla et al., 2021).....	24
Figure 2-19:	Images from the bitumen-filled cracks inside the EDZ (Kudla et al., 2021)....	25
Figure 2-20:	Images from the bitumen-filled cracks inside the EDZ, local and enhanced (Kudla et al., 2021)	25
Figure 2-21:	Shaft sealing concept based on preliminary design (Müller-Hoepppe et al., 2012)	30

Figure 2-22:	Drift sealing concept based on preliminary design, (Müller-Hoeppel et al., 2012b)	32
Figure 2-23:	Connection of hydraulic long-term calculations in a long-term safety assessment with the individual function-related assessments using the example of a shaft seal (Müller-Hoeppel et al., 2012).....	34
Figure 2-24:	Reliability methods for determining partial factors (DIN EN, 1990)	36
Figure 2-25:	Safety concept "Safe Confinement", (Krone et al., 2008).....	38
Figure 2-26:	Methodical approach to assess long-term radiological safety (Krone et al., 2008)	39
Figure 2-27:	Schematic of the ERDA-10 borehole and planned plugging program. (Modified from Gulick (1979)).....	41
Figure 2-28:	Schematic of AEC-7 borehole. The cementitious plug was emplaced from 1368 to 1370 m, just above the Belly Canyon aquifer (Modified from Christensen and Peterson, 1981).....	43
Figure 2-29:	Staging area in WIPP Room L for SSSTP-F (Ahrens and Dale, 1996). MB-139 is the gray layer below the floor of the drift, intersected by the disturbed rock zone (illustrated with fractures)	46
Figure 2-30:	Underground WIPP field test layout before emplacement of waste (Munson et al., 1997).....	47
Figure 2-31:	Layout of WIPP Rooms A1-A3 with heaters, and layout of Room B along with cross-sectional view	48
Figure 2-32:	Elevation and plan view of WIPP Room J.	50
Figure 2-33:	Elevation and plan view of WIPP Room T.....	50
Figure 2-34:	Diagram of typical seal borehole setup for SSSTP in WIPP Room M and salt block seal in Series D-Phase 1.....	51
Figure 2-35:	WIPP Large-Scale Salt Compaction Tests: a. Weight drop pattern b. Chamber used	52
Figure 3-1:	3D model of the mining areas within Asse 2 including the stopes with radioactive waste after (Lautsch, 2021).....	54
Figure 3-2:	Side view of a symmetrical EBS concept for fluid pressure from both sides, after (Fischer, 1990).....	56
Figure 3-3:	Schematic position and purpose of a flow barrier between stopes, after (Heydorn, 2006).....	58
Figure 3-4:	Basic concept for a horizontal flow barrier at Schachtanlage Asse II (Köhler et al., 2019; No. 5)	59
Figure 3-5:	Scheme of the flow barrier building process sequence after (Köhler et al., 2019; No. 5).....	59
Figure 3-6:	Asse shaft 2 and 4 sealings (Kudla et al., 2013; pp. 19-21).....	65
Figure 4-1:	Geological east-west cross-section through ERAM close to shaft Bartensleben after BGE, 2018.....	67
Figure 4-2:	ERAM mine workings of shaft Bartensleben in the foreground and shaft Marie in the background (Mauke & Herbert, 2013)	68
Figure 4-3:	Schematic drawing of a horizontal sealing after (BfS, 2016c).....	70
Figure 4-4:	Section view of the ERAM in situ Test Seal with cross-sections 1 to 5, predetermined breaking planes (metal plates) and the fluid-pressure-chamber on the left side after (Niederleithinger et al., 2019).	71

Figure 4-5:	Conceptual seal in anhydrite at ERAM with a total length of about 150 m after (Orzechowski, 2017), (Krauke & Fliß, 2008) and (Polster, 2010)	73
Figure 4-6:	Schematic profile of the large scale test in anhydrite after (BfS, 2016c).....	75
Figure 4-7:	Scheme of a shotcrete - bitumen EBS in anhydrite rock at ERAM (Carstensen, 2019).....	75
Figure 4-8:	Mixing plant for salt concrete on surface (A: silos for the storage of cement and fly ash, B: shaft Bartensleben, C: concrete batch mixer, D: tank for salination of the mixing solution, E:container for quality control) (Fischer et al., 2004).....	76
Figure 5-1:	WIPP Generalized Regional (left) and Site (right) Geologic Cross Sections.....	79
Figure 5-2:	Detailed stratigraphy near the WIPP underground facility (Roberts et al., 1999)	80
Figure 5-3:	WIPP repository layout and Shaft Seals.....	81
Figure 5-4:	WIPP Shaft Seals (Hansen & Knowles, 2000).....	82
Figure 5-5:	WIPP panel closures: Previous Salado Mass Concrete monolith design (top) and new run-of-mine salt (bottom) (from DOE, 2011).....	83
Figure 6-1:	Experiment set-up in blind raise and used materials after (Breidung, 2002)	86

List of Tables

Table 2-1:	Grain-size distribution of the different mixtures (Kudla et al., 2021).....	6
Table 2-2:	Comparison of total porosity in two test setups (Kudla et al., 2021)	13
Table 2-3:	Composition of the MgO-cast-in-place-concrete C3 (Freyer et al. 2015).....	15
Table 2-4:	Plugging plan for the four plugs with grout mixtures and curing conditions. For additional details on mixtures, see Table 1 in Gulick (1979).....	41
Table 2-5:	Small Scale Seal Performance Tests: (Knowles and Howard, 1996).	44
Table 2-6:	Seal Material Descriptions (Knowles and Howard, 1996).	44
Table 2-7:	ESC Mixture Used in SSSPT Test Series A (Stormont, 1987).....	45
Table 2-8:	Summary of test conditions of key WIPP salt consolidation projects (not inclusive).....	53
Table 3-1:	Permeabilities to gas and brine in the Asse seal (Gläß et al., 2005).....	57
Table 4-1:	Recipes of the salt concretes M2 (for stabilization of Central Part and for sealings) and M3 (for main backfilling volumes) (Engelhardt et al., 2003).....	69
Table 4-2:	Measuring devices at ERAM Test Seal, cross-sections 1 to 5 (Stahlmann et al., 2013).....	71

BGE TECHNOLOGY GmbH
Eschenstraße 55
31224 Peine – Germany
T + 49 5171 43-1520
F + 49 5171 43-1506
info@bge-technology.de
www.bge-technology.de